School of Molecular and Life Sciences

Carbonate production and loss among inshore island reefs of the Pilbara, Western Australia

Shannon Dee

This thesis is presented for the Degree of

Doctor of Philosophy

of

Curtin University

September 2021

Declaration

To the best of my knowledge and belief this thesis contains no material previously published by any other person except where due acknowledgement has been made.

This thesis contains no material which has been accepted for the award of any other degree or diploma in any university.

Signature: Date: 30/09/2021

“Don't let anyone rob you of your imagination, your creativity, or your curiosity. It's your place in the world; it's your life. Go on and do all you can with it and make it the life you want to live.”

Mae Jemison

Abstract

Coral reefs serve a number of functions that are essential for the maintanence of marine life, however, these functions are under increasing pressures with current climate change. Carbonate budgets offer a comprehensive assessment of the health and production of coral reefs, with census-based carbonate budgets having rapidly increased in popularity over the past two decades. With developing technologies and varying methodologies between studies, an uncertanty of the accuracy and comparability of studies has arisen. Additioanlly, there remains a lack in varability between reef settings with majority of studies focusing on shallow clear water reefs, and little research being conducted on turbid or marginal reef systems.
This thesis aims to quantify net carbonate production of two inshore turbid island reefs, Eva and Fly, of the Pilabra Western Australia. In doing so, the applicability of traditional and modern methodologies for quantifying benthic habitat area are compared (chapter 2), while carbonate production of calcifying encrusting organisms is measured across spatial and temporal scales (chapter 3). Aditionally, rates of cryptic endolithic bioerosion are measured, with investigations into the relationships between environmental parameters and bioeroder activity in the Pilbara, and globally (chapter 4). Finally, the knowledge of chapters 2-4 are combind with onsite coral calcification rates to calculate the net carbonate budget of Eva and Fly reefs (chapter 5). Chapter 5 also reports direct carbonate sediment production across both reefs, leading to estimates of net sediment budgets, with further discussions of what implications these rates have in the face of predicted climate change.

Reef rugosity is a measure of topographic complexity across a reef and is a prominent factor within many carbonate budget equations. Rugosity is traditionally measured with the chain and tape method which is limited by a 2-dimensional resolution. Remote sensing offers a solution to this by capturing the 3-dimensional reef bathymetry, but how representative these measures are of true coral cover is still unknown. Areial LiDAR was employed to gather 0.1m resolution bathymetric data of each reef, where 2m wide belt transects on bathymetric data were compared with insitu line transects measuring rugosity with the chain and tape method. Results showed the chain and tape method was more representive of the reef topographic complexity as awell as coral cover at each morphological scale. Meanwhile, LiDAR derived bathymetry measured little variation in rugosity across each reef geomorphic zone, and had little correlation with coral cover at any scale.

Secondary carbonate producers are valuable taxa across reefs as they fill gaps and solidify the carbonate framework. Carbonate production and lateral cover of encrusters, mainly CCA, were measured annually and seasonally alongside environmental and water quality measures. Results found CCA ws spatially more

prominent in habitats with hard substrate and less so in areas dominated by macroalgae. Seasonally, there was significantly more lateral growth in the winter season compared to the summer, which aligned with strong periods of ocean warming and sea surface temperature anomalies. However, no significant variation in carbonate prodiction between the seasons was recorded.

Opposed to carbonate producers, bioeroding taxa weaken the reef fraework. Cryptic endolithic borers are oftern overlooked with most carbonate budget studies traditionally ocused on bioerosion by external grazers (parrot fish and urchins). Experimental substrates were deployed for 12 months to capture bioeroder activity across reef zones. Macroboring worms were the most dominant bioeroding group across both reefs, with grazing rates being particularly low. Spatial variations in bioerosion rates were compared with environmental parameters which showed negative relationships with temperature and light. Further a global assessment of macroboring and environmental parameters was conducted, with temperature and chlorophyll-a both showing to be significant influencers of macroboring activity.

Combining the knowledge from the previous chapters, carbonate production by corals was quantified by first estimating coral calcification rates. This was done by the buoyant weight method which produced similar results to other local studies, although results were much lower than average Indo-Pacific rates that had been estimated from the linear growth method. When applying offsite linear growth rates, carbonate production rates by corals at Eva and Fly increased by >230%, which then carried on to estimates of net carbonate production and reef accretion potential. Net production and reef accretion estimates using onsite data were positive and compareable to other turbid and inshore reef sites within the Indo-Pacific. Furthermore, a net sediment budget was measured through direct sediment production, bioeroded sediment production, and sediment carbonate dissolution, which resulted in estimated rates comparable to “healthy” clear water reefs. Finally, the possible impacts of sea level rise on these reef settings and the adjacent islands is discussed.

This thesis provides the first full comprehensive carbonate reef and sediment budgets among turbid reefs for Western Australia. Importantly, this research also displays areas of ambiguity among methodologies adopted across modern carbonate budget studies, as well as the remaining knowledge gaps that are increasingly relevant under climate change predictions.

Acknowledgement of Country

I acknowledge that Curtin University works across hundreds of traditional lands and custodial groups in Australia, and with First Nations people around the globe. We wish to pay our deepest respects to their ancestors and members of their communities, past, present, and to their emerging leaders. Our passion and commitment to work with all Australians and peoples from across the world, including our First Nations peoples are at the core of the work we do, reflective of our institutions' values and commitment to our role as leaders in the Reconciliation space in Australia.

I would like to further acknowledge the Whadjuk Nyoongar people and the Jinigudera people of whose land this research took part on.

Acknowledgements

These have been some of the most challenging years of my life, and I could not have achieved this amazing feat without the help and support of many people. Each chapter of this thesis would not have come together if it weren't for the support of collaborators, friends, and love-ones. I would like to take this opportunity to thank them.

This project came to my attention while I was working as a barista on the Gold Coast, looking for a path to express my passion for science and love for the ocean. I could never thank Nicola Browne, Mick O'Leary, and Jennifer McIlwain enough for considering my application for this project after meeting me over a skype call, and then inviting me to come back over to the west coast to work in my favourite part of Australia. I would also like to thank Sarah Marley for encouraging me to apply for the project in the first place and offering a most likely embellished review of my abilities to Nikki. Over the past three years Nikki has been a great mentor and offered a huge amount of support to me, of which I am forever grateful for. Further, I would like to offer a huge amount of thanks to Michael Cuttler, who first became involved in this project as a somewhat related post-doc and very quickly became a very impactful and reliable supervisor and friend.

This PhD was very field-work intensive, which was only made possible due to my amazing volunteers and friends. I would like to thank Tahlia Basset, Adi Zweifler, Paula Cartwright, Flortje Burgers, Clair Ross, Brooke Gibbons, Savita Goldsworthy, Joshua Bonesso, Jake Nilsen, Dylan Benson, and Kesia Savill for their help in the water at one point or another. Thank you to Rowan KIeindienst for eventually approving all of my dive plans and putting up with me for the past three years. Thank you to Peter Barnes and the DBCA crew in Exmouth for their support and friendship over the years, and to the people of Exmouth town for being so welcoming and always offering us girls help at the boat ramp (even though we never needed it). In particular, I would like to offer special thanks to Aspa and Warren from Exmouth Boat Hire for providing quality boats for each field trip, local knowledge and advice, and the welcoming smile of an old friend every time I came into town.

I would like to thank the Reef Island Ecology and Futures (RIEF) lab for encouraging me and keeping me sane during this project. In particular I would like to acknowledge Adi Zweifler and Tahlia Basset, who were always reliable and available whenever I needed their help or emotional support. I would also like to thank the admin staff of the school of Molecular and Life Sciences at Curtin University for looking after me during this time. In particular Carrey Ryken-Rapp who resembled an admin fairy godmother and was always happy to answer all of my stupid questions and fix up my paperwork.

During my PhD I had the opportunity to join multiple communities of which provided me with opportunities to grow, learn and network. Being a part of the Australian Marine Sciences Association has been an invaluable experience and introduced me to many great marine scientists who I am now lucky enough to call friends. I would Like to offer a huge amount of thanks to the Society of Underwater Technology for having me as part of their youth committee and awarding me with the Chris Lawlor scholarship as well as offering me the opportunity to attend extremely valuable courses. Thank you also to the International Association of Sedimentologist for awarding me a research grant which was immensely appreciated.

Thank you so much to my family and friends. To my parents who have always supported me and allowed me to grow up by the sea. To my three older brothers who made me tough. To my beloved school friends “the cronies” for always believing in me. To Gabby for being my number one fan and never judging me for having another glass of wine. To the Bradshaw’s who allowed me to live with then during the never ending lockdown of 2020. To Trent for being my rock, engaging so full heartedly in my passions, and loving me through every breakdown. And to Bandit, for being my best friend and adventure buddy. I could not have survived the past three years without you, girl.

I would like to recognise and thank the anonymous reviewers for the chapters in this thesis that have already been accepted or published. Their comments helped shape each chapter into a better contribution to our field of science, and I am greatly appreciative of that.

Finally, I would like to thank Peter Mountford, who was my chemistry and physics teacher during the final years of high school and who ignited my love of science. As part of a reference letter he provided me once I finished school, he wrote “She is a person who will make a significant contribution in any chosen field”. I hope that this thesis holds true to that statement and would have made him proud.
Rest in peace.

Statement of Contributions

Chapter 2: Dee, S., Cuttler, M., O'Leary, M., Hacker, J., Browne, N. The complexity of calculating an accurate carbonate budget. *Coral Reefs* **39,** 1525–1534 (2020). https://doi.org/10.1007/s00338-020-01982-y.

Author contribution: JH collected the data. SD designed the study with help from NB and MO. SD conceived and executed the data analyses. SD wrote and edited the manuscript. NB and MC helped to develop the structure of the manuscript. All co-authors reviewed and commented on the manuscript.

Chapter 3: Dee, S., Cuttler, M., Cartwright, P., McIlwain, J., Browne, N. Encrusters maintain stable carbonate production despite temperature anomalies among two inshore island reefs of the Pilbara, Western Australia. *Marine Environmental Research* **169,** (2021). https://doi.org/10.1016/j.marenvres.2021.105386.

Author contribution: SD and PC collected the data. SD designed the study. SD executed the data analyses. SD wrote and edited the manuscript. NB and MC helped to develop the structure of the manuscript. NB, MC, and JM reviewed and commented on the manuscript.

Chapter 4: Dee, S., DeCarlo, T., Lozić, Ivan., Nilsen, J., Browne, N. Bioerosion among inshore reefs in Western Australia

Author contribution: SD is responsible for the study conception and design. Material preparations were performed by TD and SD, data collection were performed by SD and JN, and analysis were performed by SD and IL. The first draft of the manuscript was written by SD and all authors commented on previous versions of the manuscript.

Chapter 5: Dee, S., Cuttler, M., O'Leary, M., Nilsen, J., Browne, N. The application of carbonate and sediment budgets to assess the stability of marginal reef systems

Author contribution: SD is responsible for the study conception and design with assistance from NB. SD collected all data, with assistance of JN who collected DOV

data. The first draft of the manuscript was written by SD and was reviewed by MC and NB.

Table of Contents

List of Figures

List of Tables

List of Appendices

Chapter 1 General Introduction

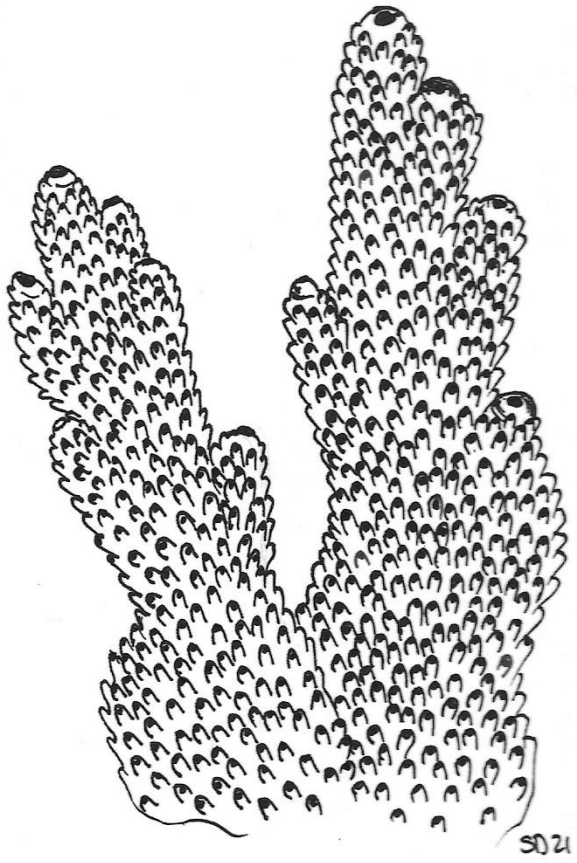

1.1 Coral reefs and environmental change

Coral reefs are some of the most biologically diverse and productive ecosystems on Earth, contributing billions of dollars annually to the global economy through tourism, food production, and cultural practices (Hoegh-Guldberg 2004; Cinner 2014; Kittinger et al. 2016). The complex carbonate framework which supports coral reefs provides several critical ecosystem services including habitat provision and protection for many fish and invertebrate species (Friedlander and Parrish 1998; Graham and Nash 2013). These frameworks provide further benefits to human life as coastal reefs act as a physical barrier that reduce wave energy, limiting shoreline inundation and coastal erosion (Perry and Smithers 2011; Beetham et al. 2017).

Coral reefs and the services they provide are currently under threat as most tropical reefs are existing at their thermal limits (Baker et al. 2008). Under the most plausible current climate projections (RCP 3.4-4.5), global mean temperature increase will likely range from 2-2.5°C by 2100, with an average sea level rise (SLR) of 0.5m (Van Hooidonk et al. 2016; Pielke and Ritchie 2021). An increase of 2°C or above will have considerable impacts on coral reefs globally with both an increase in the severity and frequency of bleaching events and subsequent coral mortality. Additionally, an increase in ocean acidification (OA) will reduce the calcification rate of marine organisms, particularly reef-building corals (Hoegh-Guldberg et al. 2007; Cornwall et al. 2021). Under these conditions, the diversity and topographic complexity of reef systems is expected to diminish, resulting in a dominance of more "hardy" coral genera that are slower growing and less structurally complex (Perry and Alvarez-Filip 2019). These estimates coupled with predicted SLR will alter the ability of reefs to dissipate wave energy, leading to an increased rate of coastal erosion and inundation. This may then result in loss of infrastructure, agriculture, freshwater supply, and in worst cases loss of human life (Harris et al. 2018). To forecast the future of reefs and predict their resilience to climate change, we need more quantitative evidence of contemporary reef processes across the diverse reef ecosystems that exist (e.g., clear water to turbid).

1.2 Carbonate budgets

The accumulation of calcium carbonate, which contributes to reef accretion and stability, is largely dependent on the rate of gross carbonate production within the reef ecosystem. The primary carbonate producers of the reef framework are hard corals, while secondary producers include encrusting organisms such as crustose coralline algae (CCA; Perry et al. 2008). The functional contribution of different corals to the reef framework varies between taxa as some are fast growing and offer higher levels of topographic complexity (branching *Acropora*), while others are slow growing and offer less contribution to overall framework accretion but are more resilient to physical damage (e.g., massive *Porites;* Darling et al. 2012; Bozec et al. 2014). As such, the composition of corals on a reef has an important long-term influence on coral reef development at geological timescales (Alvarez-Filip et al. 2013). Rates of calcium carbonate production by CCA is typically lower than that of corals, although CCA support reef accretion through biological (e.g., increasing rates of coral larval settlement; Mason et al., 2011) and geological services (e.g., cementing the reef frame framework; Rasser and Riegl, 2002). The rate of reef framework accretion is the sum of these processes, minus that of erosional processes that remove carbonate framework.

Physical, chemical, and biological erosion are natural processes that breakdown the reef framework and produce carbonate sediments. These sediments can then be reincorporated back into the reef system, carried off to deeper waters, or add to geomorphic landforms (i.e., carbonate islands; Morgan and Kench 2016). The rate at which these erosional processes take place is heavily influenced by environmental conditions. For example, an increase in nutrients may lead to an increase in bioeroding taxa (Le Grand and Fabricius 2011; Prouty et al. 2017). Further, under elevated OA corals may experience reduced skeletal density (Mollica et al. 2018), increasing vulnerability of reefs situated in cyclone hotspots that are more frequently subjected to physical damage from high energy waves (Ryan et al. 2016). Thus, understanding how environmental change influences both rates of carbonate production and erosion is crucial in predicting trends in coral reef health and stability into the future.

The balance between constructive and destructive processes that influence reef accretion over time can be estimated using the carbonate budget approach (Chave et

al. 1972; Stearn and Scoffin 1977; Hubbard et al. 1990). The most common method for estimating a carbonate budget is through the biological census-based technique (e.g., Browne et al. 2013). This method estimates net carbonate framework production by quantifying the amount of carbonate produced by calcifying reef organisms (e.g., corals and CCA) and that lost through biological and physical removal (e.g. parrot fish, urchins and boring organisms; Stearn and Scoffin 1977; Eakin 1996; Perry et al. 2008). This approach was first developed by Chave et al. (1972) and has since been used in 38 global studies that have aimed to assess various biological, physical, and chemical-driven reef processes (Browne et al., 2021). Despite the limited number of census-based studies conducted to date, this method has been growing in popularity over the last 20 years with 74% of studies being undertaken since 2000.

Census-based carbonate budgets are currently one of the most comprehensive approaches that provide a holistic view of processes that contribute to reef development (Kuffner and Toth 2016; Cornwall et al. 2021). However, a recent review by Browne et al. (2021) highlights a number of inherent issues including data collection bias, methodological inconsistencies and the use of historic or offsite data to fill gaps. There have been some improvements in recent years regarding streamlining how data for carbonate budgets are collected on reefs with the development of the *Reef Budget* approach (Perry et al. 2012, 2018a). This approach builds on the traditional census-based carbonate budget, and provides a standardised and rapid method to calculate reef carbonate production and bioerosion simply by collecting abundance data on calcifying and eroding organisms (Perry et al. 2012). Importantly, this approach still relies on the use of offsite data, which may potentially lead to spatially inaccurate estimates that result in carbonate budget estimates that are not representative of reef sites being studied.

Another key gap in carbonate budget studies is the lack of complimentary environmental data. As discussed above, environmental conditions and their interactions can have a broad influnce on the functions within reef ecosystems. Environmental data gives insight into drivers of reef carbonate production and erosional processes, and aids comparability between studies. For example, currently, it may seem as though two reef systems are comparable based on regional location and estimated net carbonate production, although one reef may be exposed to upwelling, nutrient exposure, pollution, varied levels of salinity or greater seasonal

shifts in temperatures. This reef could therefore have distinct variations in seasonal shifts in carbonate production and erosion. An increase in the inclusion of complimentary environmental data not only increases our understanding of environmental impacts on reefs, but also aids in the development of empirical relationships. This is becoming more essential with remote sensing methodologies and ecological modelling practices that may be able to predict shifts in carbonate budgets states under hypothetical climate scenarios into the future.

1.3 Carbonate sediment budget

Expanding upon the traditional reef carbonate budget, recent studies have begun to include assessments of carbonate sediment budgets (Browne et al. 2012; Perry et al. 2017; Brown et al. 2021). A carbonate sediment budget balances sediment production by carbonate organisms (e.g., forams and molluscs) and bio-physical-chemical erosion or loss of sediment due to dissolution, off reef export, and/or storage on land. Knowledge on carbonate sediment stocks is important for assessing coastal erosion as these sediments nourish and maintain shorelines (Perry et al. 2011; Morgan and Kench 2016; Cuttler et al. 2019). Low-lying coral reef islands are predominantly composed of unconsolidated carbonate sediments produced and supplied by adjacent reef platforms (Yamano et al. 2005), where overall species presence and abundance control the type of grain, size, and rate of sediment supply (Perry and Smithers 2011). Therefore, ecological transitions among the reef ecosystem are a key influence on future island resilience.

Sediment budgets are not often incorporated into reef carbonate budget assessments as the effort to quantify them is difficult to justify. For example, quantifying sediment production, transport and deposition can be logistically and technically challenging (Sadd 1984; Harney and Fletcher 2003; Morgan and Kench 2014a; Cuttler et al. 2019). Secondly, in most cases, the amount of carbonate sediment produced relative to *in situ* carbonate production is comparatively small (Browne et al. 2013). Thirdly, although sediments can infill reef frameworks, the net amount of sediment production does not directly contribute to reef accretion. Hence, if the purpose of the study was to access reef framework carbonate production and reef accretion, sediments may not need to be included. However, if we are to effectively

manage the full carbonate budget of reef systems and associated landforms, sediment budgets are a nessesary inclusion.

1.4 Turbid reefs

The vast majority of carbonate framework and sediment budget studies have been carried out across clear-water reefs, with only four being conducted on inshore reefs exposed to higher levels of turbidity or pollution (Edinger et al. 2000; Mallela and Perry 2007; Browne et al. 2013; Januchowski-Hartley et al. 2020). Inshore reefs are typically exposed to a greater degree of environmental variation than outer reef systems such as high turbidity and low-light availability, and greater fluctuations in salinity and temperature (Kleypas 1996; Kleypas et al. 1999). These harsh conditions have resulted in inshore turbid zones being considered as "marginal", existing at their environmental limits (Morgan et al. 2016). However, a growing number of studies on turbid reefs in recent years have recorded high levels of coral cover and diversity, as well as elevated adaptive capacity of these coral communities to variable light and temperature conditions (Guest et al. 2016; Morgan et al. 2016; Lafratta et al. 2017; Loiola et al. 2019). It has therefore been hypothesised that nearshore turbid reefs may represent potential refugia for corals from large-scale climatic disturbances (Cacciapaglia and van Woesik 2016; van Woesik and Cacciapaglia 2018). With impacts of anthropogenic climate change such as sea level rise, and local stressors, such as urbanisation and pollution, turbid reefs are expected to increase in relative abundance over the coming decades (Ogston and Field 2010; Heery et al. 2018; Zweifler et al. 2021). In all aspects of reef science, turbid reefs are currently less studied compared to clear water reefs, largely as a result of difficult *in situ* working conditions, leaving a significant knowledge gap in the health, production and future stability of these critical reef systems.

1.5 Aims and objectives

The aim of this research was to estimate net carbonate framework and sediment production among turbid inshore reefs of the Pilbara. A number of research methods were integrated to address critical knowledge gaps regarding carbonate production

and erosion rates on turbid reefs, and how changing environmental variables influence these processes. Specifically, key objectives of this study were to:

1) Assess the influence of different measures of reef structural complexity on carbonate budgets by comparing traditional *in situ* and modern remote sensing methods (Chapter 2),
2) Quantify rates of gross carbonate production from primary (coral) and secondary carbonate producers (e.g., calcareous algae, molluscs, bryozoans) (Chapter 3),
3) Evaluate rates of carbonate removal from external and endolithic bioeroders using modern technologies (Chapter 4),
4) Invastigate potentail links between ecological reef processes (carbonate production, erosion) with environmental data and the influences of a changing climate (Chapter 3 and 4),
5) Assess reef sediment composition and production rates (Chapter 5), and
6) Calculate net carbonate production and reef accretion rates for turbid reef systems in Western Australia (Chapter 5).

1.6 Significance

This thesis contains the first comprehensive assessment of carbonate framework production and removal for inshore turbid reefs of Western Australia, using a census-based carbonate budget approach. Globally there is an increasing need for research into the ecological functions among turbid reefs as they are considered to be future coral refugia. This study not only provides further understanding of the health and function of these reefs but provides a comprehensive assessment of the environmental conditions (e.g., temperature, light, turbidity, nutrients) that are influencing carbonate production in these marginal settings. Of the 39 census-based studies conducted to date, only three have incorporated some level of environmental data (Edinger et al. 2000; Mallela and Perry 2007; Roik et al. 2018), and such, this study is one of a very small number of studies that seeks to provide empirical data for the quantification of relationships between drivers (cause) and biological responses (effect). These relationships will be critical for developing ecological

models of reef health and accretion that can be used to predict reef response with future climate change.

Further, this study took place in a region with very minimal localized anthropogenic impacts, offering a unique “baseline” setting where these reefs are largely responding to changes in the global climate regime as opposed to local influences. The study site sits within Exmout Gulf which has recently been made a protected marine park by the West Australian Government due to the unique combination of habitat types and its use by nursing humpback whales, whale sharks, marine turtles, and threatened sea bird species.

A carbonate sediment budget for the forereef and lagoonal zones surrounding these reef islands is also included in the thesis. As such, this is only the twelfth_study globally that has attempted to combine reef framework production with carbonate sediment production, and the second study of its kind within a turbid reef environment. The sediment budget gives important insights into the amount of carbonate sediment available for island shoreline nourishment, which is increasingly critical for island stabilisation under anthropogenic pressures and predicted SLR.

1.7 Study location- Exmouth Gulf

Along the Pilbara coast, in northern Western Australia, there are a high number of well-developed reef systems with over 120 species of scleractinian corals from 43 genera (Rosser 2012; Gilmour et al. 2013; Speed et al. 2013; Ridgway et al. 2016). These reefs support one of Australia’s largest sand island archipelagos providing essential habitat for marine and terrestrial fauna (EPA 2021). The Pilbara experiences natural varying turbidity in response to wave-driven resuspension events as well as large weather patterns that drive increased river runoff (Dufois et al. 2017). It remains the most cyclone prone coastal region in Australia, with the highest frequency of cyclone coastal crossings (BOM 2021). It is estimated that on average the Exmouth area will be hit with cyclone producing winds of 90 km hr^{-1} (or more) once every two to three years. Increased sea surface temperature along the coast has also seen multiple coral bleaching events during summers of 1998, 2011, 2013, and 2016 (Moore et al. 2012; Depczynski et al. 2013; Lafratta et al. 2017; Le Nohaïc et al. 2017; Evans et al. 2020). Conditions responsible for mass bleaching events

coincide with the cause of storms and cyclones, amplifying the destructive effects of bleaching (Moore et al. 2012). Reefs within Exmouth Gulf are exposed to periods of high turbidity (e.g., 0.2-36.5 NTU) and extreme temperature fluctuations (18-32°C). Currently, Exmouth Gulf has minimal local anthropogenic pressure due to the small local population (approximately 2500 people that reside along the adjacent coastline) and minimal coastal development.

This study was carried out across two inshore island reef systems, Eva (-21.918454°, 114.433502°) and Fly (-21.804829°, 114.554003°) situated at mouth of the Exmouth Gulf (Figure 1.1). Both reef systems have similar characteristics; specifically, the surrounding reef morphology can be described as a limestone platform which forms into a fringing reef around the northern edge of each island, a macroalgae and seagrass dominated sand bar forming off the south/ south-west, and a sandy lagoon hosting spurs and buttresses around the south-east of each island. Further, as these islands are uninhabited and without any coastal infrastructure, they present an opportunity to investigate “natural” reef processes (Cuttler et al. 2020).

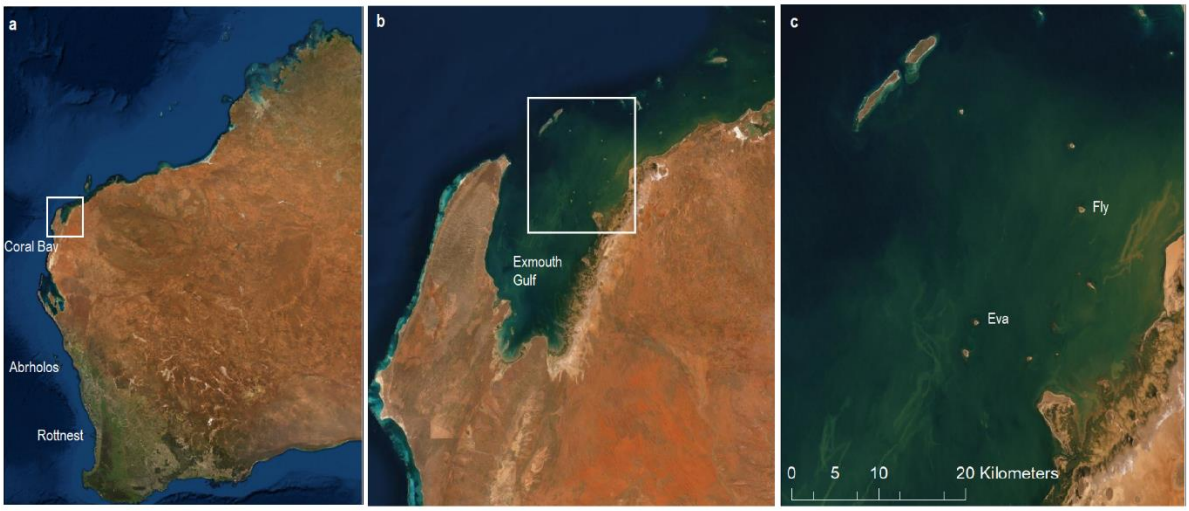

Figure 1.1(a) Western Australia, showing location of Exmouth Gulf (b), situated at the southern end of the Pilbara region, and (c) the location of Eva and Fly islands. White stars indicate the location where water quality parameters (chlorophyll-a, pH, salinity and turbidity) were measured monthly.

Fiftene diver photo transects were conducted around each island to assess benthic habitat types and coral cover and assemblage. A diver swam 1.5m above the benthos at a slow pace with photos being taken on time-laps setting capturing a photo every 2

seconds (~1m) along a 20m transect tape. 100 points were overlaid on photos within Coral Point Count with excel extension software (CPCe; Kohler and Gill 2006). Care was taken not to repeat point counts on overlapping sections of benthos through the use of identifying reef features and capturing the measuremnt of the transect tape at the point of each photo.

Following benthic identification, the marine habitats surrounding each island were sectioned into five 'zones' for spatial analysis and carbonate production calculations (Figure 1.2). These zones included a northern windward forereef (NWF; characterised by high cover of live coral and turfing algae), eastern leeward reef crest and forereef (ELC; characterised by high live coral cover), southern windward sandbar (SWS; dominated by macroalgae and rubble), southern leeward lagoon (SLL; high sand cover with occasional small coral bombie or sponges), and western windward forereef (WWF; consisting of high sediment cover with spurs and buttresses or rock; Figure 1.2). Within chapteds 3 and 4, experimental aims were to capture shallow and deeper water ecological activities in exposed and protected environments. The more'exposed' locations were within the northern sections of the reefs, with the southern section representing a more protected area year round. These four sites per reef were north offshore (i.e, ENO and FNO; NWF below), north inshore (i.e, ENI and FNI; ELC below)), south offshore (i.e, ESO and FSO; SWS below), and south inshore (i.e, ESI and FSI; SLL below).

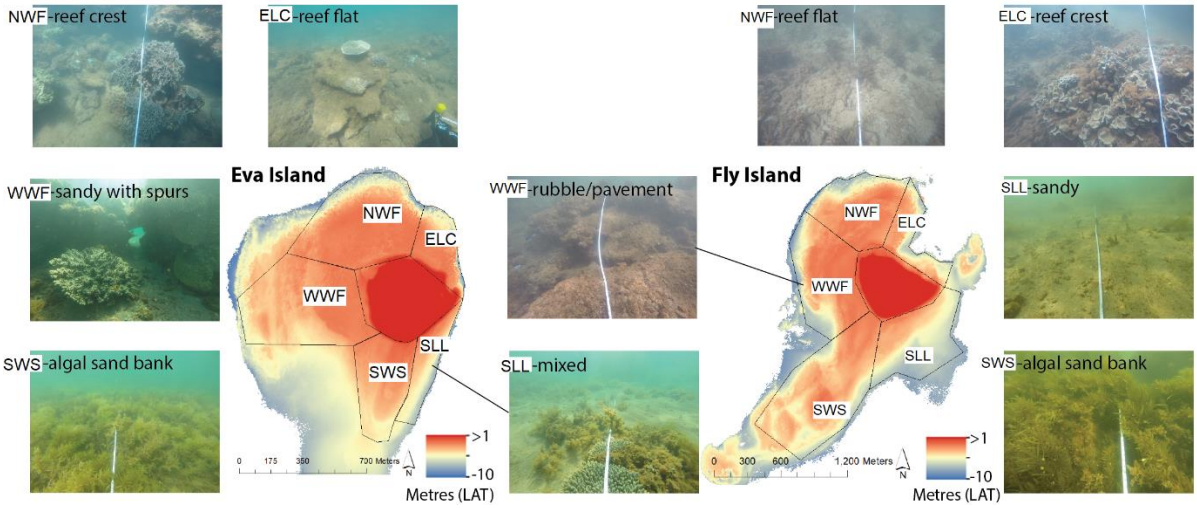

Figure 1.2 Bathymetric imagery of Fly and Eva reefs displaying the range of each geomorphic reef zone and the dominant habitat type within each zone. Reef zones include north windward forereef (NWF), east leeward crest (ELC), southern leeward lagoon (SLL), southern windward sandbar (SWS), and western windward forereef (WWF). Thesis structure and overview

The thesis opens by addressing one of the most fundamental parameters for calculating a carbonate budget, reef rugosity (chapter two). The classical 'chain and tape' method adopted since the 1970's is compared with the modern bathymetric LiDAR method, to investigate the influence of data collection methods on final rates of primary (coral) carbonate production. Chapter three then investigates secondary carbonate production by encrusting organisms, most notably crustose coralline algae (CCA; chapter three) and assess the level of contribution these organisms provide to the reef framework. In chapter four modern micro computed tomography (MicroCT) methods are applied to measure multiple scales of bioerosion (external, and endolithic microboring and macro boring). Importantly, within chapters three and four, ecological functions are combined with a comprehensive environmental data set to explore the relationships between environmental conditions and ecological functions (e.g., carbonate production rates, bioeroder activity, sediment production). Chapter five provides the completed carbonate framework and sediment budget assessment of each reef and includes additional data on *in situ* measurements of coral growth rates and reef sediment characteristics. The final discussion chapter (six) provides a synthesis of the research and explores future research needs.

The data chapters in the thesis were written and formatted as journal articles. Chapters two and three have been published, chapter four has been submitted for publication, and chapter five due to be submitted by the end of 2021. Since there is considerable overlap between references for each chapter, combined references for all chapters can be found in the "Cited Literature" section after chapter six.

1.7.1 The complexity of calculating an accurate carbonate budget (chapter 2)

Reef rugosity is a fundamental factor of multiple equations within carbonate budgets, and so accurately measuring rugosity is critical for reliable budget estimates. In chapter two the accuracy and applicability of the traditional method of measuring reef rugosity, the chain and tape method, is compared with three dimensional rugosity measurements captured from bathymetric areal LiDAR. The chain and tape method was introduced by Risk in 1972 and offers a simple two-dimensional index of surface complexity. Although cost effective, high levels of repetition are required for robust data, as this method only covers a small two-dimensional area which is

highly subjective to chain placement. Recently, studies have been applying remote sensing data, of varying resolutions, to capture three-dimensional bathymetry of the seafloor and reef habitats. Whether these remote sensing methods have the ability to measure rugosity at the coral colony scale, and hence their applicability to carbonate budgets, it yet to be assessed. Rugosity measures of line transects using *in situ* (the chain and tape method) and remote methods (aerial LiDAR) are compared to evaluate which method shows the strongest relationship with various coral morphologies and total coral cover, and what impact method selection has on final estimates of coral carbonate production. Chapter two has been published in the peer-reviewed journal *Coral Reefs* (Dee et al. 2020).

1.7.2 Encrusters maintain stable carbonate production through periods of sea surface temperature anomaly (chapter 3)

Currently there is no data on calcification rates of encrusting reef organisms for northern Western Australia, or knowledge of how their carbonate production may vary with shifts in environmental conditions. In chapter three, site specific rates of carbonate production by encrusting organisms were measured annually, and over the two dominant seasonal periods of north West Australia (the wet and dry seasons). The dominant encruster across Eva and Fly was crustose coralline algae (CCA), which is common for most reef ecosystems. Previously the only measure of CCA carbonate production rates recorded in Western Australia were from a temperate clear water reef and measured 0.148 g cm^{-2} yr^{-1}, which is a magnitude higher than average rates for the Indo-Pacific region (0.095 g cm^{-2} yr^{-1}: Perry et al. 2018a). Here, variation in carbonate production across sites is recoreded, as well as correlations between CCA growth with seasonal shifts in environmental conditions. In particular, the response of CCA to an extensive period of sea surface temperature anomaly (max SSTA of 3.6°C) is documented. Chapter three has been published in the peer-reviewed journal *Marine Environmental Research* (Dee et al. 2021).

1.7.3 Rates of endolithic bioerosion among marginal reefs of Western Australia add to our understanding of the relationships between bioeroders and their environment (chapter 4)

Chapter four explores the rates cryptic endolithic bioerosion of dead coral substrate at Eva and Fly reefs. Carbonate budget studies classically estimate bioerosion from the abundance of bioeroding taxa captured in "snap-shot" surveys, yet these methods typically only account for larger bioeroders on the surface of the substrate (urchins and sponges) or in the water column (parrotfish). Microboring organisms include algae and fungus, while macroboring taxa include various species of worms, sponges, and bivalves, all of which are difficult or impossible to quantify from visual surveys. Micro computed tomography (MicroCT) was used to measure the volume excavated by microborers, macroborers, and grazers over a 12-month period across four sites at each reef. Bioerosion rates were then correlated with environmental data from each site as a means of developing empirical relationships between key environmental parameters and rates of bioerosion. Further, a global assessment of macroboring rates recorded simultaneously with environmental data were anlaysed to further assess key quantitative relationships between endolithic bioerosion and environmental conditions. Chapter four has been submitted to the peer-reviewed journal *Marine Biology*.

1.7.4 Carbonate and sediment budgets of two marginal reefs of the Pilbara, Western Australia (Chapter 5)

Chapter five combines the knowledge and data gathered in chapters two to four with additional data on coral growth rates, sedimentation rates, sediment composition, and reef geomorphology to produce a comprehensive budget of net reef carbonate accumulation and sediment production. In total, this chapter integrates 18 site specific variables including 6 environmental parameters to provide detailed insights into *in situ* relationships between reef function and environmental fluctuations. This data set resulted in a robust assessment of carbonate reef framework and sediment production, which was then used to estimate rates of reef accretion potential (RAP) for Eva and Fly reefs while adding to global knowledge on carbonate production rates with environmental change.

1.7.5 General discussion (chapter 6)

Chapter six integrates and synthesises the research from the six data chapters, it relates the new insights stemming from this thesis to potential management solutions and discusses future avenues of research

Chapter 2 The Complexity of Calculating and Accurate Carbonate Budget

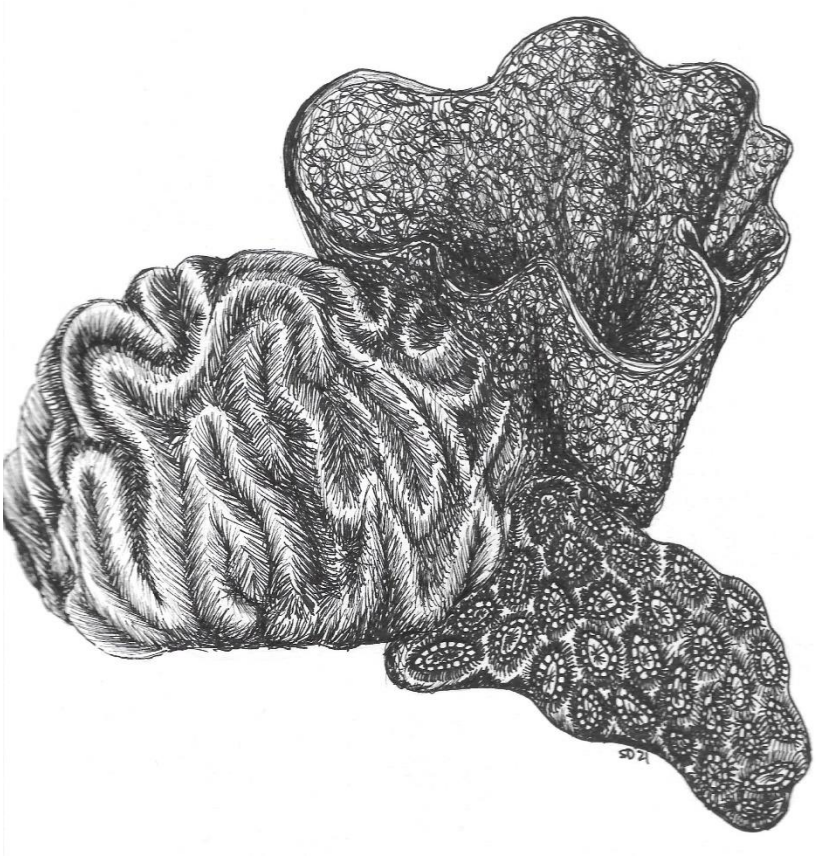

Preface: This chapter has been published in *Coral Reefs* (doi.org/10.1007/s00338-020-01982-y) and has been formatted according to the journal guidelines. The combined references for all chapters can be found in the Cited Literature section at the end of this thesis.

2.1 Abstract

A carbonate budget is a comprehensive measure of reef health and function that focuses on processes that produce and remove carbonates. A key parameter of a carbonate budget is reef topographic complexity, or rugosity, that is traditionally measured by the chain and tape method (CT). However, to overcome spatial limitations of the CT method, modern studies are moving towards remote sensing data to quantify complexity on a reef-wide scale. Here we compare rugosity values calculated using the traditional CT method with remotely sensed measures of rugosity and assess implications of methodological approach for carbonate production estimates. Remotely sensed values of rugosity were calculated from high resolution (0.1 m) LiDAR bathymetry from two turbid reefs in the Exmouth Gulf, Western Australia, and included virtual chain and tape (VCT), arc-cord ratio (ACR), and surface area to planar area (SAPA). Rugosity values varied significantly between methods (ranges: CT=1.04-2.15, VCT=1.01-1.10, ACR and SAPA = 1.00-1.07). Coral carbonate production rates calculated using the CT method were typical of turbid water reefs (2.9 and 3.8 kg m^{-2} yr^{-1}) were 30% greater than rates calculated using remote sensing. This variation questions the reliability and comparability of carbonate budgets using remote assessments of reef rugosity with previous budget studies that used the CT method. Given the limitations of remote sensing when capturing fine-scale reef rugosity, we propose that CT is currently a more appropriate method than remote sensing for quantifying rugosity within carbonate budget studies.

2.2 Introduction

Reef structural complexity, defined as the three-dimensional shape or physical architecture of the ecosystem (Graham and Nash 2013; Bozec et al. 2015; Pygas et al. 2019), is a key driver of reef health and ecosystem function (Dahl 1973). Structural complexity in reef systems is typically driven by coral cover and composition (morphology) but can also be influenced by other benthic features such as limestone structures, sponges and, on temperate reefs, kelp forests (Graham and Nash 2013). Corals grow in a diverse range of morphologies including encrusting (low structural complexity), massive, foliose, and branching (high structural complexity). Coral species with higher structural complexity tend to grow faster thereby creating reef habitats that support reef biodiversity and regulate the functional structure of reef communities (Bozec et al. 2015; Darling et al. 2017). However, structural dependency on branching corals has future implications for reef biodiversity given that this coral morphology is more susceptible to bleaching (Welle et al. 2017; Magel et al. 2019) and physical damage from storms (Scoffin 1993). In response to these and other global climate stressors (i.e., elevated sea surface temperatures, and altered sea water chemistry), many modern-day reefs have become degraded, and are now characterised by low structural complexity and biological diversity (Hoegh-Guldberg et al. 2007; Wild et al. 2011; Denis et al. 2017; Perry and Alvarez-Filip 2019).

A comprehensive method that evaluates reef structural complexity, health and function is the census based carbonate budget (Mallela and Perry 2007; Perry et al. 2008; Browne et al. 2013). This budgetary approach sums up sources of carbonate production (e.g., corals, crustose coralline algae, mollusc) and subtracts carbonate loss (e.g., mechanical, and biological erosion), to calculate the net weight of carbonate accumulation per area per year (kg m^{-2} yr^{-1}; Stearn and Scoffin 1977, Mallela and Perry 2007; Browne et al. 2013). A positive carbonate budget suggests that the reef is accreting and therefore maintaining some level of structural complexity and ecosystem stability (Perry and Alvarez-Filip 2019). In carbonate budget studies, reef structural complexity is represented by topographic complexity, or the reef surface roughness commonly referred to as reef rugosity (Dustan et al. 2013; Denis et al. 2017). Several equations used to calculate net carbonate

production using the budget approach incorporate rugosity as a scalar to account for the actual reef surface area (e.g., reef surface area (m^2) = planimetric area (m^2) x rugosity). Since rates of reef accretion or erosion are calculated per unit area, accurately measuring surface area is required for sound and comparable estimates of net carbonate production.

The most common method used to measure reef rugosity is the chain and tape method (CT), which has been used extensively since the 1970's (Risk 1972; Dahl 1973). This method consists of a diver laying a chain that closely follows the reef surface and divides the chain length by the horizontal distance covered (Risk 1972). Hence values of 1 indicate a flat terrain and higher values indicate more complex reef topographies (McClanahan and Shafir 1990; Friedman et al. 2012). However, this method is labour intensive, not easily repeatable and data is often spatially and temporally sparse (Friedman et al. 2012). More importantly, this method only provides a measure of complexity across a two-dimensional space and therefore, may not capture the true three-dimensional structure of the reef's surface (Dahl 1973, Friedman et al. 2012). Beyond *in situ* CT, new methods are rapidly developing that calculate rugosity from remotely sensed bathymetry.

Remote sensing methods for capturing reef rugosity allow for repeatable measurements over a large three-dimensional space (Friedman et al. 2012). Today, there are several methods available for quantifying reef rugosity remotely due to the increased accessibility of high-resolution bathymetric point cloud data (e.g., LiDAR). LiDAR data collection generates a point cloud, where point depth is calculated based on the return time of a laser beam (Brock et al. 2004, 2006; Wedding and Friedlander 2008). A bathymetric digital elevation model (DEM) can be made from this point cloud and be used to assess the scale of reef rugosity over a two or three-dimensional surface (Du Preez 2015). The resolution of a DEM refers to the horizontal pixel size, where a 1 m resolution DEM has a real pixel size of 1 m x 1 m, with one elevation value (derived from all points within that grid cell) assigned to each pixel. Remotely-derived DEM resolution in reef systems has varied from fine-scale 1 m (Brock et al. 2004; Du Preez 2015; Storlazzi et al. 2016; Hamylton and Mallela 2019), to broad scale > 400 m (Ferrari et al. 2018). The resolution dictates the scale of features that

can be resolved and in turn the scale of rugosity, with higher resolutions (<1 m) more likely to capture rugosity at the coral colony scale.

Several metrics have recently been developed for calculating rugosity from DEMs within common geospatial software (e.g., ESRI ArcGIS; Walbridge et al. 2018), including the arc-cord ratio (ACR) and surface area to planar area (SAPA) (descriptions of all rugosity methods and references are provided in Table 2.1). These methods quantify rugosity as ratios of surface topography to the area of an orthogonal projection onto a plane (expressed as surface indices comparable to the CT method; Dahl 1975) with 1 indicating flat terrain and rugosity increasing with larger values (Jenness 2004; Friedman et al. 2012; Du Preez 2015). Additionally, when using GIS software, a transect line can be placed across a DEM to measure a virtual CT value (VCT). Virtually calculating rugosity over georeferenced 3D bathymetry is a logistically simpler method for assessing rugosity over a greater spatial scale, with no *in situ* fieldwork causing little to no environmental impacts (Friedman et al. 2012). Due to these advantages, remotely sensed methods are increasing in popularity within fields of marine science (Zoffoli et al. 2014). However, remote sensing methods have only been applied in two of census based carbonate budget studies (supplementary table 2.1) and it is currently unclear how comparable these rugosity measures are to that of the CT method. If these methods are to be utilised in future carbonate budget studies, their ability to accurately capture reef rugosity needs to be assessed.

In this study, reef rugosity and coral carbonate production was assessed across two reefs located in Exmouth Gulf, Western Australia. Rugosity was measured *in situ* using the traditional CT method as well as from an airborne LiDAR-derived DEM (resolution of 0.1 m). We also collected benthic cover and coral composition data to calculate coral carbonate production following the census based carbonate budget approach (Stearn and Scoffin 1977; Mallela and Perry 2007). Specifically we: 1) calculated three LiDAR-derived measures of reef rugosity (VCT, ACR and SAPA) and compared these with measures using the CT method, 2) correlated changes in live coral cover and morphological composition (branching, foliose and massive) with reef rugosity to assess how different methods captured coral community scale topographic complexity, and 3) calculated hypothetical coral calcium carbonate

production rates to assess the impact of different rugosity methods on carbonate production calculations.

Table 2.1 Definitions of each method used for quantifying rugosity in this study. Please see cited studies for more detailed descriptions and visual representations of how rugosity measures are calculated from Digital Elevation Models

Method	***Acronym***	***Description***
Chain-and-Tape	CT	In-situ diver lays a chain that closely follows the reef surface and divides the chain length by the horizontal distance covered (Risk 1972).
Virtual Chain-and-Tape	VCT	Virtually calculated a CT value by drawing a transect line along a DEM and dividing the line distance by the surface area of the line (Storlazzi et al., 2016).
Surface Area to Planar Area	SAPA	Computes rugosity by using a 3x3 cell window (central cell and the eight surrounding) where a line from the centre of each surrounding cell links to the centre of the central cell. The resultant network of eight triangles makes a contorted area that is then divided by the cell window area as projected onto a plane of local slope. The rugosity equated for a selected surface area is the average value equated of all cells (Jenness et al, .2004; Walbridge et al., 2018).
Arc-chord Ratio	ARC	Similar to SAPA, ACR takes a contorted area of the surface, developed by creating a triangulated irregular network, and divides the sum of the triangle areas by the area of a surface orthogonally projected onto a plane of best fit, which is a function of the boundary data (Du Preez 2015).

2.3 Methods

2.3.1 Study Site

Exmouth Gulf is relatively shallow (mean depth ~11.9 m) with most of the seabed sediments characterised as shelly-muddy sands (Brunskill et al. 2001). Eva and Fly islands are low lying carbonate islands located off the eastern coast of the Gulf (Figure 2.1). Both islands are surrounded by similar reef systems, with shallow reef flats off the northern edge of the island, macro algae dominated sand bars off the

southern edge, and coral bommies scattered all around. The Gulf often experiences high turbidity primarily due to sediment resuspension from: (1) oceanic swells that propagate through the gap between Northwest Cape and South Murion Island and enter the Gulf from a north-west direction; (2) local wind-driven waves that form during periods of prevailing southerly winds; and (3) net tidal currents that flow in a south-westward direction at up to 1 m s^{-1} and tend to circulate in a clockwise direction around the Gulf (Dufois et al. 2017). Reefs situated in the Gulf are therefore naturally turbid reef systems and are dominated by sediment tolerant coral species (e.g., *Turbinaria, Goniastrea, Porites*). The region is also highly prone to cyclones (13 cyclones making landfall or impacting the region in the last 10 years) that often produce large waves (~5 m on average;) and storm surge of several metres or more (Nott and Hubbert 2005). Overall, the north-western to north-eastern sides of the reefs experience higher wave energies and the reefs on the southern sides experience lower wave energies.

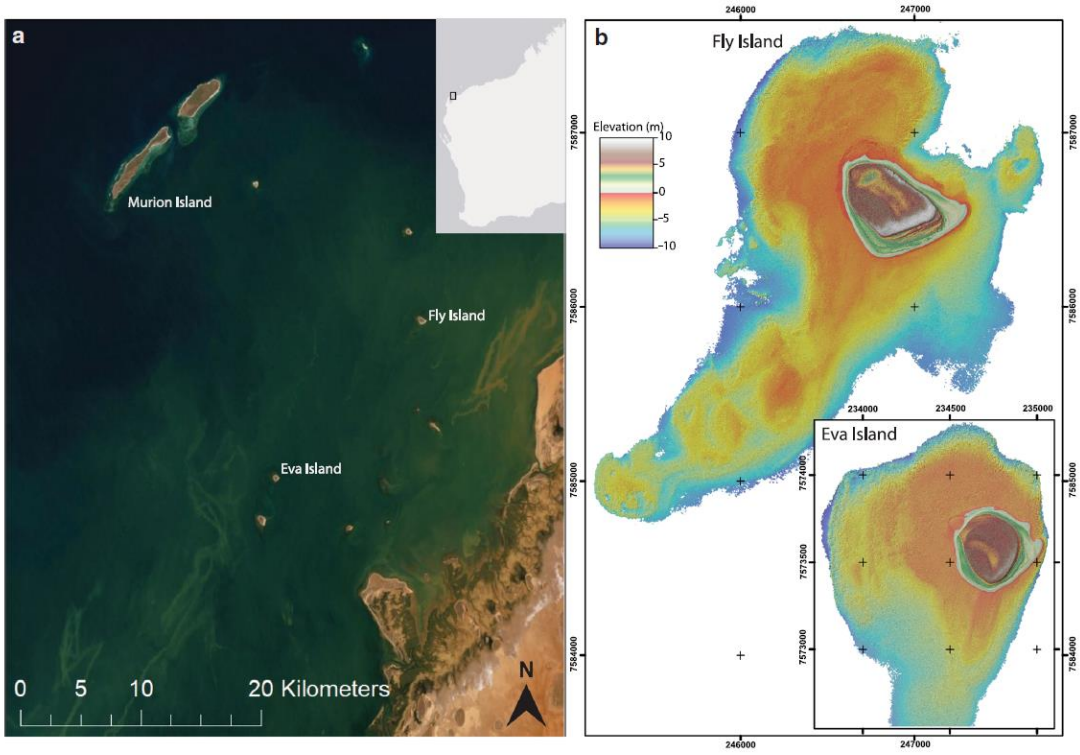

Figure 2.1 a) shows satellite imagery of the north-east coast of Exmouth Gulf where Eva and Fly islands are located and where they are situated in relation to the West Australian coast (in grey). b) displays the raw LiDAR DEM of both islands and their surrounding reef networks, from the shallow reef flats highlighted in red and orange, to the shallow reef crest at - 5 m displayed in light blue, and the deeper drop off shown in dark blue

2.3.2 Data collection

Fifteen, 20 m-long shore parallel permanent line transects were laid around each island's reef between 1-4 m depth. Transects were stratified into low (south) and high (north) wave energy sites as well as nearshore and offshore to capture the variety of benthic habitats (e.g., reef flat, reef crest and slope, macro algae/seagrass, and sandy bottom) that surround the islands. Along each transect, photos were taken every two seconds (<1 m apart) by a diver (approximately 1 m above seabed), totalling approximately 20 photos per transect. These photographs (capturing an area of approximately 2 m^2) were used to assess benthic habitat and coral community using Coral Point Count software (CPCe, Kohler and Gill 2006). Within CPCe, each photo was overlaid with 100 random points that were used to classify the benthos into either coral, macro algae (kelp or seagrass), turfing algae (predominantly growing on dead coral), sandy bottom, rubble, sponge, crustose coralline algae (CCA), or pavement (rock). Corals were classified into morphological groupings and identified to genus level. Following benthic identification, the marine habitats surrounding each island were sectioned into five 'zones' for spatial analysis and coral carbonate production calculations. Reef zones include north windward forereef (NWF), east leeward crest (ELC), southern leeward lagoon (SLL), southern windward sandbar (SWS), and western windward forereef (WWF). *In situ* CT rugosity measurements were taken at the start and 10m point of each transect with a six-meter-long chain (links were 5 mm wide and 15 mm long).

Airborne LiDAR data was collected by Airborne Research Australia (ARA) using two LiDAR systems (Riegl Q680i-S (topographic) and a Riegl VQ-820-G (topo-bathymetric) mounted to a light aircraft. For the Riegl Q680i-S, the laser pulse repetition rate was set to 400 kHz, and for the VQ-820-G to 284 kHz. The Riegl VQ-820-G topo-bathymetric green (532nm) laser LiDAR system uses a rotating multi-facet mirror with the scan axis tilted by ~20° with respect to the nominal flight direction so that the angle of incidence of the laser beam to the water surface varies by ~1° over the entire scan range of up to 60°. This results in an arc-like scan pattern on the seafloor. Refraction correction has to be applied when the laser beams pass from the air into the water. To handle target situations with complex multiple echo

signals, the VQ-820-G gives access to detailed target parameters by digitizing the echo signal by performing online waveform processing.

All elevations were referenced to the Australian height datum (approximately mean sea level). The point cloud density averaged 10-25 points per square metre depending on flight line overlap and water depth. The subsequent point clouds were post-processed using RapidLasso's LAStools (Isenburg, 2014). The LASnoise utility was used to denoise point clouds as well as remove false returns and other non-ground features. The LASground utility was used to clarify the point cloud with the 'last return' used to identify ground points as it avoids interference from objects floating on the water's surface and/or in the water column; only ground-classed returns were retained for analysis. Overlapping flight-lines within each sub-area were then strip-aligned using BayesMap's BayesStripAlign.exe utility (Version 2.09). All points below the waterline were corrected for refraction at the air-water boundary using ARA's LASrefract utility. Finally, the corrected point cloud was grid cell averaged to a 0.1 m resolution DEM in BlueMarble Graphics' Global Mapper (version 19).

The LiDAR data was used to calculate three measures of remoting sensed reef rugosity (VCT, ACR, SAPA). Rugosity values using the VCT were determined by plotting the GPS co-ordinates of the start and finish of the *in situ* line transects onto the DEM in ArcMap10. The VCT ratio line surface analysis was then overlayed across these points. For three-dimensional analysis (ACR, SAPA), a 2-meter-wide belt transect area was used (1 meter each side) along the 20 m permanent line transects. Rugosity along each 2x20 m belt transect was assessed using the ACR and SAPA extensions of the Benthic Terrain Modeller application within ArcMap10.

2.3.3 Statistical Analysis

To compare reef rugosity values derived from the CT and remote methods a correlation matrix was created using Spearman's rank correlation (for non- normally distributed data) in R (Hmisc package; Harrell Jr 2015). Rugosity values were also correlated with total coral cover (%) as well as the total percentage of foliose, branching and massive corals to identify the method that best captured fine-scale changes in relief (e.g., due to branching corals) and rapid changes in benthos height

(e.g., due to massive species). To examine the effect of rugosity methods on estimating carbonate production, we calculated gross coral carbonate production (kg m^{-2} yr^{-1}) across all zones of both reefs. Production was calculated using coral cover, coral species calcification rates from the literature and measured rugosity values (Browne et al., 2013; Table 2.2 and 2.3). Calcification rates used here had previously been measured on comparable reef types (e.g., inshore Great Barrier Reef; Browne et al. 2012).

Table 2.2 Calcification rates found in the literature based on turbid reefs or reefs within the Indian Ocean for coral genus found at the study site. These rates were used to calculate primary carbonate production

Morphology	Genus	Density (g cm^{-3})	Extension rate (mm yr^{-1})	Calcification Rate (g cm^{-2} yr^{-1})	Source
Branching	*Acropora*	1.0	63.0	6.3	Browne 2012
	Pocillopora	1.4	26.0	6.0	Tortolero-Langarica et al. 2016
Foliose/plate	*Turbinaria*	1.3	10.5	3.8	Browne 2012
	Montipora	0.9	29.0	1.5	Browne 2012
	Pavona	1.4	17.7	2.0	Wellington and Glynn 1983
Massive	*Porites*	1.3	13.4	1.7	Lough and Barnes 2000
	Goniopora	1.3	13.4	1.72	Highsmith 1979
	Favites	1.2	8.2	1.1	Highsmith 1979
	Platygyra	1.2	8.8	1.7	Weber and White 1974

Table 2.3 Equations to calculate coral carbonate production

Variable	*Symbol*	*Units*	*Equation*
Zone habitat surface area	A	m^2	Planimetric area (m^2) x **rugosity**
Coral carbonate production	CCP	kg yr^{-1}	Coral cover (%) x A x calcification rate (kg m^{-2} yr^{-1})
Gross coral carbonate production	Gcor	kg yr^{-1}	$\sum$ CCP
Normalised coral carbonate production rate	GcorN	kg m^{-2} yr^{-1}	Gcor / planimetric area (m^2)

2.4 Results

2.4.1 Reef habitat

Reefs surrounding Eva and Fly Islands were characterised by similar coral assemblages and habitat. Off the north edge of both islands are reef crests with higher levels of rugosity (CT rugosity = 1.6-2) and coral cover (approx. 23% at both reefs). Eva reef has marginally higher average coral cover over the entire reef (10% compared to 8% at Fly). Massive (Eva = 4%, Fly = 4%) and foliose corals (Eva = 4%, Fly = 3%) dominate the coral assemblage at both reefs, with only 2% and 1% branching coral cover at Eva and Fly reefs, respectively.

2.4.2 Rugosity method comparison

Rugosity values measured using the traditional CT method varied between 1.33 to 1.57 across Eva reef, and 1.04 to 2.14 across Fly reef (Table 2.4). Zones with the highest coral cover (approximately 23% at Eva NWF and Fly ELC) showed similar average CT rugosity values (1.57 at Eva and 1.65 at Fly). Across both reefs, VCT and SAPA rugosity values ranged from 1.00 to 1.10, whereas rugosity values at all but three transects calculated using the ACR method were 1.00, suggesting the reef topography at Eva and Fly was completely flat (Table 2.4).

A correlation matrix was used to compare the different methods for estimating rugosity values (Figure 2.2). CT was significantly correlated with SAPA measures ($r = 0.43$, $p = 0.02$), but not with ACR ($r = 0.26$, $p = 0.17$) or VCT ($r = 0.15$, $p = 0.43$). The only significant correlation between the remotely sensed methods was between VCT and ACR ($r = 0.37$, $p = 0.04$). The CT method was the only measure of rugosity that had a strong positive relationship with total coral cover ($r = 0.72$, $p<0.01$; Figure 2.2). This correlation appears to be driven by foliose ($r = 0.58$, $p<0.01$) and massive ($r = 0.94$, $p<0.01$) coral coverage. SAPA measures were correlated with total coral cover ($r = 0.46$, $p = 0.01$), foliose corals ($r = 0.38$, $p = 0.04$), and, most strongly, branching coral cover ($r = 0.47$, $p = 0.01$). In contrast, ACR and VCT were not significantly correlated with any of form of coral cover.

Average gross coral carbonate production rates calculated using the CT method (Eva=3.8$\pm$1.9, Fly=2.9$\pm$1.3 kg m^{-2} yr^{-1}) were approximately 30% greater than rates

produced using the VCT, ACR and SAPA methods (Table 2.4). The remote methods all produced similar estimates ranging from 2.6 to 2.8 kg m^{-2} yr^{-1} for Eva reef and 1.8 to 1.9 kg m^{-2} yr^{-1} for Fly reef.

Table 2.4 Average rugosity values of each zone for each method with ± standard error. Average reef coral carbonate production rates (GcorN; kg m^{-2} yr^{-1}) are also provided for each method ± standard error in bold.

Zone	*Coral Cover (%)*	*CT*	*SAPA*	*ACR*	*VCT*
Eva West (WWF)	3	1.43 ± 0.07	1.06 ± 0.01	1.00 ± 0.00	1.05 ± 0.01
Eva North (NWF)	23	1.57 ± 0.27	1.07 ± 0.03	1.01 ± 0.01	1.10 ± 0.04
Eva East (ELC)	11	1.45 ± 0.05	1.09 ± 0.04	1.01± 0.01	1.08 ± 0.00
Eva South (SWS)	2	1.33 ± 0.11	1.03 ± 0.00	1.00 ± 0.00	1.01 ± 0.00
Eva S. Lagoon (SLL)	6	1.42 ± 0.01	1.04 ± 0.01	1.00 ± 0.00	1.02 ± 0.01
Carbonate production		**3.8 ± 1.9**	**2.8 ± 1.3**	**2.6 ± 1.2**	**2.8 ± 1.3**
Fly West (WWF)	1	2.15 ± 0.67	1.04 ± 0.00	1.00 ± 0.00	1.05 ± 0.02
Fly North (NWF)	6	1.47 ± 0.28	1.05 ± 0.02	1.00 ± 0.00	1.02 ± 0.00
Fly East (ELC)	23	1.65 ± 0.14	1.05 ± 0.01	1.00 ± 0.00	1.04 ± 0.02
Fly South (SWS)	0	1.15 ± 0.04	1.05 ± 0.02	1.00 ± 0.00	1.04 ± 0.02
Fly S. Lagoon (SLL)	1	1.04 ± 0.03	1.03 ± 0.01	1.00 ± 0.01	1.06 ± 0.03
Carbonate production		**2.9 ± 1.5**	**1.9 ± 0.9**	**1.8 ± 0.9**	**1.9 ± 1.0**

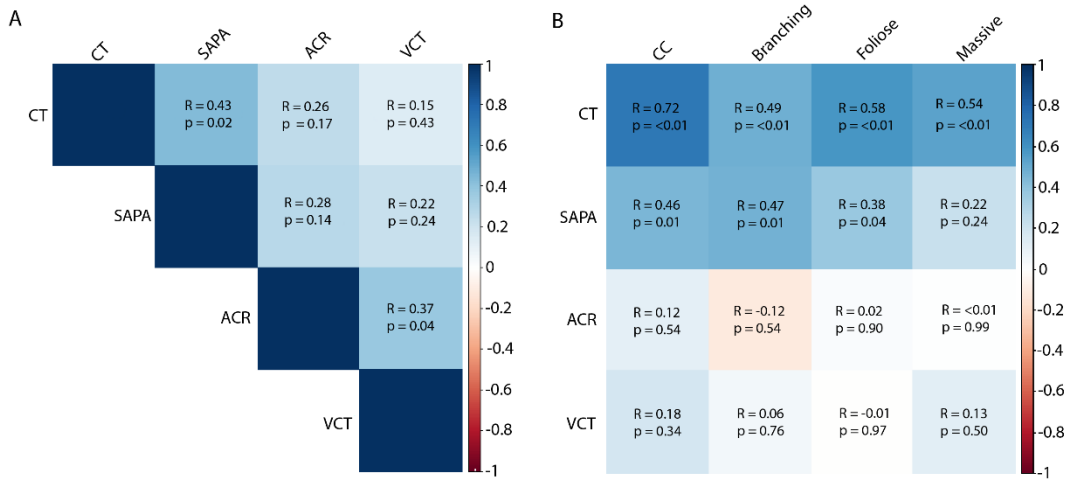

Figure 2.2 Visual plots displaying strength of correlations of rugosity measures between different methods (a) as well as correlations between rugosity measures of each method with total coral cover, as well as cover of three key coral morphologies: branching, foliose, and massive (b)

2.5 Discussion

Here we highlight the significant difference in reef rugosity measurements between traditional CT and remote data collection methods. This has important implications for assessing how reef topographic complexity varies over time, and for assessments of reef health (e.g., carbonate budgets) that rely on accurate rugosity data. CT-derived rugosities at both Eva and Fly were typical for a turbid reef environment. Average rugosity values ranged from 1.4 to 1.5 and are comparable to those measured on turbid inshore reefs of the Great Barrier Reef (1.2 to 1.3; Browne et al. 2013) and turbid sites off the coast of Tanzania (1.2 to 1.5; Herrán et al. 2017). In contrast, rugosity values calculated from LiDAR (using a 0.1 m resolution DEM) ranged from 1.00 to 1.10.

Estimates of rugosity from remote sensing at Eva and Fly reef were comparable to previous assessments that also used high resolution DEMs. For example, a recent carbonate budget study by Hamylton and Mallela (2019) in the clear water Cocos (Keeling) employed the use of SAPA rugosity analysis over reef zones using ground-truthed satellite imagery at 1 m resolution. Average rugosity across the zones was low (average of 1.15), similar to measures recorded in this study. Similarly, LiDAR coupled with SAPA analysis has previously been used by Brock et al. (2004) across Florida reefs where rugosity values ranged from 1.01-1.10 using a 1 m resolution DEM. Storlazzi (2016) also recorded low values of rugosity using SAPA with LiDAR (1 m resolution) and sonar data (0.1 m resolution), with average findings of 1.00 and 1.05, respectively. Du Preez (2015) introduced the ACR method to correct for slope and provided case studies with rugosities between 1.00 and 1.02 when using LiDAR derived DEMs. These low rugosity values (with limited variability) would suggest that there is little to no reef rugosity across these reefs, and that they are essentially flat. This is not the case, at least, across sites within this study as evidenced from *in situ* visual observations of structurally complex reefs during habitat surveys (Figure 2.3). CT measures appeared to give a more accurate representation of varying reef rugosity across transect sites, while remote measures provide extremely low rugosity estimates across all sites.

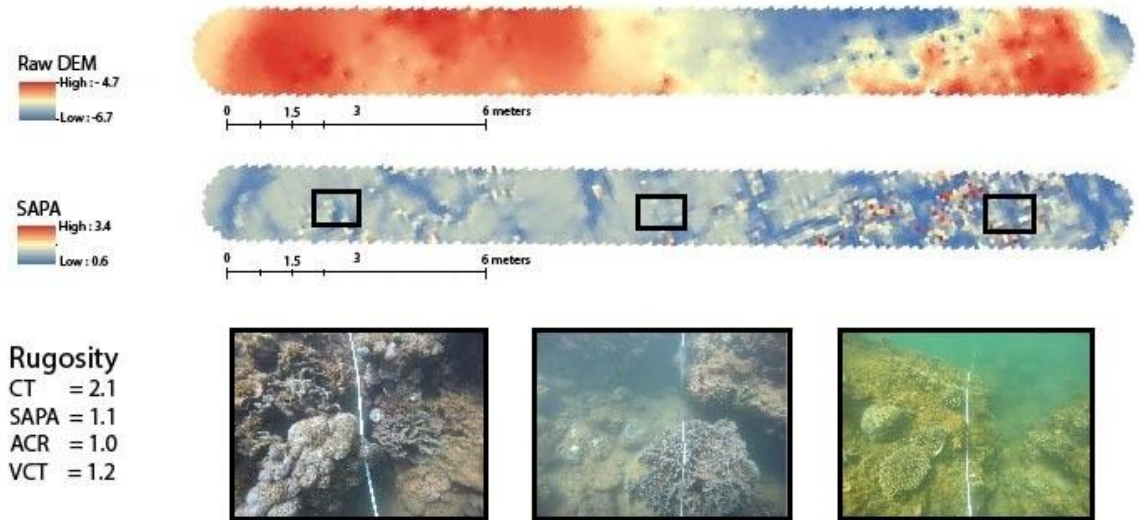

Figure 2.3 Comparison of raw DEM created from LiDAR data and SAPA analysis of the same line transect, as well as imagery of the reef substrate at different stages along the transect. Rugosity measures of this transect from the various methods are shown on the bottom left
uncommon

When compared to remote measures of rugosity, CT was found to be significantly positively correlated with the SAPA method, and no others. However, hypothetically, the CT and VCT should have been strongly correlated as they are both taking a two-dimensional measure of the same line transect. There are two explanations for this discrepancy. Firstly, it is unlikely that both two-dimensional methods were applied over exactly the same line transect. This is due to potential error in GPS readings of up to 5 m, meaning transects plotted on a DEM from *in situ* coordinates may be lying a few meters adjacent to where CT measurements were taken. Secondly, VCT was found to be poorly correlated with coral cover and did not recognise any coral morphology, whereas CT was strongly correlated to coral cover and all morphologies. Therefore, even if CT and VCT line transects were both measured over exact locations, CT measures will gather much more detailed rugosity measures. Additionally, SAPA rugosity values were the only remote measures that showed a positive correlation with coral cover, which appears to be driven by a strong correlation with branching coral cover (as opposed to the weak and insignificant correlation with massives). This explains the significant correlation found between SAPA and CT measures and illustrates the influence coral growth form on the ability of LiDAR derived methods to detect changes in benthic relief. For example, fine-scale changes in rugosity, or sudden vertical drops (typical over

massive corals) that characterise different growth morphologies are easily captured by the CT method, particularly when using chains with smaller link lengths (e.g., 2 mm; Knudby and LeDrew 2007). However, the remote methods tested here are unable to capture the full topographic complexity of the underwater reef structure in the same manner and thus underestimate reef rugosity. The reasons for this are both simple and complex but can generally be considered as limitations in LiDAR data collection and processing.

LiDAR data is derived from reflectance of a laser beam off subaerial or submerged structures. As the beam is shot from the aircraft it first passes through the atmosphere and *then* the water column before interacting with benthos at the seabed. Therefore, any large particle, bubble or even fish can result in high amplitude backscatter that may be recorded as a false seabed return. Automated de-noising algorithms work well where these false returns have a large separation distance from other clusters of points (representing the true seabed surface), but where false returns occur close to the seabed it becomes a challenge to accurately separate the actual seabed returns from in water column returns. This problem becomes more acute when surveying over very shallow waters < 0.5 m depth, which is not uncommon for reef flats. Similarly, despite advanced interactive filtering of the point cloud data, the actual seabed returns can be misinterpreted as water column returns and, when removed, can reduce the elevations (and rugosity) of the LiDAR point cloud. LiDAR data is often filtered using first and last return to distinguish ground- from non-ground returns in terrestrial applications; however, these approaches can be more problematic in marine applications. For marine applications, vertical point density-related algorithms and principles are required to identify the seafloor. In a complex coral environment, these methods will not always yield the 'true' seabed due to lack of vertical resolution of the returning waveforms. The situation becomes even more complicated if the benthos is dominated by macroalgae or seagrass. Together, these indicate LiDAR processing complications that reduce the ability of LiDAR data to accurately reflect *in situ* rugosity in coral reef environments.

It may be possible to define a scaling constant that corrects the LiDAR underestimation by comparing individual *in situ* CTs with analyses of the LiDAR-based SAPA along the same transect (though this was not the goal of this study).

This would provide a correction factor that can be applied to specific reef habitat types, (i.e., those dominated by branching or massive corals) and, importantly, allow much larger reef areas to be accurately measured for rugosity using bathymetric LiDAR. This would then promote rapid SAPA rugosity assessments of reefs using LiDAR data in an accurate and comparable manner suitable for fine-scale assessments of coral carbonate production and carbonate budget assessments. The magnitude of potential scaling offset can be seen from differences in carbonate production rates calculated for Eva and Fly reefs using CT and remote methods (Table 2.4).

Previous studies calculating carbonate production at similar turbid shallow island reef sites using CT have reported production rates of 1.8 kg m^{-2} yr^{-1} (turbid Jamaican reef; Mallela and Perry 2007), and 3.2 kg m^{-2} yr^{-1} (turbid island reef in Indonesia; Edinger et al. 2000). This study calculated similar CT derived carbonate production rates ranging from 2.9 $\pm$ 1.5 kg m^{-2} yr^{-1} (Fly) to 3.8 $\pm$ 1.9 kg m^{-2} yr^{-1} (Eva), with the average CT derived production rate approximately 30% higher than rates derived from remote sensing methods (which equates to an additional 1.2 kg m^{-2} yr^{-1}). Although this difference lies within the standard error associated with CT derived production rates, differences in averages of this magnitude may still have implications for reef status assessments (i.e., actively accreting and stable versus actively eroding and unstable). For example, these CT production rates would suggest that these reefs are actively accreting, whereas rates generated from remote sensing, were closer to production thresholds (<1 kg m^{-2} yr^{-1}) and may suggest these reefs are entering a state of diminished to no reef growth potential (Perry et al. 2013, 2014).

This study has shown that the CT method provides a more comparable and applicable measure of reef rugosity when considering carbonate budget calculations given the limitations of remote sensing when capturing fine-scale reef rugosity. However, protocols and precautions should be put in place to ensure consistent data collection between studies. The spatial heterogeneity of reef environments and subjectivity of chain placements along transects can result in significant variations in rugosity measurements. This can be controlled for by collecting data from a minimum number of measurements per reef determined by the size of the reef area,

as well as standardised chain length and link to ensure rugosity measures are more reliable and comparable. The use of remote sensing for carbonate budgets has the potential to improve reef wide assessments of rates of carbonate production and loss. However, until these methods improve in resolution and can be accurately scaled to an appropriate range, *in situ* CT rugosity continues to be a more appropriate and relevant method than remote sensing for rugosity estimates.

Postscript: The next chapter investigates the relative contribution to carbonate production that calcifying encrusting organisms have across Eva and Fly reefs. We also investigate seasonal and spatial variations in carbonate production and growth.

Chapter 3 Encrusters maintain stable carbonate production despite temperature anomalies among two inshore island reefs of the Pilbara, Western Australia

Preface: This chapter has been published in the peer-reviewed journal *Marine Environmental Research* (doi.org/10.1016/j.marenvres.2021.105386) and has been formatted according to journal guidelines. The combined references for all chapters can be found in the Cited Literature-section at the end of this thesis.

3.1 Abstract

Encrusting reef organisms such as crustose coralline algae (CCA), serpulid worms, bivalves, bryozoans, and foraminifera (collectively termed encrusters) provide essential ecosystem services and are a critical part of the reef framework. Globally, research into *in situ* growth and carbonate production of encrusters has focused on clear water fore-reef settings in the Pacific and Caribbean, with limited studies being conducted on marginal reef systems or within the Indian Ocean. Here we examined spatial and temporal variation in CCA coverage (%) and total encruster carbonate production rates (g cm^{-2} yr^{-1}) across two inshore turbid island reefs of northern Western Australia. We recorded average carbonate production rates of 0.039 ± 0.002 g cm^{-2} yr^{-1}, which are comparable to healthy reef sites globally. Our results show variation in lateral CCA cover over small spatial scales, with a strong seasonal signature, while constant average carbonate production rates were maintained. Additionally, we recorded *in situ* water temperatures above predicted coral bleaching threshold of 29°C for four weeks and found annual patterns of sea surface temperature anomalies (SSTA) of 2°C or more being a regular occurrence over the hotter months. Encrusters on these reefs are considered to have a vital contribution to the reef carbonate budgets, and if they maintain stable carbonate production through periods of SSTA, they may support net positive reef carbonate budgets.

3.2 Introduction

From the equator to the poles, crustose coralline algae (CCA) and other calcifying encrusting taxa such as serpulid worms, bivalves, bryozoans, and foraminifera (hereon referred to as encrusters), play a critical role in tropical and temperate reef ecosystems (Steneck, 1986). These organisms contribute to the construction and stabilisation of reef frameworks (Fabricius and De'ath, 2001; Rasser and Riegl, 2002), bind sedimentary particles (Rasser and Riegl, 2002), and add to reef systems' carbonate sediments (Perry, 2005; Yamano et al., 2005; Gischler, 2006). In particular, CCA provide additional ecosystem services through the provision of settlement substrate for invertebrates such as coral larvae (Heyward and Negri, 1999; Fabricius and De'ath, 2001; Mason et al., 2011; G´omez-Lemos et al., 2018). As such, CCA contribute to the reef carbonate budget directly, and also indirectly through enhanced coral recruitment, thereby facilitating both reef accretion and reef consolidation (Chisholm, 2003; Mason et al., 2011). However, like corals, CCA (and other encrusters) are vulnerable to impacts of climate change (Anthony et al., 2008; Kuffner et al., 2008; Martin and Gattuso, 2009; Diaz-Pulido et al., 2012), with declines in CCA expected to reduce coral larval recruitment rates (Webster et al., 2011; Doropoulos et al., 2012), and therefore, reef accretion.

Over the past three decades, *in situ* studies of CCA have covered a diverse range of topics including growth rates (Potin et al., 1990; Martin et al., 2006; Roik et al., 2016), carbonate production (Mallela, 2007, 2013; Morgan and Kench, 2014b, 2017; Chisholm, 2000), patterns of succession and accretion (Matsuda, 1989; Mariath et al., 2013), cover and dispersal across environmental gradients (Fabricius and De'ath, 2001; Dean et al., 2015), community structure (Lei et al., 2018), and competition (Belliveau and Paul, 2002; Steneck, 2011; Vermeij et al., 2011). These studies have primarily focused on clear water, shallow (<10 m) fore-reef environments of the Great Barrier Reef, the Caribbean, or the Mediterranean. In contrast, only three *in situ* studies have been undertaken within the Indian Ocean, with two based in the Maldives (Morgan and Kench, 2014b, 2017) and one from temperate Western Australia (Short et al., 2015). These Indian Ocean based studies investigated carbonate production rates by encruster (predominantly CCA) growth on artificial substrates, quantified by weight and/or extension rates. Morgan and Kench (2014b,

2017) studied tropical CCA growth and carbonate production on a clear-water reef over a year but did not assess the impacts of seasonality or environmental parameters on CCA. In contrast, Short (2015) assessed seasonal differences in temperate CCA carbonate production on a clear water reef following the 2010/2011 marine heatwave along the Western Australian coast and found CCA mortality due to thermal stress, but no seasonality in calcification rates. Short's findings contradict a multitude of studies that have recorded increased calcification with seasonal increases in water temperatures (Blake and Maggs, 2003; Martin et al., 2006; Kamenos and Law, 2010). Such contradictions show a paucity of knowledge on CCA responses to environmental fluctuations within a range of environmental settings (e.g., marginal reefs) where key influences of CCA growth may vary.

It is well established that temperature is a key driver of spatial and temporal growth and calcification of encrusters, particularly CCA (Adey and McKibbin, 1970; Kuffner et al., 2008; Hetzinger et al., 2013; Dean et al., 2015). Investigations of CCA physiology with changing temperatures (*in situ* and laboratory) have found higher growth rates during the warmer months (King and Schramm, 1982; Potin et al., 1990; Blake and Maggs, 2003; Martin and Gattuso, 2009). This is expected as warmer waters are more suitable for increased respiration rates (Martin et al., 2007) and photosynthesis (V´asquez-Elizondo and Enríquez, 2016; Vogel et al., 2016). However, exposure to temperatures outside of thermal limits are likely to reduce CCA growth rates and carbonate production (King and Schramm, 1982; Short et al., 2015; Roik et al., 2016; Cornwall et al., 2019; Anton et al., 2020), but at present CCA thresholds to rising temperatures remain ambiguous or largely unknown. This is further compounded by the fact that thermal thresholds may vary spatially and among species, adding further challenges to understanding the effects of thermal stress and temperature sensitivity on CCA and other encrusters.

Despite the recent increase in attention on the responses of CCA to environmental stressors over the last few decades, the number of studies is considerably less than that for corals. A meta-analysis of laboratory based CCA studies (Cornwall et al., 2019) found only 78 research papers on impacts of ocean acidification (OA) and 14 research papers on rising sea surface temperature (SST) effects (or interactions with OA) on CCA calcification. These studies have shown that OA tends to decrease

CCA carbonate production rates (Cornwall et al., 2018; Anthony et al., 2008; Kuffner et al., 2008), however, the response varies alongside synergistic interactions with other environmental variables (e.g., temperature, light, nutrients; Hofmann et al., 2014; Ordo˜nez et al., 2017; Celis-Pl´a et al., 2015; Comeau et al., 2019). Furthermore, as most previous research into the impacts of environmental stress on CCA growth and carbonate production have been conducted in a laboratory setting (e.g. Anthony et al., 2008; Martin and Gattuso, 2009; Cornwall et al., 2018), a better understanding of *in situ* response of CCA to changing environments is required. Doing so will facilitate the identification of CCA (and encruster) environmental thresholds and enable more accurate predictions of future reef stability and development.

Given there is currently little to no knowledge on *in situ* carbonate production rates and thermal thresholds of encrusters within the subtropical Eastern Indian Ocean, this study aimed to quantify rates of CCA carbonate production (g cm^{-2} yr^{-1}) and additional encrusting taxa for two inshore marginal island reefs of the Pilbara, Western Australia. Specifically, we: 1) provide the first encruster carbonate production rates for subtropical Western Australia and the Eastern Indian Ocean, 2) assess *in situ* spatial and temporal variations in CCA and encrusting community growth and carbonate production, and 3) identify key environmental and habitat characteristics associated with encruster cover and carbonate production. Finally, we discuss the level of importance encrusters play in the carbonate budgets of these marginal reef systems.

3.3 Methods

3.3.1 Study Site

This study was carried out across two inshore island reefs (Eva and Fly) located in Exmouth Gulf, which is situated at the southern end of the Pilbara coast. Eva reef (-21.918454◦, 114.433502◦), and Fly reef (-21.804829◦, 114.554003◦) have similar fringing reef morphology, coral cover (8–10%) and diversity (Shannon-Weiner index 0.73 and 0.76 respectively), and wave exposures (high exposure at northern reef

sites, with less wave energy experienced at southern sites; Cuttler et al., 2020; Chapter 2).

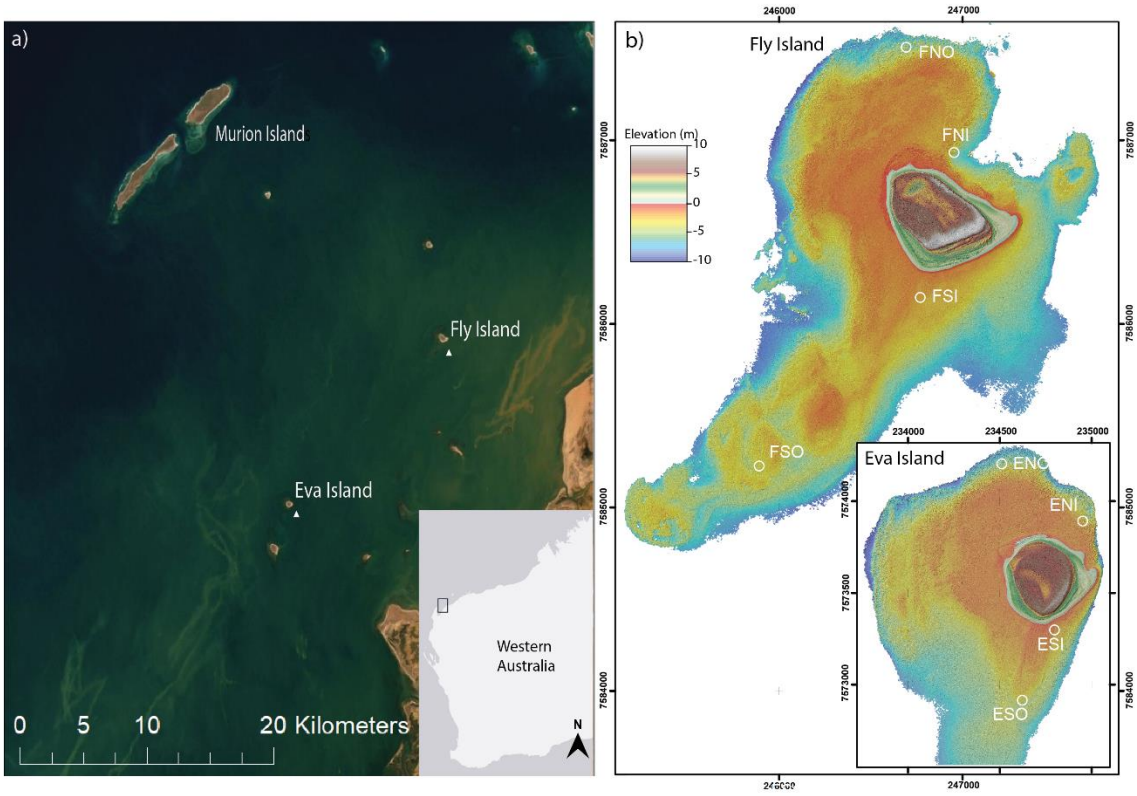

Figure 3.1 Location of Eva and Fly islands relative to each other with white triangles depicting where water quality was measured monthly; b) and the geomorphology of surrounding reefs, with white circles indicating the location of experimental tiles and *in situ* data loggers for light and temperature. Experimental tile locations at Eva were Eva north offshore (ENO), Eva north inshore (ENI), Eva south offshore (ESO), Eva south inshore (ESI); and at Fly were Fly north offshore (FNO), Fly north inshore (FNI), Fly south offshore (FSO), Fly south inshore (FSI)

The Pilbara has a dry arid climate, characterised by two main seasons: hot and humid summer, and mild winter (Leighton, 2004). Temperatures in the summer average between 36 and 37°C from November to April, with winter temperatures averaging 28–29°C from May to October. Rainfall is variable annually and is greatest during the summer and early autumn months due to tropical cyclones and storms (Leighton, 2004). In this study we focus on these two dominant seasons, and refer to the hot summer months between November and April as the "wet season", and cooler months between May and September as the "dry season".

Encruster growth experiments were set up at four locations per reef (Figure 3.1). These four sites consisted of two northern "exposed" sites (one offshore and one inshore) and two southern "protected" sites (one inshore and one offshore)

3.3.2 Encruster composition and carbonate production

To obtain encruster population characteristics and carbonate production rates, encruster growth tiles were deployed at four sites (two northern and two southern) at each of the two island reefs (**Error! Reference source not found.**). Encruster tiles were made of PVC (10 cm × 10 cm) as this material has previously been shown to produce consistent estimates of carbonate production and abundance representative of communities among adjacent reef substrate (Kennedy et al., 2017). Tiles were lightly sanded and weighed (to within 0.001 g) before deployment and fixed using a screw and stainless-steel plate onto limestone blocks, with the tile placed approximately 4 cm above the substrate. A total of 32 tiles per island were deployed in April 2019, with eight tiles at each of the four sites. Four tiles at each site were removed after the six-month dry season and replaced with four clean tiles to capture growth over the wet season. The remaining four tiles remained *in situ* for 12 months to provide annual encruster cover and carbonate production rates.

Once collected, tiles were placed into individually labelled sealable plastic bags and rinsed with distilled water in the laboratory to remove silt or debris. Tiles were then dried for 24 hours at 50°C before both sides were photographed. Community composition was determined by overlaying 200 random points across each image using the Coral Point Count software (CPCe; Kohler and Gill, 2006). A 1cm border was placed around the tile perimeter to discount any edge effect (Mallela, 2007), and encrusting organisms (CCA, serpulids, bryozoan, coral, bivalve, foraminifera) under each point were identified to the lowest taxonomic group possible (Mallela, 2007, 2013; Browne et al., 2013).

Carbonate production rates by encrusting species were calculated by measuring the weight of calcium carbonate deposited on the tiles over the experimental period. Tiles were treated with a 5% solution of sodium hypochlorite (NaClO) for 24 h to remove organic tissue, leaving carbonate deposits intact. After rinsing in distilled water, tiles were dried at 50°C for 24 hours. Each tile was weighed and then placed

in a dilute (10%) solution of hydrochloric acid (HCl) to dissolve all calcium carbonate. Tiles were again rinsed, dried and reweighed. Carbonate production (g cm^{-2} yr^{-1}) was calculated as the total mass (g) of carbonate accretion (initial weight minus end weight), divided by the deployment duration (days) and surface area of the tile (cm), then multiplied by 365 days to provide annual rates (Mallela, 2007). Calcification rates by encrusters across Eva and Fly reefs were calculated based on net rates of carbonate production, and the proportion of reef area (m^2) available for encruster growth derived from census based benthic surveys (see Chapter 2).

3.3.3 Environment and water quality

Monthly water quality data (chlorophyll-a, conductivity, salinity, pH, turbidity) was also collected offshore of each reef (**Error! Reference source not found.**) during neap tides between February 2019 and February 2020 (12 months). *In situ* sampling was undertaken using a vertical profiling method with a multi-parameter EXO Sonde 2 (YSI Inc./Xylem Inc.). The Sonde was set to continuous mode, with data logging at 1 Hz. Profiles were obtained by manually lowering the instrument from the surface to the bottom of the water column, and the average value through the profile (minus the top and bottom meter to capture the mid-water column) was used for each water quality parameter.

During periods of tile deployment, temperature loggers (°C; Hobo Pendant UA-001-64) and photosynthetic active radiation (PAR) loggers (µmol photons m^{-2} s^{-1}; Odyssey submersible PAR logger) were deployed at each site with logging intervals of 60 min for benthic temperature and 10 min for PAR loggers. Sea surface temperature (SST) and anomaly (SSTA) data were obtained from the NOAA Coral Reef Watch (CRW) daily global 5 km satellite coral bleaching heat stress monitoring product suite Version 3.1 (https://coralreefwatch.noaa.gov/pro duct/5km/, Liu et al., 2014) to provide insight into long term SST conditions across the study sites (where SSTA data was established from long term SST averages from 1984 to 2012). Reef benthic habitat data used in this study was collected using line intercept transects across both reefs in September 2018 (method details are described in Chapter 2).

3.3.4 Statistical analysis

Prior to statistical analysis, carbonate production rate data was square-root transformed to meet assumptions of normal distribution (Shapiro-wilks test) and equality of variance (Levene test). Unfortunately, CCA cover could not be transformed to meet parametric assumptions and were analysed using non-parametric methods. Analysis was then conducted using encrusting carbonate production rates and lateral CCA cover data, as CCA dominated the encrusting community. We performed Spearman's correlation analysis (confidence level = 0.95) between carbonate production rates and lateral CCA cover to determine if the lateral cover of CCA was the primary contributor to carbonate production rates.

For each reef, data from the two southern deployment sites were pooled to represent the "southern zone" of the reef, and the same was done for the two northern sites. This resulted in a two layer nested design where zone (north or south) was nested within the factor of reef (Eva or Fly). Annual carbonate production rates and lateral CCA cover from tiles deployed over 12 months were used to assess spatial variability among reef zones, with tiles deployed over wet and dry seasons used to assess temporal variability. Three-way analysis of variance (ANOVA) was used to test the effects of season, reef, and zone on carbonate production rates. Non-parametric Kruskal-Wallis (KW) test was employed to test for variation in lateral CCA cover between spatial levels (reef, zone) and seasons, with a multiple-comparisons Bonferroni correction of $p \leq 0.0167$ to control for multiple tests. Any significant results of KW test for factors with more than two levels were followed by a post-hoc Dunn's test to investigate the source of variance.

Principal Component Analysis (PCA) was used to identify key environmental variables and reef habitat data (spatial only) that were associated with sites depending on the reef (Eva, Fly), or the reef zone (north, south). In addition, we carried out Distance Based Linear Modelling (DistLM, PERMANOVA) to identify key environmental and habitat variables related to both spatial and temporal variations in CCA cover and carbonate production rates. CCA cover and encrusting carbonate production rates were square-root transformed, and resemblance matrices were calculated using the Bray Curtis similarity index. Water quality and habitat data were normalised and DistLM models were determined using the 'Best' procedure

and Akaike information criterion (AIC) selection criterion with 9999 permutations. DistLM analysis was implemented in Primer7 software (version. 7.0.13), with all other analyses performed in RStudio (version 1.1.463) using the vegan (Oksanen et al., 2019), ggplot2 (Wickham, 2011), and Dunn's test (Dinno 2017) packages.

3.4 Results

3.4.1 Carbonate production and encruster cover

On average, encrusters covered 77 ± 4.9% and 64 ± 5.0% of the PVC tile surface area at Eva and Fly reefs, respectively. Across both reefs, CCA was the dominant encrusting organism with cover ranging from 37 to 95% (of encrusting cover; 72% mean) of the tile surface. Other encrusters found on the tiles, but in smaller quantities included bryozoans (mean cover = 1.2%), serpulids (mean cover = 0.9%) and coral recruits (mean cover = 0.8%). CCA cover and carbonate production rates were positively correlated across all deployment periods, with more than 50% of the variation in CCA cover correlated to carbonate production rates (Dry season: R = 0.53, p = 0.005; Wet season: R = 0.50, p = 0.018; Annual: R = 0.61, p = 0.002; Figure 3.2). The data also revealed variability between these two parameters, whereby high CCA cover does not always equate to higher carbonate production.

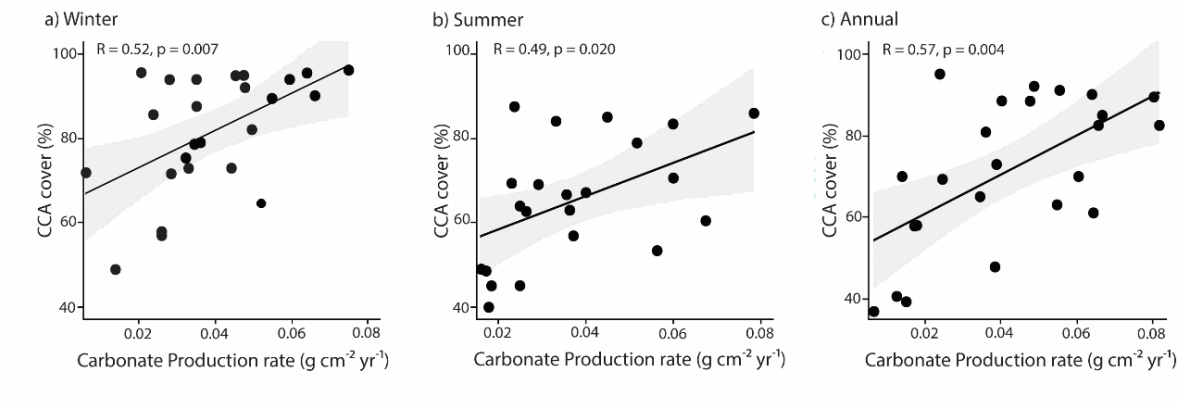

Figure 3.2 Spearman rank correlation between CCA tile coverage (%) and encruster carbonate production rates (g $cm^{-1}yr^{-1}$) from a) dry season deployment, b) wet season deployment, and c) Annual deployment periods. All results are significant at confidence interval 95%

Table 3.1 Three-way analysis of variance (ANOVA) to test for effects of season, reef, and zone on rates of carbonate production from encrusting taxa on settlement tiles. Significant values are presented in bold text.

	df	*ms*	*F value*	*p value*
Season	1	0.000	0.021	0.885
Reef	1	0.007	4.350	0.040
Zone	1	0.032	18.743	**4.51 e-05**
Season: Reef	1	0.001	0.427	0.515
Season: Zone	1	0.000	0.126	0.724
Reef: Zone	1	0.019	10.969	**0.001**
Season: Reef: Zone	1	0.009	5.058	**0.027**
Residuals	76	0.002		

Table 3.2 a) non-parametric Kruskal-Wallis test to show variation in CCA lateral cover between reefs, zones, and seasons with a multiple-comparisons Bonferroni correction of 0.0167 applied. Post-hoc Dunn's test (Bonferroni method) was caried out to investigate variation in b) reef specific zones and c) seasons.

	Chi-square	*df*	*p-value*
a)			
Reef	3.533	1	0.060
Zone	24.585	1	**8.32e-07**
Season	9.25	2	**0.010**
b)			
	Eva S - Eva N	*Eva S - Fly S*	*Eva N - Fly S*
Z	-4.079	1.361	5.117
p-value	**0.000**	0.521	**0.000**
	Eva S - Fly N	*Eva N - Fly N*	*Fly S - Fly N*
Z	-2.066	2.147	-3.275
p-value	0.117	0.096	**0.003**
c)			
	Dry-Wet	*Dry- Annual*	*Wet- Annual*
Z	3.745	2.459	-1.322
p-value	**0.000**	**0.021**	0.279

Annual average carbonate production rates ranged from 0.024 to 0.062 g cm^{-2} yr^{-1} (mean = 0.039 ± 0.002 g cm^{-2} yr^{-1}) and varied between reefs (Eva = 0.042 ± 0.003 g cm^{-2} yr^{-1}, Fly = 0.035 ± 0.003 g cm^{-2} yr^{-1}, F = 4.350 p = 0.040, Figure 3.3a). This equates to annual carbonate production rates of 0.436 ± 0.029 and 0.329 ± 0.044 kg

m^{-2} yr^{-1} at Eva and Fly reefs, respectively. There was a significant interaction effect between factors reef and zone (F = 10.969, p =0.001, Table 3.1) on encruster carbonate production, with the highest carbonate production rates in the northern zone of Eva reef (average = 0.056 ± 0.003 g cm^{-2} yr^{-1}). Although annual CCA cover was more than 10% higher at Eva reef (Eva = 77%, Fly 64%) there was no statistically significant variation in CCA cover between reefs (H = 3.533, p = 0.060, Table 3.2 Figure 3.3 b). There was, however, a significant variation in CCA coverage between zones (H = 24.585, p = 8.32e-07), with post-hoc tests identifying significantly higher CCA coverage at the northern zones at both reefs (Figure 3.3; Table 3.2b).

Patterns in seasonal encruster carbonate production were not consistent both between reefs, and zone (F = 5.058, p = 0.027; Table 3.1). For example, highest rates were recorded on annual tiles at Eva north, whereas highest rates during the dry season were recorded on tiles at Eva south, and wet season tiles at Fly south (Figure 3.3a). In contrast, lateral cover of CCA was consistently higher in the dry season compared to the wet season across all locations (Dunn's test p = <0.001, Table 3.2c, Figure 3.3b). Given annual tiles were deployed for twice as long as seasonal tiles, it was interesting to see the average cover of CCA on annual tiles (total average = 72 ± 3.7%) was only 6% greater than that of wet season tiles (total average = 65 ± 3.1%), and 16% lower than dry season tiles (total average = 81.1 ± 2.7%, Dunn's test p = 0.021).

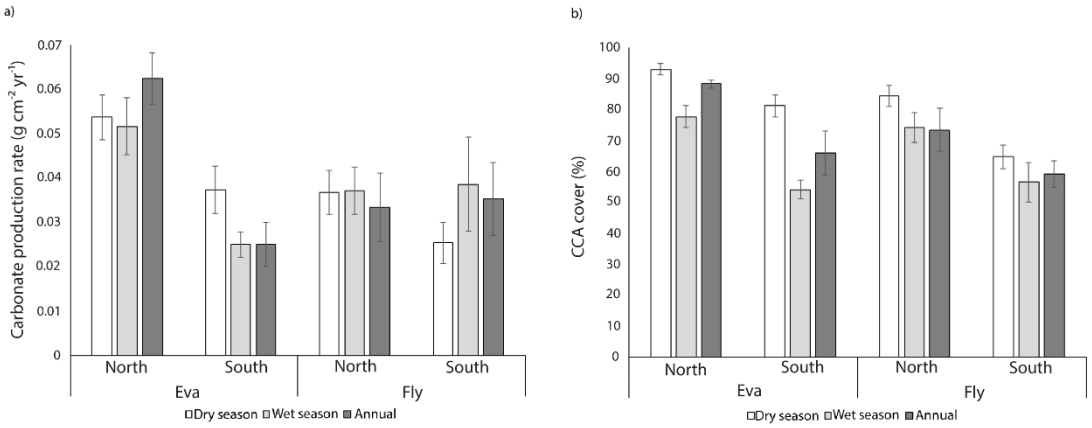

Figure 3.3 a) Carbonate production rates (g cm^{-2} yr^{-1}) across the four zones (Eva north, Eva south, Fly north, Fly south) between the two reefs (Eva and Fly) during the dry season (April-September), the wet season (October-March) and annually. b) Lateral coverage of CCA across each of the four zones during the dry and wet seasons, as well as annual coverage.

3.4.2 Environmental influence on spatial variation of carbonate production and lateral CCA cover

Annual averages in environmental and habitat data at each of the four zones were used to identify key environmental parameters that were associated with spatial differences in carbonate production rates and lateral CCA cover. Average water temperatures taken at the benthos were comparable between reefs (Fly 24.9 ± 0.02 °C; Eva 24.8 ± 0.02 °C), as was salinity (Fly mean = 38.16 ± 0.42 psμ; Eva mean = 38.34 ± 0.46 psμ), and conductivity (Fly mean = 57149 ± 982 μS/cm; Eva mean = 57150 ± 965 μS/cm; Supplementary table 3). However, Fly reef experienced nearly 50% higher turbidity levels (Fly mean = 2.27 ± 0.36 FNU; Eva mean = 1.48 ± 0.33 FNU), as well as slightly higher chlorophyll-a (Fly mean = 0.49 ± 0.05 μg. L^{-1}; Eva mean = 0.38 ± 0.05 μg. L^{-1}) and pH (Fly mean = 8.19 ± 0.03; Eva mean = 8.17 ± 0.01; Figure 3.4a, Supplementary Table 3). Whereas Eva was exposed to higher levels of light (Fly mean = 177.52 ± 1.73 μmol photons m^{-2} s^{-1}; Eva mean = 228.06 ± 2.38 μmol photons m^{-2} s^{-1}; Figure 3.4Figure 3.5). In addition, benthic temperatures were comparable between reef zones (north = 24.95 ± 0.02 ◦C, south = 24.92 ± 0.02 °C), whereas light was typically higher in the southern zones (north = 124.63 ± 1.59 μmol photons m^{-2} s^{-1}, south = 220.95 ± 2.50 μmol photons m^{-2} s^{-1}; Figure 3.4Figure 3.5).

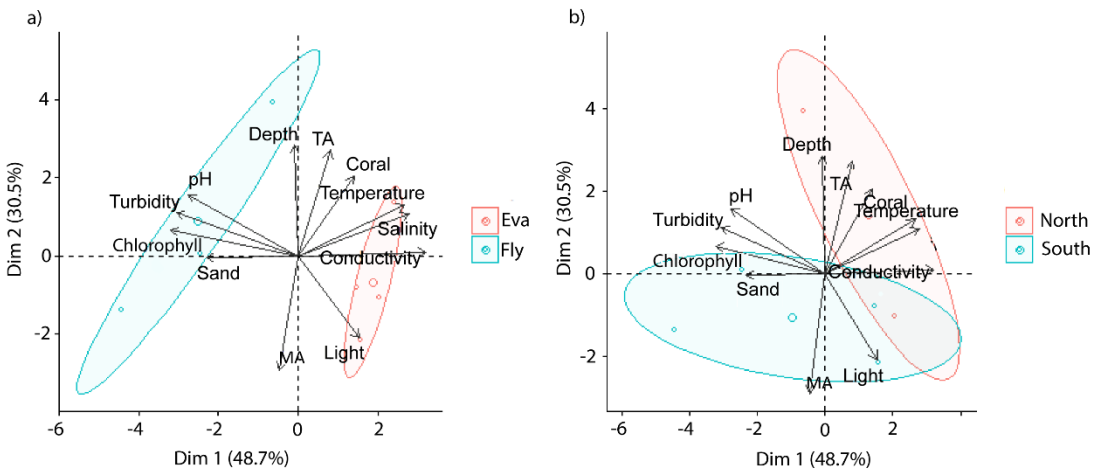

Figure 3.4 Principle component analysis (PCA) of environmental and habitat variables between reefs (a), and between reef zones (b). The x-axis is the first principal component, and the y-axis is the second principal component. MA = Macroalgae, TA = turfing algae

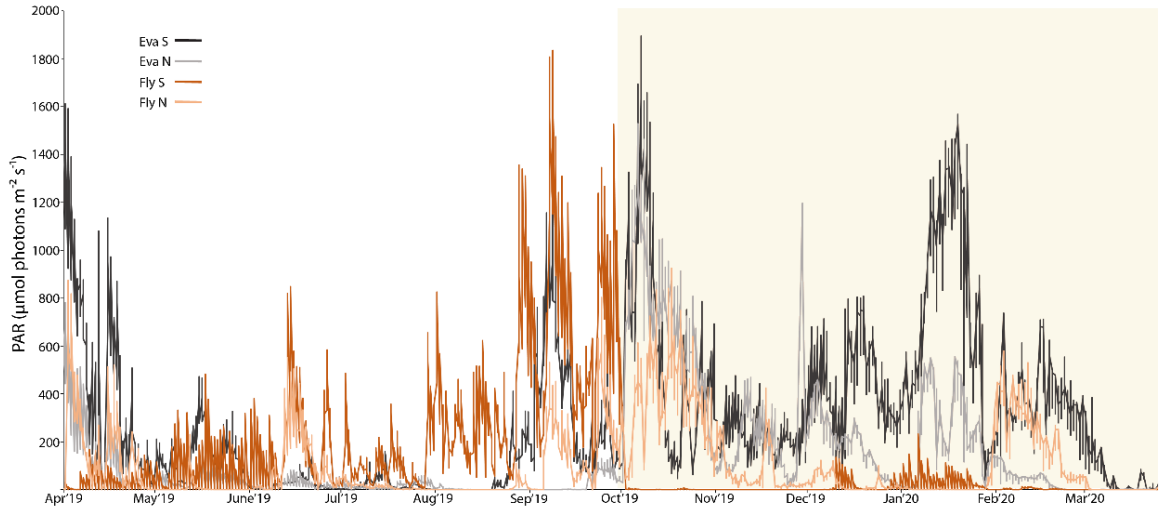

Figure 3.5 Light levels collected by photosynthetic active radiation (PAR) loggers at the benthos during encruster growth at north and southern sites at each reef between April 2019–April 2020. Loggers were changed out in early October 2019 at the beginning of the wet season, which is shaded in orange.

Table 3.3 Distance based linear modelling (DistLM) of spatial environmental and habitat data considering a) carbonate production rates (g cm^{-2} yr^{-1}) and b) lateral CCA cover (%) on experimental tiles. The model with the lowest AIC values was selected (in bold).

AIC	R^2	*RSS*	*No.Vars*	*Selections*
a)				
121.44	**0.61**	**2294**	**5**	**Light, Coral, Macroalgae, Turfing Algae, Sand**
121.74	0.61	2323	6	Temp, Chlorophyll, Turbidity, Salinity, Coral, Sand
122.10	0.56	2563	4	Temperature, Light, Salinity, Sand
b)				
89.10	**0.43**	**648**	**4**	**Temp, Light, Salinity, Sand**
89.12	0.43	649	4	Temp, Salinity, Turfing Algae, Sand
90.39	0.45	629	5	Light, Coral, Macroalgae, Turfing Algae, Sand

Benthic cover was comparable between reefs with similar coral cover (8% at Fly, 10% at Eva) and fleshy algal cover dominating the benthos (macro-algae = 35% at Fly, 56% at Eva; turfing algae = 15% at Fly and 16% at Eva; Chapter 2). However, there were distinct differences in benthic cover between south and north reef zones (Figure 3.4b, Supplementary table 2). Southern zones were characterised by higher macroalgae cover (52–67% for Fly and Eva respectively) and exceptionally low coral cover (1–2%). Whereas northern zones displayed lower macroalgae cove (0–28%) and higher coral cover (29–37%), and high cover of turfing algae (16–35%) with the latter growing predominantly on dead coral substrate.

Environmental and habitat data explained 61% and 43% of the spatial variation (using annual tiles) in carbonate production rates and lateral CCA cover, respectively (Table 3.3). Carbonate production rates were found to be predominantly associated with benthic cover (coral, macroalgae, turfing algae) and light, whereas CCA cover was influenced by environmental factors including temperature, light, salinity, and sand cover (Table 3.3). Marginal tests found temperature and coral cover to have the strongest influence explaining 18% and 19% of the variation in lateral CCA cover, respectively (Supplementary Table 4). In contrast, macroalgal cover was the only significant factor associated with carbonate production rates, explaining 18% of the spatial variation.

3.4.3 Environmental influence on temporal variation of carbonate production and lateral CCA cover

The wet season was characterised by more than double light levels (WS = 224.78 ± 2.04 μmol photons m^{-2} s^{-1}; DS = 105.72 ± 1.50 μmol photons m^{-2} s^{-1}; Figure 3.5 and Figure 3.6); higher conductivity (WS = 59109.25 ± 1010.74 μS/cm; DS = 55550.29 ± 754.80 μS/cm) and higher salinity (WS = 39.22 ± 0.13 psμ; DS = 37.41 ± 0.54 psμ; Figure 3.6, Supplementary table 3). The wet season also experienced higher benthic temperatures (WS = 29.0 ± 0.4 °C, DS = 24.3 ± 0.6 °C, measured with *in situ* loggers) as well as sea surface temperatures (WS = 25.7 ◦C ± 0.8, DS = 23.4 ± 0.9 °C). During the wet season, specifically between December 2019 to January 2020, SST anomalies (SSTA) ranged from 1 to 3.2 °C (Figure 3.7). This level of SSTA is not uncommon for Exmouth Gulf, as SSTA of 2 °C or more have occurred annually during December and January (excluding 2018) since 2003 (Figure 3.7c). Dry season SST for the duration of this study were comparable to historic temperatures, with the exception of June and July 2019 that experienced average SSTA of -1.8 ◦C and -1.5 ◦C (Figure 3.7d). Further, the dry seasons experienced higher levels of chlorophyll-a (0.54 μg. L^{-1} ± 0.04, WS 0.33 μg. L^{-1} ± 0.05) and turbidity (2.03 FNU ± 0.38, WS 1.61 FNU ± 0.13, Figure 3.6).

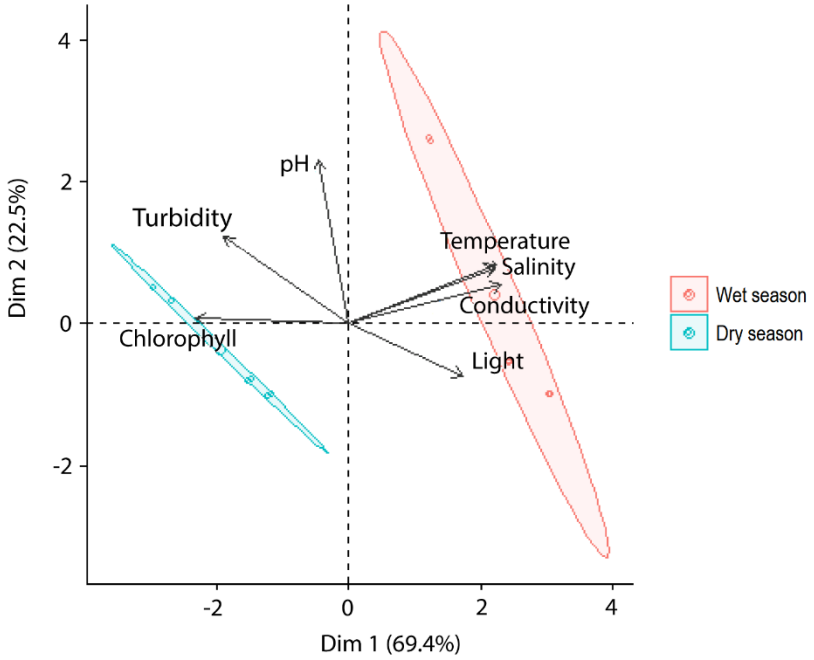

Figure 3.6 Principal component analysis of environmental variables driving seasonal variation between dry (April-September), and wet (October-April) seasons 2019-2020.

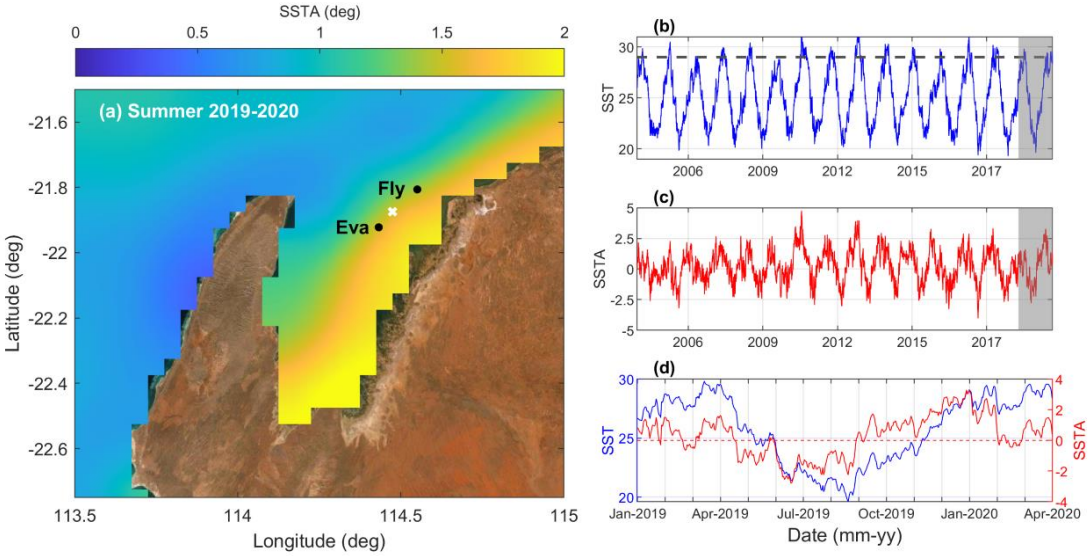

Figure 3.7 Temperature patterns within the Exmouth Gulf showing a) SSTA recorded over the wet (summer) season 2019–2020 for the Exmouth Gulf and Ningaloo coast, b) monthly average sea surface temperatures (SST) recorded between 2003 and 2020, c) monthly average sea surface temperature anomaly (SSTA) recorded between 2003 and 2020, d) daily SST and SSTA recordings from January 2019 to April 2020. All data obtained from by

NOAA Coral Reef Watch (CRW) daily global 5 km satellite coral bleaching heat stress monitoring product suite Version 3.1 (https://coralreefwatch.noaa.gov/product/5km/.).

Table 3.4 . Distance based linear modelling results for seasonal mean environmental and water quality measures explanation for a) carbonate production rates and b) lateral CCA cover %. The model with the lowest AIC values was selected (in bold).

AIC	*R^2*	*RSS*	***No.Vars***	*Selections*
a)				
240.76	**0.11**	**6126.30**	**3**	**Temperature, Conductivity, Chlorophyll-a**
240.80	0.07	6392.6	2	Light, Turbidity
240.88	0.07	6403.0	2	Conductivity, Chlorophyll
241.1	0.07	6437.9	2	Salinity, Conductivity
b)				
158.84	**0.31**	**1111.80**	**3**	**pH, Salinity, Conductivity**
158.84	0.31	1111.80	4	pH, Salinity, Conductivity, Chlorophyll-a
158.84	0.31	1111.80	4	pH, Salinity, Chlorophyll, Turbidity

Environmental data explained 11% and 31% of the temporal variation in carbonate production and lateral CCA cover, respectively (Table 3.4). Lateral coverage of CCA between seasons were associated with shifts in pH, salinity, and conductivity (AIC = 158.84, R2 0.31), while marginal tests also found benthic temperature to be a significant influencing factor (Pseudo-F = 13.18, p = 0.001, Prop = 0.223, Supplementary Table 5). CCA cover was significantly lower in the wet season when temperatures, salinity and conductivity were all relatively high. Temperature, together with conductivity and chlorophyll-a were also found to be related to changes in carbonate production rates (Table 3.4b). However, DistLM marginal tests found no significant association of environmental variables when modelled individually with carbonate production rates (Supplementary Table 5). This is most likely due to a lack of constant variation in carbonate production rates between seasons.

3.5 Discussion

This study provides the first carbonate production rates of encrusters for inshore subtropical reefs within the Eastern Indian Ocean and Western Australia. Annual carbonate production rates of encrusting organisms at Eva and Fly reefs varied from 0.024 to 0.062 g cm^{-2} yr^{-1} (mean = 0.039 ± 0.002 g cm^{-2} yr^{-1}), which are comparable to rates recorded in the tropical Indian Ocean, subtropical Atlantic, and from inshore reefs in the Pacific. For example, clear water reefs in the Maldives had mean carbonate production rates at the upper range of our study at 0.056 ± 0.029 g cm^{-2} yr^{-1} (Morgan and Kench, 2017), with similar rates recorded in a different ocean basin (e.g., Florida Keys at 0.054 g cm^{-2} yr^{-1}; Kuffner et al., 2013). In the Pacific, inshore sites of the Great Barrier Reef returned highly variable rates of between 0.009 ± 0.001 to 0.058 ± 0.012 g cm^{-2} yr^{-1} (Browne et al., 2013), and inshore sites from Tahiti and Moorea recorded higher rates of 0.020 ± 0.019 and 0.065 ± 0.042 g cm^{-2} yr^{-1}, respectively (Pari et al., 1998). Among all these sites, CCA was the dominant encrusting taxa (45–99% of encruster cover), which was also found across sites within this study (77 ± 4.9% and 64 ± 5.0% at Eva and Fly reefs, respectively).

Although we found a mild relationship between lateral CCA cover and carbonate production rates, measuring lateral CCA cover on reef substrate may not be an appropriate proxy for carbonate production. At some sites high CCA cover did not produce higher carbonate production rates, a disconnect that occurred between reefs and seasons. Specifically, annual settlement tiles from Eva reef and tiles deployed during the dry season (at both reefs), displayed significantly higher CCA cover than annual tiles at Fly reef and tiles deployed over the wet season, respectively. Yet mean carbonate production rates were approximately equal at Eva and Fly and across seasons. This disconnect between lateral CCA cover and carbonate production could potentially be due to different CCA growth morphologies and differences in environmental conditions (e.g., light, temperature, salinity) over small spatial scales that may favour CCA taking on different growth strategies over time. We know that early successional CCA species with thin thalli (crust) opportunistically recruit (within two weeks) on to bare substrate and then spread laterally (Adey and Vassar, 1975; Mariath et al., 2013). These crusts have very little biomass (g) and, therefore, do not provide a substantial contribution to final carbonate production rates, as

opposed to successor species that develop thicker crusts (Matsuda, 1989; Mariath et al., 2013). The development of thicker crusts by successor species often results in lower lateral growth (Steneck, 1986) because of the energetic trade-off between lateral growth and maintaining nonphotosynthetic tissue within the crust (Mccoy and Kamenos, 2015). This nonphotosynthetic tissue produces seasonal growth banding, whereby warmer summer temperatures result in wider bands (see Kamenos and Law, 2010). Therefore, if CCA cover on reef substrate is surveyed during warmer months where taxa are prioritising vertical growth, it is suggested that employing lateral cover of CCA as a proxy for carbonate production may lead to underestimating production rates.

Within this study, carbonate production and lateral CCA cover of encrusters was greater among northern reef sites that were more characteristic of "healthy" reef systems. High coral cover (29–37%) found in northern zones of Eva and Fly reef, provide hard substrate and greater topographic complexity for encruster settlement and offers some protection from grazing predators (Graham and Nash, 2013). In contrast, southern zones were characteristic of lagoonal habitats with higher coverage of macroalgae, which compete with CCA for space and irradiance (Dethier, 1994; Marcia et al., 1996). Furthermore, it is known that CCA species with thin crust, such as *Mesophyllum spp*., are predominantly found under macroalgal canopies (Figueiredo and Steneck, 2000). Although southern zones were moderately shallow and exposed to high levels of light, inadequate substrate (soft sand and patchy macroalgae) meant there are less established CCA with thick crusts to provide recruits to settlement tiles. This spatial variation in habitat demonstrates a limited potential for substantial carbonate production in habitats characterised by high levels of macroalgae and minimal hard substratum.

Seasonally, carbonate production rates varied inconsistently, maintaining stable average seasonal production rates across all zones. Meanwhile, lateral CCA cover showed consistent seasonal fluctuations. Annual tiles were expected to have the greatest lateral coverage of CCA since they were deployed for twice as long as seasonal tiles, however, tiles deployed over the six month dry season had the highest lateral CCA cover. This suggests that established CCA on the annual tiles may have died off or been physically removed during the wet season. We propose multiple

theories to explain these findings. Firstly, there may have been an increase in predation by grazers of thin crusts (e.g., urchins and fish; Padilla, 1984; Steneck, 1986) on tiles during the wet season. Secondly, partial or total mortality of dry season recruits during the wet season, with replacement by recruits employing different growth strategies (vertical rather than lateral growth). We propose the later theory is more likely considering the relationship between warmer waters and crust thickness discussed above, as well as high SST recorded during the wet season that were potentially above thermal thresholds of some CCA.

Sea surface temperatures above 29 °C and SSTA over 2 °C have caused significant thermal stress on encrusters globally as well as among temperate West Australian reefs. For example, SST's from 25 to 29 °C (SSTA 1–4 °C) affected the health and survival of CCA and bryozoan species in the Mediterranean (Martin and Gattuso, 2009; Pag`es-Escol`a et al., 2018), while SST's between 26 and 33 °C reduced carbonate production rates of CCA in the Red Sea (Roik et al., 2016), and SST's from 28 to 31 °C (SSTA 2–4 °C) reduced calcification and survival of CCA from the Great Barrier Reef, Australia (Webster et al., 2011; Diaz-Pulido et al., 2012). Short et al. (2015) recorded thermal stress and mortality of CCA off temperate Western Australia due to consecutive summer periods (2012 and 2013) with SSTA of 2 °C during a major marine heatwave event along the West Australian coast (Feng et al., 2013; Lafratta et al., 2017). Given these findings, as well as a decline in lateral CCA cover, we expected a decline in carbonate production rates on tiles deployed over the wet season in response to substantial SSTA experienced at Eva and Fly reefs. But carbonate production only declined among the southern zone of Eva reef, while all other zones displayed constant rates across seasonal deployment periods. A comparison with historical SSTA confirms that over the last eight years, the inshore reefs of Exmouth Gulf are regularly exposed to prolonged SSTA of 2 °C during the wet season. As a decline in carbonate production was not observed in this study, we hypothesise that CCA and encrusting taxa inhabiting these reefs may be tolerant to these annual conditions.

Encrusters play an important role in the consolidation and stabilisation of reef framework, therefore consistent carbonate production by encrusters is vital to a reef's carbonate budget. Calcification rates by encrusters across Eva and Fly reefs were

estimated based on net rates of production, and the proportion of reef area (m^2) available for encruster growth to be 0.436 ± 0.029 and 0.329 ± 0.044 kg m^{-2} yr^{-2}. These calcification rates are approximately 11.4% of the rates produced by corals across both reef sites (see Chapter 2). This contribution to the overall carbonate budget is a magnitude higher than that of inshore reefs of the Great Barrier Reef, where encrusters contributed 0.94–4.27% of the calcification rates produced by corals (Browne et al., 2013). Similarly, calcification rates of encrusters from an inshore site of Jamaica contributed 2.61% of that produced by corals (Mallela and Perry, 2007). The rates recorded for Eva and Fly show that encrusters (particularly CCA) make up a vital portion of the carbonate budgets of these inshore reefs, and if they have the potential to maintain stable carbonate production with rising ocean temperatures, could result in net positive carbonate budgets in periods where carbonate production by corals is impeded.

We have documented the maintenance of stable carbonate production by CCA through a period of high SSTA. However, we stress that we are not able to confirm long-term encruster community adaptations or shifts in CCA growth morphologies from this study due to data being collected over one annual cycle. In order to fully understand the effects of thermal stress and temperature sensitivity of CCA (and other encrusters), future works should be conducted over multiple years and include seasonal, reef scale experiments. Species identification to determine population and morphology shifts that occur seasonally, as well as *in situ* measurements of CCA physiology on temporal and spatial scales, would bring greater understanding of how CCA are responding to ocean change within their reef settings. This knowledge will be valuable for carbonate budget and reef growth estimates given that expected climate change scenarios (RCP 8.5) are predicted to lead to declines in coral cover and reef health (van Woesik and Cacciapaglia, 2018). As CCA is a preferred settlement substrate for coral larvae, a better understanding of how CCA respond to climate stressors *in situ* would give more confidence to predictions of reef recovery after a disturbance.

Postscript: The next chapter delves into cryptic endolithic bioerosion activity across Eva and Fly reef, and how this varies spatially and relates to local environmental patters. Additionally, the relationship between endolithic bioerosion and environmental parameters is explored at a global scale.

Chapter 4 Bioerosion among inshore reefs in Western Australia

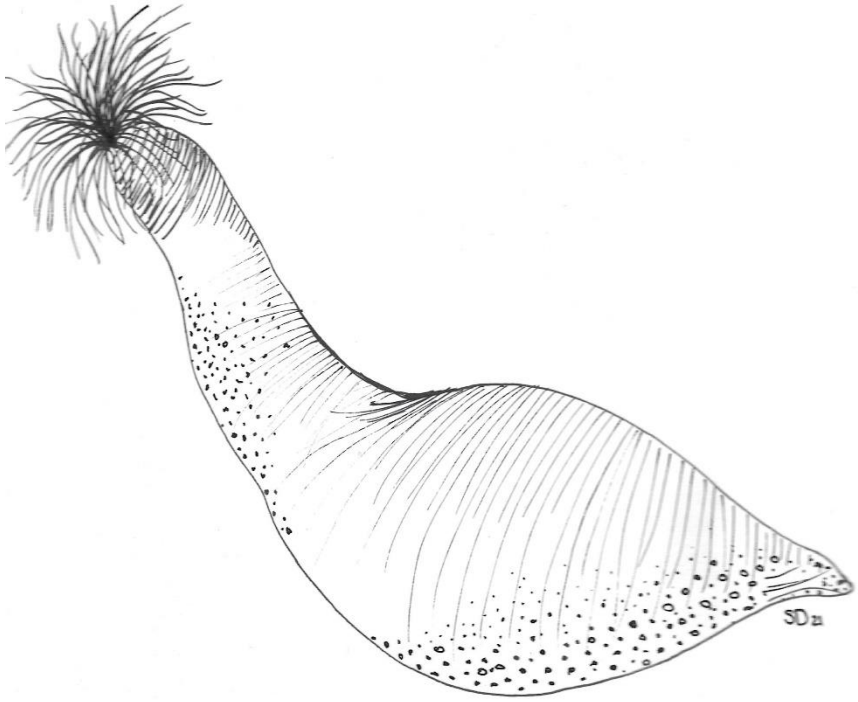

Preface: This chapter has been submitted for peer-review to the journal *Marine Biology* on the 03/09/2021 and has been formatted according to journal guidelines. The combined references for all chapters can be found in the Cited Literature-section at the end of this thesis.

4.1 Abstract

Bioerosion on turbid inshore reefs is expected to increase with global climate change reducing reef stability and accretionary potential. Most studies investigating bioerosion have focused on external grazers, such as parrotfish and urchins, whose biomass is more easily measured. Yet, cryptic endolithic bioeroders such as macroboring (worms, sponges and bivalves) and microboring taxa (fungus and algae) have the potential to be the dominant bioeroders, especially among inshore reef systems exposed to increased nutrient supply. We measured bioerosion rates of three bioeroder groups (microborers, macroborers, and grazers), and their response to environmental parameters (temperature, turbidity, light, chlorophyll a, salinity, pH) across two inshore reefs of north Western Australia. Total bioerosion rates were low (0.152 ± 0.012 kg m^{-1} yr^{-1}) compared to average global rates but were comparable to other inshore turbid reefs. Macroboring worms were the dominant source of bioerosion and displayed a significant negative relationship with temperature (r^2= 0.24, P=0.008) and light (r^2= 0.16, P=0.037). A global assessment of environmental influences on bioerosion further identified chlorophyll-a as a significant driver of macroboring (r2= 0.60, P=<0.001). Low bioerosion rates among marginal inshore reefs is encouraging as these reefs may be able to maintain a positive carbonate budget state despite lower coral cover and gross carbonate production rates. These data also highlight the necessity of reducing local impacts such as nutrient loads, which drive increases in chlorophyll a, to support marginal reef systems with climate change. Further, the development of empirical relationships that quantitatively link bioeroder activity and rates of environmental change will improve our ability to predict reef responses to environmental change, and better manage reefs into the future.

4.2 Introduction

Globally, rates of bioerosion driven reef breakdown are likely to increase with climate change (Davidson et al. 2018; Cornwall et al. 2021). Bioerosion processes include external grazing from taxa such as parrotfish or urchins, as well as endolithic boring and chemical dissolution from "microborers" (fungus or algae), and larger "macroborers" (sponges, worms, or bivalves; Hutchings 1986). As many of these boring organisms are heterotrophic, increases in bioerosion have been shown to increase with eutrophication and warming waters (Chazottes et al. 2002; Le Grand and Fabricius 2011). Additionally, ocean acidification has been shown to influence bioerosion rates as acidic waters weaken the calcium carbonate framework, increasing its susceptibility to bioeroding organisms (Schönberg et al. 2017). Inshore reefs are considered to be particularly vulnerable to increasing bioerosion rates as they are often exposed to elevated nutrients and sediment runoff, and are situated in shallower, warmer waters (Prouty et al. 2017). As such, many inshore reefs are typically considered to be "marginal", living at the edge of their environmental limits (Browne et al. 2012; Loiola et al. 2019). Yet, these reef systems are likely to expand their geographic range in coming years due to sea level rise inundating coast lines, changing weather patterns (e.g., increased rain fall and river runoff) and continued modification of coastal catchments (Zweifler et al. 2021). As such, we need to better understand how these reef systems are and will be impacted by potential increases in processes such as bioerosion that destabilise reef systems.

Increased rates of bioerosion will reduce the capacity of coral reefs to deliver key biological (habitat structure and diversity), economic (tourism, source of protein, coastal protection), and social services (cultural significance). The influence of bioerosion on reef function and long-term development can be estimated using reef carbonate budgets. Carbonate budgets consider factors of reef accretion (primarily through the growth of scleractinian corals), and reef erosion (bioerosion) to calculate an estimated rate of net reef accretion (Stearn and Scoffin 1977). If the rate of erosion outweighs the rate of accretion, the reef is considered to be in a negative budgetary state and is assumed to be degrading in terms of coral health and structural complexity (Kennedy et al. 2013; Perry et al. 2014; Januchowski-Hartley et al.

2017). This has carry on effects to other ecological reef functions such as loss of habitat and biological diversity (Perry and Alvarez-Filip 2019). Therefore, accurately estimating the rate of bioerosion is critical for assessing long-term reef health and stability, particularly given that drivers of bioerosion, particularly on inshore reefs, (e.g., eutrophication, warming oceans) are likely to increase in coming years.

Most bioerosion studies have focused on external bioeroders whose abundance is easily measured from snapshot *in situ* observations. This has resulted in carbonate budget studies heavily skewed to external grazing rates driven by the abundance of parrotfish and urchins (Browne et al., 2021). Rates of bioerosion are then typically calculated based on offsite and/or historic relationships between these grazers, their size and bioerosion rates (e.g., Bruggemann et al. 1994; Bellwood 1995). It is possible these observations may overestimate or underestimate species abundance depending on season, recent local disturbance, as well as specimens fleeing the path of observing divers. For example, recent studies have shown that there may be significant spatial variation in parrotfish bioerosion activities across an individual reef platform (Perry et al. 2017; Yarlett et al. 2020), and that grazing may be more intense at specific times of the day, as well as between species (Yarlett et al. 2018). Grazing can also intensify as a result of increased endolithic microborer and macroborer activity in response to environmental drivers (e.g., increased nutrients: Chazottes et al. 1995; Carreiro-Silva et al. 2009; Rice et al. 2020). Rates of endolithic bioerosion are largely unknown as it is more difficult to quantify compared to external grazing rates (Browne et al., 2021). These difficulties are largely because boring organisms are often small to microscopic, patchily distributed (e.g., bivalves) and are cryptic in nature (e.g. sponges and polychaetes; Diaz and Rützler 2001; Pari et al. 2002; Hutchings 2008; Schönberg 2015).

Traditionally endolithic bioerosion has been measured through two-dimensional (2D) image analysis of coral cross-sections. Originally, heads of live massive *Porites* were removed from the reef and cut into cross-sections that were then X-rayed to determine the area of carbonate removed (Sammarco and Risk 1990; Holmes et al. 2000). A less destructive method uses coral rubble, which is cut into cross-sections, and the volume of carbonate removed is determined using image analysis software (Harney and Fletcher 2003; Mallela and Perry 2007; Browne et al. 2013). This

method is, however, come with ambiguity as the age of coral rubble cannot be confidently estimated without carbon dating, which is an expensive practice when large amounts of rubble are required to produce a robust dataset. Consequently, previous research has used either a known event (e.g. bleaching, cyclone) or the state of the coral rubble (e.g. <1 year if corallites intact and limited algal growth; Browne et al. 2013) to time-stamp the death of the coral and its availability for bioerosion. A more accurate approach is to use pre-weighed *Porites* skeleton blocks, which are deployed on to a reef (attached to the substrate) for 12 or more months (Davies and Hutchings 1983; Kiene and Hutchings 1994; Pari et al. 1998; Chazottes et al. 2002). This method is both less destructive (blocks are cut from cores) and is time-stamped. On removal from the reef, the block can be weighed to determine the mass of carbonate removed over time and cut into cross sections to measure volume and identify boring organism (e.g., mollusc, serpulid worm). More recently, experimental *Porites* blocks have been scanned using micro computerized tomography (microCT) before and after deployment (Beuck et al. 2007; Enochs et al. 2016; Silbiger et al. 2016). The high resolution scans obtained by microCT allow the user to analyse total volume loss and relate a percentage volume loss to macro and microboring. These methods likely provide some of the best estimates of endolithic bioerosion. However, they are both time consuming (several years) and expensive to conduct.

Environmental conditions are a key driver of bioerosion rates and could be used to estimate changes in endolithic bioerosion activity. Furthermore, tracking changes in environmental parameters (e.g., light, temperature, pH etc.) is logistically easier and less labour intensive than current methods used to estimate endolithic bioerosion. Within a review of 31 global studies reporting rates of endolithic bioerosion, only 7 included environmental data (Supplementary Table 6). Of the studies that did measure one or more environmental parameters, strong relationships between bioerosion rates and environmental conditions such as eutrophication (Chazottes et al. 2002; Webb et al. 2017; Rice et al. 2020), ocean acidification (DeCarlo et al. 2014; Enochs et al. 2016), and temperature (Achlatis et al. 2017) were observed. However, there is a considerable lack of *in situ* data that have coupled bioerosion activity with environmental conditions highlighting the need for studies that can provide data and development an understanding of empirical relationships.

A lack of data on endolithic bioerosion and a poor understanding on how bioerosion may alter with environmental change, limits our ability to accurately quantify total bioerosion (external and endolithic) and assess how rates will change with future climate shifts at a local and global level. There are currently no recorded rates of endolithic bioerosion from West Australian reefs, with an additional paucity in bioerosion data from marginal reef systems globally. In this study we provide much needed endolithic bioerosion data for inshore north West Australia, with a comprehensive assessment of important environmental variables (light, turbidity, temperature, water quality). We also collect data on grazing pressure (fish and urchin abundance) to demonstrate that endolithic bioerosion is the primary loss of biological carbonate material from these reef systems. Further, to improve our knowledge of how environmental conditions influences internal bioerosion rates, we assessed a sample of studies that incorporated data on both endolithic bioerosion of coral substrate and environmental parameters. In doing so, we aim to fill an important knowledge gap and promote the development of empirical relationshups that could aid in estimating changes in bioerosion activity over time.

4.3 Methods

4.3.1 Study site

This study was carried out at four sites on each of two inshore island reefs (Eva and Fly) located in Exmouth Gulf (Detailed in Chater 1. At each reef, sites included two northern wave exposed locations and two southern sheltered lagoon locations (Figure 4.1). Sites were referred to as being inshore or offshore in relation to the central island, though there was no major habitat variation between inshore and offshore sites (Chapter 2). The sites within this study were Eva south offshore (ESO), Eva south inshore (ESI), Eva north inshore (ENI), Eva north offshore (ENO), Fly south offshore (FSO), Fly south inshore (FSI), Fly north inshore (FNI), and Fly north offshore (FNI).

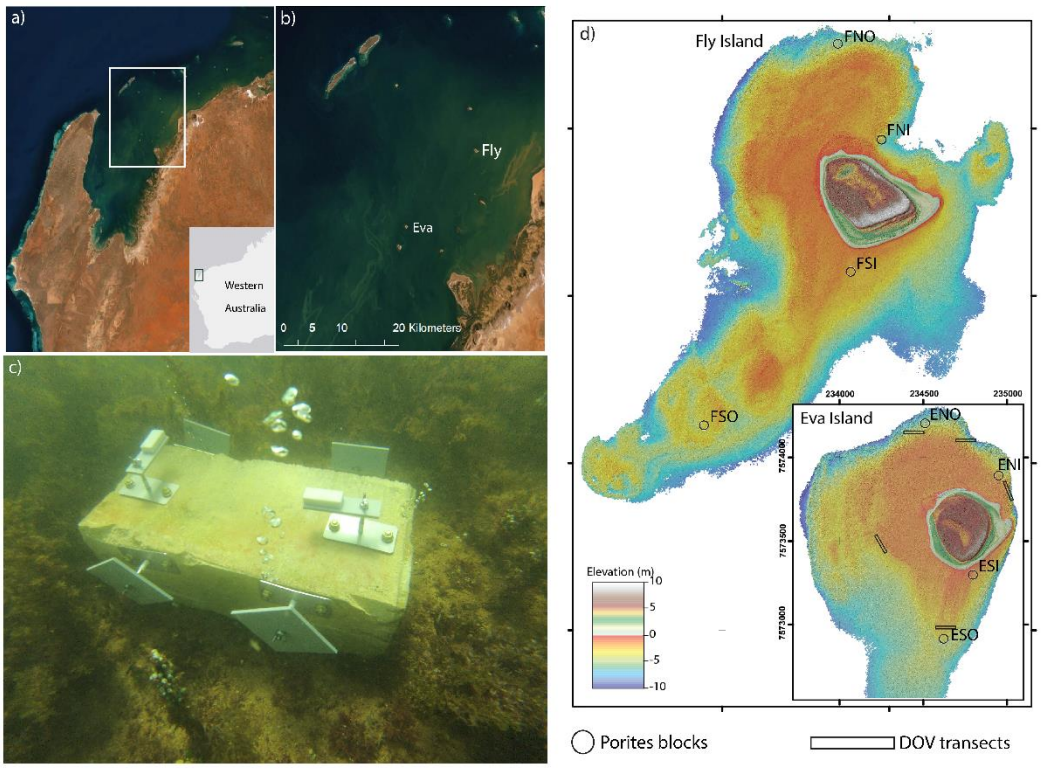

Figure 4.1 The West Australian coast shown in grey with a zoomed satellite image of Exmouth Gulf (a), highlighting the area around Eva and Fly Island reefs (b). Panel (c) shows one of two limestone blocks deployed at each of eight study sites, with the two bioerosion blocks on top. Study sites are shown by black circles across Eva and Fly reefs in panel (d) on the right. The eight sites within this study were Eva south offshore (ESO), Eva south inshore (ESI), Eva north inshore (ENI), Eva north offshore (ENO), Fly south offshore (FSO), Fly south inshore (FSI), Fly north inshore (FNI), and Fly north offshore (FNI). Five 50 m long diver operated video (DOV) surveys were conducted around sections of Eva Reef to estimate the abundance and biomass of grazing fish. DOVs were conducted at ENI, ESO, ENO (x2), and the western zone.

4.3.2 Environmental variables

This study was conducted from April 2019 to May 2020. Temperature loggers (^{o}C; Hobo Pendant UA-001-64) and photosynthetic active radiation (PAR) loggers (µmol photons m^{-2} s^{-1}; Odyssey submersible PAR logger) were deployed at each site with logging intervals of 60 minutes for benthic temperature and 10 minutes for PAR loggers. Water quality variables of chlorophyll-a (µg L^{-1}), salinity, pH and turbidity (FNU) were measured *in situ* monthly during neap tides at one site per reef (see Chapter 3) Sampling was undertaken using a vertical profiling method with a multi-parameter EXO Sonde 2 (YSI Inc./Xylem Inc.; details of testing methods outlined in Chapter 3). Habitat data at each site was gathered by line intercept transects (20 m)

and image analysis using Coral Point Count with excel extension (CPCe ref; see details of habitat analysis in Chapter 2)

4.3.3 Porites blocks and MicroCT

At each site, four blocks were deployed in early April 2019 and retrieved in mid-June 2020 (total number of blocks = 32). Each block measured 5x2x1 cm with average density = 1.56 g cm^3 , which is comparable to previous studies (). Blocks were obtained from cores of *Porites lutea* collected from the South Cay of Willis Island within the Coral Sea. Although cores were not collected at the study site, *Porites lutea* is the dominant massive coral at Eva and Fly reefs. Blocks were individually weighed and attached to PVC plates (8x2x0.4 cm) with marine epoxy before being imaged using microCT at the NIF Bioimaging Facility located at the Centre for Microscopy, Characterisation and Analysis at the University of Western Australia, Perth, Australia. MicroCT scans were undertaken with a SkyScan 1176 microCT (Bruker-microCT, Kontich, Belgium) at 90 kV and 273 µA. Initial and post deployment scans were run at 35 µm resolution with a 0.1 mm Cu filter. Scans were reconstructed into image stacks using Bruker NRecon software using a modified Feldkamp cone-bream algorithm with ring artifact reduction of 20 and beam hardening of 20%. Pre and post deployment scans were directly compared through three-dimensional registration of the two data sets with Skyscan Data-Viewer software using the pseudo-3D registration strategy. From here we generated a bitmap "difference" image stack from the overlapped data sets, where eroded mass appeared white (bitmap value = 255), accretion appeared black (bitmap value = 0), and constant mass was grey. Three-dimensional analysis of this dataset in CTAn (version 1.18) allowed erosion to be measured by applying a threshold to isolate the white (bioeroded) regions. After the entire block was processed, a region of interest (ROI) was drawn for the interior area, excluding approximately 1 mm outer edge, to measure macroboring. This 1 mm exclusion was applied to measure microboring following evidence of microborers among inshore reefs of the Great Barrier Reef (Low Isles and Snapper Island), and other Indo-Pacific sites, boring to average depths of 1mm over a 1-year period (Chazottes et al. 1995; Tribollet 2008; Tribollet et al. 2010). ROIs were also placed around obvious areas of scraping to measure

external grazing (displayed in orange in Figure 4.2). Rates of bioerosion (kg m^{-2} yr^{-1}) for each *P.lutea* block by grazers, microborers, and macroborers were measured as:

$$Bioerosion\ rate\ (\ kg\ m^{-2}\ yr^{-1}) = (Voli \times Di) \div (SAi \times time) \quad \text{Eq.4-1}$$

Where Vol_i is the volume of carbonate loss in the region of interest (areas of external grazing, internal and remaining outer 1mm), D_i is the density of the individual block of *P.lutea*, SA_i is the surface area of the individual block, and time is the number of years the block was exposed (number of days/365; DeCarlo et al. 2014; Silbiger et al. 2016). Identification of macroborers were based on the characteristics of their borings following descriptions by Sammarco and Risk (1990).

Figure 4.2 Experimental block of Porites lutea before and after 12 months of deployment, along with micro computerized tomography (microoCT) scan of the block post deployment. Varying sources of bioerosion displayed on the µCT image include grazing (orange), microboring (yellow), and macroboring by polychaetes and sipunculans (red)

4.3.4 Fish and urchin abundance

To further assess potential grazing pressures that may not be captured by experimental blocks, abundance data was gathered for bioeroding fish and urchins. Diver-operated stereo-video (DOV) was used to collect data on fish abundance across Eva reef, to identify grazing species present and estimate fish biomass. Four 50 m transects separated by 10 m were carried out by a SCUBA buddy pair at five sites (Figure 4.1). Transects were kept linear and to a consistent depth profile (mean depth across all sites= 3.3 m). The DOV system used two Sony ActionCams (FDR-X3000) mounted on either side of the base, approximately 800 mm apart, which were calibrated prior to fieldwork (for more information on the DOV system setup and its applications, see Goetze et al. (2019). Video footage was analysed using the computer software EventMeasure (www.seagis.com.au), which allows for accurate abundance and length measurements with a pre-populated species list (Goetze et al. 2019). All fish observed were measured to fork length and identified to their lowest possible taxonomic resolution. Count data was used where length measurements were not possible (i.e., due to limited visibility or obstruction of view). To ensure accurate identification and length measurements, values were excluded if their residual mean square (RMS) error exceeded 20 mm, and if measurement to length ratio precisions exceeded 10%. All measurements farther than 7 m from the DOV and outside of the 5 m wide belt transect were also excluded (Goetze et al. 2019). Biomass was calculated using fish fork length as a proxy for weight, in the equation:

$$Weight\ (g) = a\ \times Length\ (cm) \quad \text{Eq. 4-2}$$

where a is the relevant slope of a given species (Karakulak et al. 2006). Slopes at the family and genus level were used cautiously for species without published slope data, and for fish that were not identified to species level. Slope values and fish feeding guilds were derived from the FishBase website (https://www.fishbase.se/search.php) and relevant published literature (Schramm et al. 2021). DOV's were not carried out across Fly reef due to limited days in the field, but as there is no significant variation in habitat types between Eva and Fly reef (Dee et al. 2020, chapter 2), and similar abundances have been witnessed at Fly reef previously (Pers. Obs.), we are confident that the abundance and biomass of grazing fish would be similar to that of Eva reef. Species-specific and size-scaled grazing rates for fish were determined using the "Indo-Pacific" data spreadsheet available from the *Reef Budget* website

(https://geography.exeter.ac.uk/reefbudget/indopacific/; Perry et al. 2018a). Urchin abundance estimates were conducted along each line transects at Eva and Fly reef. There were negligible amounts of urchins found across both reefs (<5 individuals per reef) and so they were excluded from analysis.

4.3.5 Statistical analysis

Prior to undertaking analysis, data were $\log_{10}(x+1)$ transformed to meet assumptions of normality and equality of variance. We used linear regression to determine if the density of experimental blocks had influenced total bioerosion rates, but found no significant influence (n=32 r2 = 0.54, F 7,27 =2.48, P = 0.108). Three-way analysis of variance (ANOVA) was run to investigate if there was a significant difference in bioerosion rates between the three functional groups of bioeroders on the experimental substrate (grazers, macroborers and microborers), spatial variation in bioerosion rates of each functional group at reef and site level, as well as to identify any interaction between reef and site. Tukey HSD (Honestly Significant Difference) post hoc test adopted to identify any source of variance. Principal Component Analysis (PCA) was used to identify spatial differences in key environmental variables associated with reefs and sites, and linear regression was used to investigate relationships between bioeroder functional groups and environmental parameters measured at Eva and Fly during periods of block deployment.

4.3.6 Global endolithic bioerosion assessment

31 studies that measured *in situ* endolithic bioerosion from around the globe were reviewed and used to investigate relationships between environmental variables and bioerosion rates. These studies were discovered during an extensive literature search for studies on bioerosion, or that included bioerosion in ecological assessments (i.e., carbonate budget studies). The region of each study, methods undertaken, experimental substrate used, reef type, what (if any) environmental parameters recorded, and bioerosion rates measured (micro, macro, and grazing; Supplementary Table 6) were all noted. No sound relationships could be quantitified between bioerosion rates and environmental drivers due to a lack in studies containg data (i.e., six studies not including this manuscript recording macroboring rates and at least one

environmental variable). There were additional studies that included environmental data with microboring rates (3 studies), or solely focused on sponge bioerosion rates (3 studies), but these were also excluded due to limited data available (Supplementary Table 6).

4.4 Results

4.4.1 Rates of bioerosion on *Porites* blocks

Rates of carbonate removal varied significantly between the three bioeroder functional groups (Figure 4.3; F (1,76)=19.87, P=<0.001;Table 4.2). Macroboring was responsible for the greatest amount of bioerosion (average = 0.084 ± 0.008 kg m^{-2} yr^{-1}) and grazing the least (average = 0.024 ± 0.033 kg m^{-2} yr^{-1}). Average macroboring rates were slightly higher at Fly reef than at Eva reef (F (1,76)=2.18, P=0.144; Table 4.2). There were significant differences in bioerosion activity among sites (F (1,76)=5.07, P=0.027; Table 4.2) with FSO experiencing highest levels of macroboring, and most inshore sites experiencing the least (Figure 4.3). A significant interaction effect between reefs and sites confirmed that the spatial difference at reef level was largely driven by greater micro-boring activity at Eva's southern sites only (ESO, ESI; Figure 4.3).

All blocks showed presence of polychaete and sipunculans borings (Figure 4.2). The highest number of sipunculans borings were seen at sites ESO (average 5.5 ± 0.5 borings per block), FSO (average 3 ± 1 borings), and FSI (average 2.5 ± 1.0 borings). There was no evidence of bivalve or sponge boring.

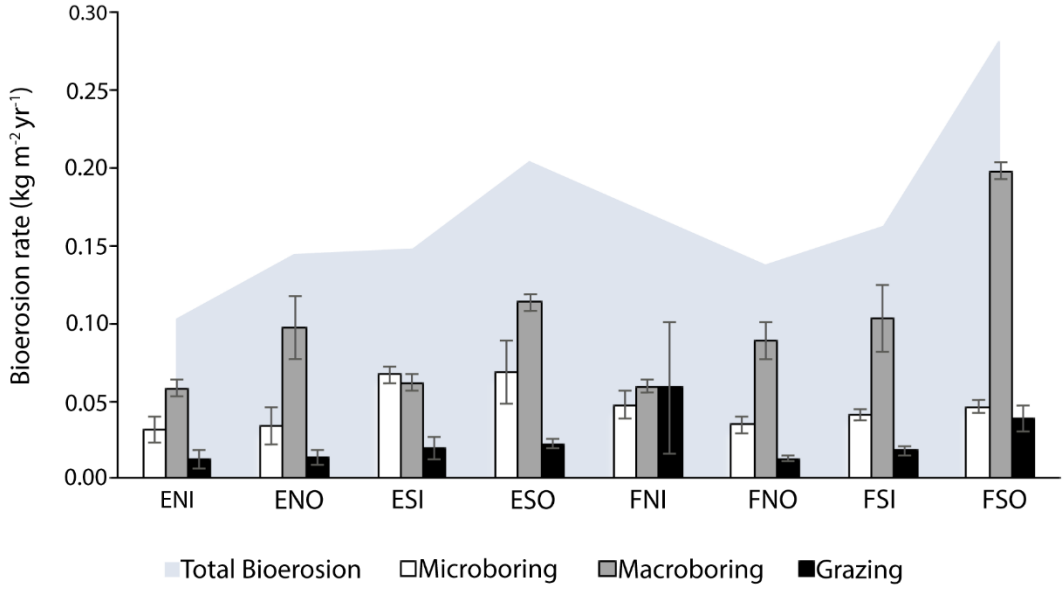

Figure 4.3 Comparative rates (kg m^{-2} yr^{-1}) of grazing, macro and micro bioerosion to total bioerosion rates measured across sites using micro computerized tomography (microCT)

Table 4.1. Average substrate (% cover) dominated by coral, macroalgae (MA), turfing algae (TA- mostly on dead coral), and sand (Dee et al., 2020). Mean annual environmental variables measured monthly throughout 2019/2020 at Fly and Eva reefs, and average µCT (microboring, macroboring, grazing and total) and rubble bioerosion rates (kg m^{-2} yr^{-1}) measured for each site.

			Substrate cover (%)				Environment						Bioerosion rates (kg m^{-2} yr^{-1})			
Reef	Site	Depth (m)	Coral	MA	TA	Sand	Light (PAR)	Temperature (°C)	Chlorophyll (µg L^{-1}))	pH	Turbidity (FNU)	Salinity	*microCT micro*	*microCT macro*	*microCT grazing*	*microCT total*
Eva	ENI	3.1	9.51	56.44	19.02	13.50	311.17 (±73.15)	27.15 (±0.80)	0.38 (±0.05)	8.18 (±0.01)	1.48 (±0.33)	38.16 (±0.42)	*0.032 (±0.008)*	*0.058 (±0.006)*	*0.013 (±0.006)*	*0.103 (±0.011)*
Eva	ENO	3.5	65.35	0.00	13.52	5.07	142.04 (±59.90)	27.15 (±0.80)	0.38 (±0.05)	8.18 (±0.01)	1.48 (±0.33)	38.16 (±0.42)	*0.034 (±0.012)*	*0.097 (±0.020)*	*0.013 (±0.005)*	*0.144 (±0.035)*
Eva	ESI	2.7	2.06	62.06	3.82	19.41	311.17 (±73.15)	26.90 (±0.86)	0.38 (±0.05)	8.18 (±0.01)	1.48 (±0.33)	38.16 (±0.42)	*0.067 (±0.006)*	*0.062 (±0.005)*	*0.019 (±0.007)*	*0.148 (±0.010)*
Eva	ESO	3.6	1.19	71.85	5.12	7.77	142.04 (±59.90)	26.90 (±0.86)	0.38 (±0.05)	8.18 (±0.01)	1.48 (±0.33)	38.16 (±0.42)	*0.068 (±0.020)*	*0.114 (±0.005)*	*0.022 (±0.003)*	*0.204 (±0.011)*
Fly	FNI	4.5	29.12	0.00	34.71	20.29	106.62 (±36.10)	27.20 (±0.89)	0.49 (±0.06)	8.19 (±0.03)	2.27 (±0.36)	38.34 (±0.46)	*0.047 (±0.009)*	*0.059 (±0.004)*	*0.059 (±0.042)*	*0.166 (±0.051)*
Fly	FNO	4.0	6.24	29.46	32.10	7.07	106.62 (±36.10)	27.20 (±0.89)	0.49 (±0.06)	8.19 (±0.03)	2.27 (±0.36)	38.34 (±0.46)	*0.035 (±0.005)*	*0.089 (±0.012)*	*0.013 (±0.001)*	*0.137 (±0.015)*
Fly	FSI	3.0	1.06	35.98	4.76	35.71	127.08 (±65.53)	27.32 (±0.89)	0.49 (±0.06)	8.19 (±0.03)	2.27 (±0.36)	38.34 (±0.46)	*0.041 (±0.004)*	*0.103 (±0.021)*	*0.018 (±0.003)*	*0.162 (±0.023)*
Fly	FSO	3.1	0.00	67.58	1.21	21.06	127.08 (±65.53)	27.32 (±0.89)	0.49 (±0.06)	8.19 (±0.03)	2.27 (±0.36)	38.34 (±0.46)	*0.046 (±0.007)*	*0.098 (±0.024)*	*0.039 (±0.006)*	*0.183 (±0.019)*

Table 4.2 Three-way analysis of variance (ANOVA) comparing rates of bioerosion between functional groups (microboring, macroboring, and external grazing), measured on Porites blocks and spatial variations at site and reef levels

Variable	DF	MS	F value	P value
Functional group (FG)	1	2.348	19.874	<0.001
Site	1	0.599	5.067	0.027
Reef	1	0.257	2.179	0.144
FG: Site	1	0.155	1.315	0.255
FG: Reef	1	0.047	0.400	0.529
Site: Reef	1	0.081	0.687	0.410
FG: Site: reef	1	0.000	0.001	0.969
Residuals	76	0.118		

4.4.2 Fish abundance and erosion rates

DOV data showed low abundance of herbivorous fish species across Eva (compared to neighbouring Ningaloo reef; see discussion), with the only parrotfish species (*Scarus ghobbin*) showing particularly low numbers (average 2.6 ± 0.75 per 1000 m^2; Figure 4.4). Estimates of *Scarus ghobbin* biomass and bioerosion rates (kg m^{-2} yr^{-1}) for each DOV site were calculated using the *Reef Budget* data sheet for the Indo-Pacific. Average biomass was 15.53 ± 7.33 kg per 1000 m^2 resulting in an estimated average bioerosion rate of 0.059 ± 0.030 kg m^{-2} yr^{-1}. This is more than double the average grazing rate recorded by blocks at Eva (0.016 ± 0.003 kg m^{-2} yr^{-1}).

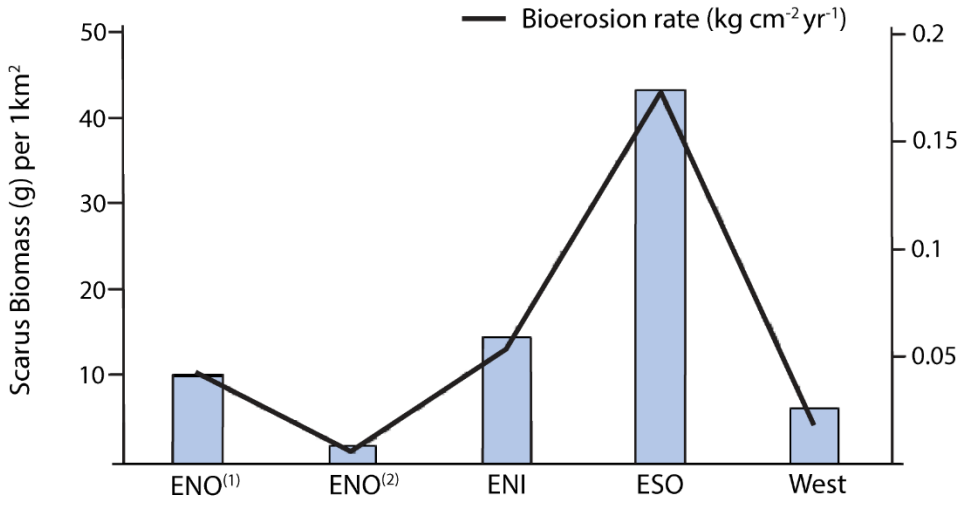

Figure 4.4 Estimated biomass of grazing herbivore *Scarus ghobban* across five DOV transects and the estimated bioerosion rate (kg m^{-2} yr^{-1}) calculated using the *Reef Budget* data sheet for the Indo-Pacific (available at https://geography.exeter.ac.uk/reefbudget/indopacific/)

4.4.3 Environmental relationships in Exmouth Gulf

PCA plots showed environmental disparity between Eva and Fly reefs. Fly was characterised by higher levels of chlorophyll a (Fly mean = 0.49 ± 0.06 µg L^{-1}; Eva mean = 0.38 ± 0.05 µg L^{-1}), turbidity (Fly mean = 2.27 ± 0.36 FNU; Eva mean = 1.48 ± 0.33 FNU), and pH (Fly mean = 8.19 ± 0.03; Eva mean = 8.18 ± 0.01), while Eva recorded higher light levels (Fly mean = 177.52 ± 1.73 µmol photons m^{-2} s^{-1}; Eva mean = 228.06 ± 2.38 µmol photons m^{-2} s^{-1}; Figure 4.5a).

Linear regression of bioerosion rates from microborers, macroborers and grazers with environmental variables measured across Eva and Fly reef found that spatial differences in macroboring were significantly driven by temperature and light (Table 4.3). Specifically, as temperature and light levels increased, rates of macroboring decreased accounting for 24% and 16% of the spatial variation, respectively (Figure 4.5b, c; Table 4.3). Further, we also saw a significant negative influence of temperature on total bioerosion likely due to the fact that macroboring was the dominant bioeroding agent and would hence be driving this relationship.

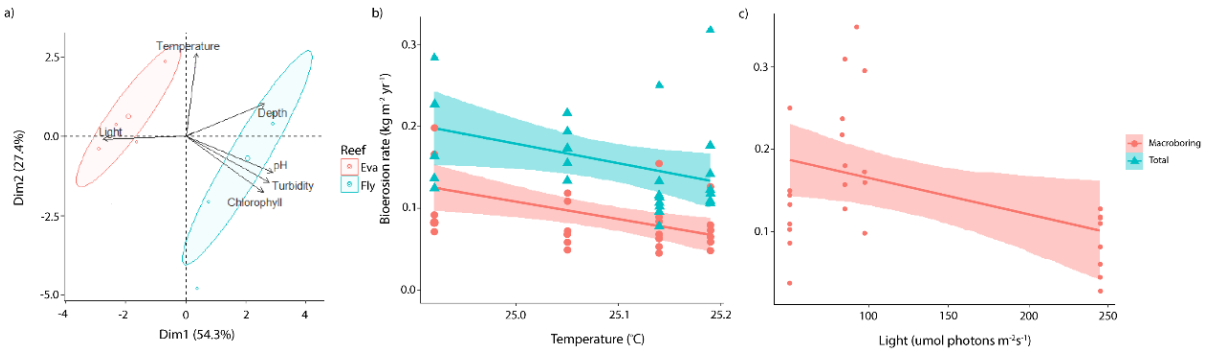

Figure 4.5 a) PCA plot of annual mean environmental parameters across Eva and Fly reefs, b) linear regression of mean temperature with macroboring and total bioerosion rates across all sites, c) linear regression of macroboring rates and mean light levels across all sites

Table 4.3 Linear regression results for relationships between bioerosion functional groups (macroboring, microboring and grazing) and yearly average environmental variables (temperature, chlorophyll-a, pH, turbidity, light, and salinity) measured within this study

Variable	*Estimate*	*S.E.*	*T value*	*df*	*r2*	*F value*	*P value*
Microboring							
Temperature	-0.148	0.101	-1.470	26	0.077	2.160	0.154
Chlorophyll	-0.011	0.052	-0.209	26	0.002	0.044	0.836
pH	-0.004	0.021	-0.209	26	0.002	0.044	0.836
Turbidity	-0.097	0.465	-0.209	26	0.002	0.044	0.836
Light	42.670	81.910	0.521	26	0.010	0.271	0.605
Salinity	-0.003	0.016	-0.209	26	0.002	0.044	0.836
Macroboring							
Temperature	-0.280	0.098	-2.852	26	**0.2383**	8.135	**0.008**
Chlorophyll	0.072	0.054	1.330	26	0.064	1.768	0.195
pH	0.029	0.022	1.33	26	0.064	1.768	0.195
Turbidity	0.642	0.483	1.330	26	0.064	1.768	0.195
Light	-178.620	81.000	-2.205	26	**0.157**	4.863	**0.037**
Salinity	0.022	0.016	1.330	26	0.064	1.768	0.195
Grazing							
Temperature	-0.051	0.054	-0.935	26	0.033	0.874	0.358
Chlorophyll	0.044	0.026	1.701	26	0.100	2.893	0.101
pH	0.018	0.010	1.701	26	0.100	2.893	0.101
Turbidity	0.396	0.233	1.701	26	0.100	2.893	0.101
Light	-60.080	41.790	-1.438	26	0.074	2.068	0.162
Salinity	0.013	0.008	1.701	26	0.100	2.893	0.101
Total bioerosion							
Temperature	-0.616	0.292	-2.108	26	**0.146**	4.444	**0.045**
Chlorophyll	0.079	0.061	1.297	26	0.061	1.722	0.206
pH	0.032	0.024	1.297	26	0.061	1.722	0.206
Turbidity	0.707	0.545	1.297	26	0.061	1.722	0.206
Light	-144.870	95.320	-1.52	26	0.082	2.174	0.141
Salinity	0.024	0.018	1.297	26	0.061	1.722	0.206

4.5 Discussion

Total average bioerosion rates across Eva and Fly reefs were 0.152 ±0.012 kg m^{-2} yr^{-1}, with macroboring being the dominant agent of bioerosion (average = 0.084 ± 0.008 kg m^{-2} yr^{-1}). This is below typical average macroboring rates for reefs globally (0.314 ± 0.333 kg m^{-2} yr^{-1}: Lange et al. 2020). However, these rates are comparable to some studies at similar reef sites, and studies that assessed macroboring through the use of microCT with experimental *Porites* blocks. For example, Tribollet and Golubic (2005) assessed rates of bioerosion at two inshore island reefs (Snapper Island and Low Isles) of the Great Barrier Reef (GBR) using 2D image analysis of experimental *Porites* blocks. These sites have similar fringing reef structure and turbidity levels to Eva and Fly and recorded total bioerosion rates of 0.27 kg m^{-2} yr^{-1} at Snapper Island and 0.18 kg m^{-2} yr^{-1} at Low Isles (0.13 and 0.01 kg m^2 yr^1 due to macroboring, respectively). Silbiger et al. (2015, 2016, 2017) used microCT of experimental *Porites sp.* blocks and also found similar endolithic bioerosion rates ranging between 0.072 and 0.15 kg m^{-2} yr^{-1} at sites in Hawai'i. Further, Enochs et al. (2016) employed microCT with blocks of *Porites sp.* and recorded rates ranging from 0.026 to 0.13 kg m^{-2} yr^{-1} in Papua New Guinea, although these results were recorded at sites with low CaCO3 saturation. Global averages in bioerosion rates may be inflated by measures reported in older studies due to less accurate methodologies, or due to a shift in dominant bioeroding taxa populations over time. For example, early work on bioerosion in the Caribbean reported macroboring rates of 0.443 kg m^{-2} yr^{-1} (Rutzler 1975; Lange et al. 2020). This is a magnitude higher than average macroboring rates gathered for the Caribbean in the past decade (~0.062 kg m^{-2} yr^{-1}; Perry et al. 2014; Murphy et al. 2016), and is expected to be due to a significant decline in bioeroding taxa as result of a rapid decline in coral cover and structural complexity. More so than macroboring, grazing pressure on Caribbean reefs has also declined as these previously complex reef systems continue to shift to less complex macroalgae dominated systems, similar to that of Eva and Fly reefs.

Low grazing rates are typical of turbid inshore reefs characterised by low populations of parrotfish and urchins. As such, Eva and Fly reefs recorded low rates of external erosion on experimental blocks (average = 0.016 kg m^{-2} yr^{-1} at Eva and 0.031 kg m^{-2} yr^{-1} at Fly) compared to clear water reefs (e.g., up to 4.31 ± 0.43 kg m^{-2} yr^{-1} at

Reunion Island, Indian Ocean: Chazottes et al. 2002). Here we relate the external erosion observed on the blocks to be due to herbivorous fish, such as parrotfish, given that the blocks were not accessible to urchins. Across Eva reef herbivorous fish had a low mean abundance of <10 per 1000 m^2, with the only grazer species recorded being *Scarus ghobbin* with a mean biomass of 15.53 ± 7.33 kg per 1000 m^2 and estimated average bioerosion rate of 0.059 ± 0.030 kg m^2 yr^{-1}. This estimate is almost four times the average rate of external erosion captured on experimental blocks (0.016 ± 0.003 kg m^{-2} yr^{-1}). This variation displays the uncertainty of capturing grazing with small experimental units, especially in algae dominated settings where herbivorous grazers have an abundance of food across the reef substrate.

Previously, the only research into bioerosion (external and internal) from north Western Australia has been from Ningaloo Reef where studies focused on external grazing of parrotfish and urchins using snapshot abundance data combined with offsite grazing rates from previous GBR studies (Bellwood 1995; Bonaldo and Bellwood 2009). Across Ningaloo, estimates of parrotfish (*Chlorurus microrhinos and Chlorurus sordidus)* erosion ranged from 1.18 kg m^{-2} yr^{-1} to 2.30 kg m^{-2} yr^{-1} (Johansson et al. 2010). Additionally, Johansson et al. (2010) found that urchin grazing rates (*Diadema* sp. and *Echinometra mathaei*) at Ningaloo ranged from 0.00 to 0.55 kg m^{-2} yr^{-1} with a later study by Langdon et al. (2013) suggesting that rates were as high as 1.00 - 4.50 kg m^{-2} yr^{-1}. Although the grazing rates we have recorded for Eva and Fly reefs are an order of magnitude lower than that recorded at Ningaloo, they are comparable to similar inshore sites of the GBR that employed the use of experimental substrates (<0.01-0.02 kg m^{-2} yr^{-1} at Snapper Island and <0.01-0.06 kg m^{-2} yr^{-1} at Low Isles; Osorno et al. 2005; Tribollet and Golubic 2005). There is also the potential for over-estimation of grazing bioerosion rates based purely on a snapshot measure of taxa abundance and biomass (see Perry et al. 2017 and Yarlett et al. 2020 for further discussion).

Within this study, the majority of bioerosion measures across Eva and Fly reefs were from macroboring polychaete and sipunculan worms. Given that previous studies have suggested that experimental substrate should be exposed for a minimum of three years to allow for full borer succession (Kiene and Hutchings 1994), the lack of

macroborer diversity may be due to the short (1 year) deployment of the experimental blocks. Bioeroder successions patterns are variable over time (Chazottes et al. 1995; Osorno et al. 2005; Tribollet and Golubic 2005; Carreiro-Silva and McClanahan 2012), as well as over small spatial scales (Davies and Hutchings 1983; Sammarco and Risk 1990; Kiene and Hutchings 1994; Hutchings and Peyrot-Clausade 2002), likely due to both variable biotic (e.g., reproduction) and abiotic factors (e.g., substrate density, environmental variables). Typically, within Australia, microborers inhabit dead coral substrate rapidly, followed by short lived polychaete species such as *Polydora* (Spionidae) and *Fabriciniids* (Sabellidae) (Hutchings 2011). Within two to six months sipunculans bore into cracks made in the substrate by polychaetes (Hutchings 2011). Kiene and Hutchings (1994) suggest that it is not until three years of exposure that bivalves and sponges populate available substrate. However, Tribollet and Golubic (2005) recorded macroboring of sponges and bivalves in experimental substrate that had been deployed *in situ* for 1 year at multiple sites across the GBR. Additionally, Wizemann et al. (2018) recorded bivalves in substrate after two months of exposure at reefs off Costa Rica. These more recent studies demonstrate that one year of substrate exposure may be adequate to detect other boring organisms. Furthermore, low coverage of sponges across both Eva and Fly reef substrate have been observed (average 0.42%; Chapter 2) suggesting that sponge borings may not be observed here even after three years of exposure. Therefore, endolithic boring rates recorded here are potentially representative of long-term bioerosion, although these rates could fluctuate with environmental change.

Across Eva and Fly reefs, spatial variation in microboring and macroboring activities were recoreded, with greater microboring rates at Eva reef and greater macroboring rates measured at Fly Reef. Eva Reef was characterised by higher light levels whereas Fly Reef had greater chlorophyll-a. These spatial differences in micro and macroboring at each reef suggests that these groups of bioeroders may be driven by different environmental conditions particularly given that the habitat between reefs is comparable. Linear regression further found that macroboring was negatively correlated with both temperature and light. The negative effects of temperature on macroboring are potentially due to temperature anomalies (up to 3.6°C) recorded during the summer months, which may have caused thermal stress and decreased the

activity of macroboring taxa. We offer two theories for the negative relationship found between macroboring and light; firstly, Hutchings et al. (2005) suggest that sedimentation at inshore reef sites may inhibit the settlement and development of epilithic and endolithic algae, which limits grazing, and in turn facilitates recruitment of macroboring taxa. Secondly, sites with lower light levels may be associated with higher levels of chlorophyll-a and other nutrients essentail to zooplankton that are predated on by filter feeding macroborers (Le Grand and Fabricius 2011), increasing their abundance and activity. The lack of a relationship between chlorophyll-a and macroboring is likely due to the fact that chlorophyll-a data (as well as turbidity, salinity, pH) were collected at a lower spatial (one site) and temporal (monthly) resolution. Given that macroborers were significantly correlated with light and temperature collected at a high spatial and temporal resolution, we suggest that future studies attempt to collect all environmental data at this resolution as a means of further developing understandings of environmental influence on bioerosion rates over time.

Within this study, we provide the first rates of endolithic bioerosion for marginal reef systems in Western Australia, where data for both Western Australia and marginal reefs are severely lacking. We found lower than expected rates of bioerosion compared to average global rates, yet rates were comparable to other studies on inshore turbid reefs of the GBR, and studies adopting microCT analysis. Macroborers were the dominant drivers of bioerosion at Eva and Fly reefs and were also more sensitive to environmental change than microborers or grazers. Lower rates of bioerosion across marginal inshore reefs is encouraging as these reefs may be able to maintain a positive carbonate budgets despite lower carbonate production rates. However, as our findings showed global macroboring rates were significantly influenced by chlorophyll-a, the control of nutrient loads may be more important to the survival of inshore reefs than temperature. With changing climates and increasing anthropogenic pressures, the importance of understanding relationships between environmental parameters and ecosystem processes (i.e., bioerosion) has increased exponentially. As we were only able to find seven studies that reported environmental data coupled with bioerosion rates, it is apparent that this is an important knowledge gap. Therefore, an increase in data for the development of empirical relationships between bioerosion activities and environmental parameters,

will allow for high resolution (site specific) environmental data to act as reliable and rapid proxies of bioerosion rates and facilitate the development of ecological models that aim to predict reef carbonate loss and net reef accretion.

Postscript: In the next chapter I combine the knowledge from chapters 2-4, with additional research into site specific calcification rates for two abundant coral species to quantify a detailed estimate of net carbonate production across geomorphic reef zones of Eva and Fly reefs. A comprehensive sediment budget is also quantified from estimates of direct sediment production, bioerosion, and estimates of sediment dissolution.

Chapter 5 The application of carbonate and sediment budgets to assess the stability of marginal reef systems

Preface: This chapter is in preparation for publication and has been formatted according to the journal of *Marine Biology* guidelines. The combined references for all chapters can be found in the Cited Literature-section at the end of this thesis.

5.1 Abstract

Coral reefs and their associated landforms (carbonate islands and shorelines) are under increasing threat from the effects of anthropogenic climate change, including sea level rise (SLR). A reef's ability to 'keep up' with SLR depends on the capacity and rate of which it accretes calcium carbonate. Census-based carbonate budgets offer a comprehensive technique to quantify rates of net calcium carbonate production and, as such, they have been increasingly applied to estimate reef accretionary potential (RAP). To date, most carbonate budget studies have been undertaken in clear-water settings resulting in a limited understanding of how inshore reefs are functioning amongst changing costal environments. Many of these inshore reefs offer protection from wave energy to adjacent shorelines, as well as offering nourishment through carbonate sediment production. Here, we applied census-based carbonate framework and sediment budgets across two inshore island reefs exposed to episodes of high turbidity within the Pilbara, Western Australia. Low net carbonate production (mean = 1.11 and 0.62 kg $m^{-2}yr^{-1}$) were predominantly driven by low coral cover (<10%) and calcification rates. Importantly, bioerosion rates were also low (<0.6 kg $m^{-2}yr^{-1}$), maintaining positive carbonate budgetary states. In contrast, net sediment production rates were high (mean = 1.2 and 3.1 kg $m^{-2}yr^{-1}$) and were found to be mostly derived from mollusc material (34 and 40%). Calculated RAP estimates are below current and predicted rates of SLR, suggesting that these reefs will soon struggle to keep up with increasing water depth and shoreline inundation, leaving little hope for future stability of associated islands. Within this study we also highlight the importance of methodological consistency, and display how variations may impact carbonate budget estimates and interpretations.

5.2 Introduction

More than ever, there is a growing dependence on the stable accretion of coral reefs as rates of sea-level rise (SLR) continue to increase. With rising sea levels, coral

reefs may become ‘drowned’ if they are unable to ‘keep up’ with increasing water depths. Reef accretion is largely driven by scleractinian corals, whose association with the symbiotic algae *Symbiodinium*, promotes rapid rates of calcium carbonate production (Putnam et al. 2017). When alive, these calcifying organisms provide key habitats for a range of marine organisms, promoting biological diversity and supporting important economic and social functions (e.g., tourism, fisheries and culture; Kittinger et al. 2016). Further, higher percentages of live coral cover is intrinsically linked to increased reef structural complexity, which in turn reduces wave energy and resultant coastal erosion of associated landforms (e.g., islands, beaches; Harris et al. 2018). Reef carbonate production is also supported by other calcifying organisms such as crustose coralline algae, which help to build and stabilise the reef framework (Rasser and Riegl 2002) as well as foraminifera, molluscs and *Halimeda* (i.e., direct sediment producers; Harney and Fletcher 2003). These organisms either support reef construction (and accretion) by infilling the reef framework (Perry 1999), or are transported towards shore contributing to landform building, or offshore into deeper waters (Sadd 1984; Kench 1998). Rates of calcium carbonate production are, however, increasingly threatened by both warming temperatures and increasing ocean acidification (Crook et al. 2013; Cornwall et al. 2021). This has implications for the long-term stability of coral reefs and their associated landforms.

The ecological processes that drive reef development and long-term stability can be quantified through the application of the census-based carbonate budget technique. Carbonate budgets measure the net production of reef calcium carbonate. Reef carbonate inputs come from primary (scleractinian corals) and secondary (calcifying encrusters) sources, while the loss of carbonate from the framework occurs through physical, chemical, and biological erosion. These processes can be measured by taking direct measurements of carbonate producing organisms (abundance and carbonate production rates), and eroding functions (abundance of bioeroding taxa, bioerosion rates, and chemical dissolution). The resulting rate of net carbonate production is therefore what determines the rate of reef accretion potential (RAP, Perry et al. 2018). This approach was first developed by Chave et al. (1972) and has since been used in 39 global studies, 75% of which have occurred since the turn of the century (Browne et al. 2021).

Although carbonate budgets are growing in popularity, distinct knowledge gaps and concerns remain. Firstly, there is a lack of diversity of reef type, with the majority (~90%) of census-based carbonate budgets conducted on tropical clearwater reefs (i.e., Caribbean, Stearn and Scoffin 1977; Sadd 1984; Mallela and Perry 2007; Perry et al. 2013; de Bakker et al. 2019; Great Barrier Reef, Hamylton et al. 2013). In particular, there is a lack of carbonate budget data from "marginal" reef systems such as turbid reefs. Secondly, there are inconsistencies in the methodologies used to collect key data components across studies (e.g., coral calcification rates; Browne et al. 2021). Thirdly, studies rarely incorporate carbonate sediment budgets despite the fact that there are a growing number of studies now attempt to link carbonate budgets to associated landform stability (e.g., Perry et al. 2011; de Bakker et al. 2019; Kane and Fletcher 2020). Lastly, very few studies have included environmental data reducing our ability to confidently relate how rates of net carbonate production and reef accretion may change under varying climate scenarios (Browne et al. 2021).

In the past two decades, only four census-based carbonate budget studies have been conducted on inshore reefs exposed to turbidity or urban pollution (Edinger et al. 2000; Mallela and Perry 2007; Browne et al. 2013a; Januchowski-Hartley et al. 2020). Inshore reefs are typically exposed to a high levels of fluctuations of turbidity, salinity, and temperature (Kleypas 1996; Kleypas et al. 1999). These harsh conditions have led to the perception that these reefs are existing at their environmental limits and therefore support lower coral cover and diversity (Morgan et al. 2016). However, recent studies have recorded high levels of coral cover and diversity among turbid settings, as well as a capacity to withstand or quickly recover from disturbance events (Browne 2012; Richards et al. 2015; Cacciapaglia and van Woesik 2016; Guest et al. 2016; Lafratta et al. 2017; Morgan et al. 2017; Evans et al. 2020). With predicted impacts of anthropogenic climate change such as SLR, coupled with local stressors from coastal land-use change, turbid reefs are expected to increase in relative abundance over the coming decades (Ogston and Field 2010). As such, an improved understanding of how ecological drivers of carbonate production and loss will react to changing climatic conditions is becoming increasingly important for global reef conservation efforts.

For census-based carbonate budgets to be of value to reef conservation and coastal landform management, methodologies that capture local ecological processes should be applied. Corals typically drive reef carbonate production rates; therefore, carbonate budgets are heavily influenced by estimated rates of coral growth and carbonate production. Rates of coral carbonate production are influenced by both biological (e.g., species specific growth rates, skeletal density, colony size and morphology; Ryan et al. 2019) and environmental factors (e.g., temperature, pH, light; Venti et al. 2014), and vary considerably over space and time (Bakker et al. 2016; Perry et al. 2017; Ross et al. 2019). There are multiple methods available to quantify coral calcification rates, with measures of linear growth rates being the most popular within carbonate budget studies (Perry et al. 2012; Browne et al. 2013a). Calcification rates (g cm^{-2} yr^{-1}) estimated from linear growth incorporate skeletal extension rates ($cm^{-1}yr^{-1}$) and skeletal density (g cm^{-3}), but do not consider uneven growth across colony surfaces, or variation in density (Edinger et al. 2000; Lough and Barnes 2000; Morgan and Kench 2012). An alternative method is the buoyant weight technique, where a colony (or section of) is weighed while suspended in seawater of a known density before and after a period of time (Bak 1973; Jokiel et al. 1978; Ross et al. 2015; Roik et al. 2016). The advantage of the buoyant weight technique is that it incorporates size and skeletal density, providing accurate and repeatable measures of carbonate production (Herler and Dirnwöber 2011). Although considered more accurate, the buoyant weight method is not often applied within carbonate budget studies, which has likely reduced the accuracy of carbonate production estimates.

Most carbonate budget studies to date have not included an assessment of reef carbonate sediment production. Knowledge on rates of carbonate sediment production (termed the carbonate sediment budget) and how they vary over space and time is critical to understanding the geo-ecological link between reefs and associated landforms (Kench and Cowell 2006; Hamylton et al. 2016). A sediment budget includes rates of direct sediment production minus that lost through dissolution (Cyronak et al. 2013; Eyre et al. 2014; Andersson 2015; Brown et al. 2021) and off reef transport (Kench 1998; Browne et al. 2013b; Morgan and Kench 2014a). Sediment budgets compliment the carbonate 'framework' budget as the type and size of sediment grains, and the rate of their production, is directly related to the

presence and abundance of sediment producing taxa, which are in turn dependent on the functions of the reef framework (Perry et al. 2011). The lack of inclusion of sediment budgets in census-based carbonate budget studies is likely due to either: the difficulties in accurately assessing rates of sediment production (see review by Browne et al. 2021); or that the aim of the study was focused on framework carbonate production and reef health as opposed to the link between reefs and landforms. None the less, there has been a growing interest in applying sediment budgets to predict how unconsolidated carbonate landforms will respond to predicted SLR scenarios (de Bakker et al. 2019; Kane and Fletcher 2020). These assessments require knowledge of carbonate sediment stocks and rates of sediment transport from reefs to islands to accurately make such predictions (Yamano et al. 2005; Kench and Cowell 2006; Morgan and Kench 2016; Cuttler et al. 2019).

This study aimed to produce a comprehensive census-based carbonate reef and sediment budgets for two turbid reef systems situated in northern Western Australia. Importantly, these turbid reefs are associated with small reef islands (<60 hectares; Bonesso et al. 2020) that support endemic terrestrial species (e.g., shore birds) and are of local culture significance (e.g., Indigenous cultures and recreational activities; EPA 2021). As such, our estimates of net carbonate production, RAP, and sediment budgets, provide some of the first insights into the long-term stability of these reefs and their associated islands. Further, we employed the buoyant weight method to estimate rates of carbonate production and compared these to those employed in previous carbonate budget studies to investigate the influence of off-site data on final net carbonate production estimates. Lastly, we have provided a detailed complimentary and comprehensive environmental dataset that links ecological responses to environmental change.

5.3 Methods

5.3.1 Study sites

The southern Pilbara coast of north Western Australia hosts approximately 64 carbonate reef islands. The fringing reef systems that surround these inshore islands are exposed to frequent episodes of high turbidity (36.5 NTU), fluctuating ranges in

temperature (18-32°C) and salinity (35.4-39.6), and high energy storm events (Cyclones; McKenzie et al. 2009; Richards et al. 2016). Yet, they are relatively remote and therefore predominantly void of local anthropogenic pressures.

This study was carried out across two inshore island reef systems, Eva (-21.918454°, 114.433502°) and Fly (-21.804829°, 114.554003°) situated at mouth of the Exmouth Gulf (Figure 5.1). Both reef systems have similar characteristics; specifically, the surrounding reef morphology can be described as a limestone platform which forms into a fringing reef around the northern edge of each island, a macroalgae and seagrass dominated sand bar forming off the south/ south-west, and a sandy lagoon hosting spurs and buttresses around the south-east of each island. Further, as these islands are uninhabited and without any coastal infrastructure, they present an opportunity to investigate "natural" reef processes (Cuttler et al. 2020).

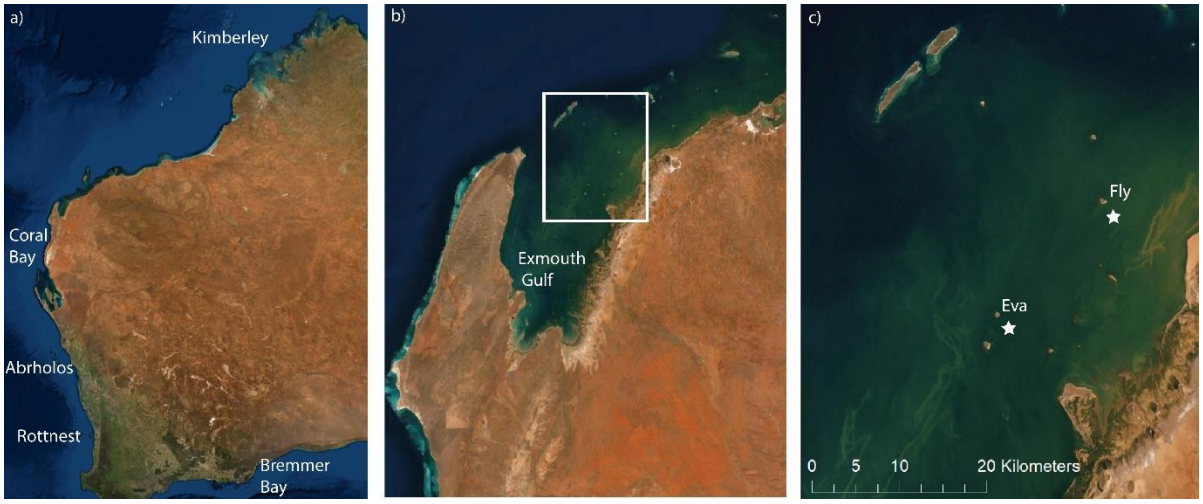

Figure 5.1 (a) Western Australia, showing location of Exmouth Gulf (b), situated at the southern end of the Pilbara region, and (c) the location of Eva and Fly islands. White stars indicate the location where water quality parameters (chlorophyll-a, pH, salinity and turbidity) were measured monthly.

5.3.2 Reef Geomorphology, Habitats, and Zones

To capture the variety of benthic habitats that surround each island, fifteen 20 m long photo line transects were laid parallel to the shore between 1-4 m depth. Along each transect photos were taken with a GoPro (Hero4) set to capture an image every 2 seconds (~0.5 m above seabed) against a measuring tape for an absolute scale, with approximately 60 photos per transect. These photographs (capturing an area of

approximately 2 m^2) were used to assess benthic habitat and coral community using Coral Point Count software (CPCe, Kohler and Gill 2006). Within CPCe, each photo was overlaid with 20 random points that were used to classify the benthos into either coral, macro algae (kelp or seagrass), turfing algae (predominantly growing on dead coral), sandy bottom, rubble, sponge, crustose coralline algae (CCA), or pavement (rock). Corals were classified into morphological groupings (branching, foliose, massive) and identified to genus level. Following benthic identification, the marine habitats surrounding each island were sectioned into five 'zones' for spatial analysis and carbonate production calculations (Figure 5.2). These zones included a northern windward forereef (NWF; characterised by high cover of live coral and turfing algae), eastern leeward reef crest and forereef (ELC; characterised by high live coral cover), southern windward sandbar (SWS; dominated by macroalgae and rubble), southern leeward lagoon (SLL; high sand cover with occasional small coral bommie or sponges), and western windward forereef (WWF; consisting of high sediment cover with spurs and buttresses; Figure 5.2; Table 5.1). *In situ* chain and tape rugosity measurements (*Rug*) were taken with a six-meter-long chain (links were 5 mm wide and 15 mm long) from the start of each transect, which were applied to calculate the habitat area (m^2) of each zone (A_Z);

$$A_Z = A \times Rug_Z \qquad \textit{(Eq.5-1)}$$

Where A_Z is the zone habitat area (m^2), and Rug_z is the average rugosity measured from line transects within that zone, and (A) is the planimetric area of each zone (m^2). Planimetric area was measured from high resolution bathymetric LiDAR data (Chapter 2).

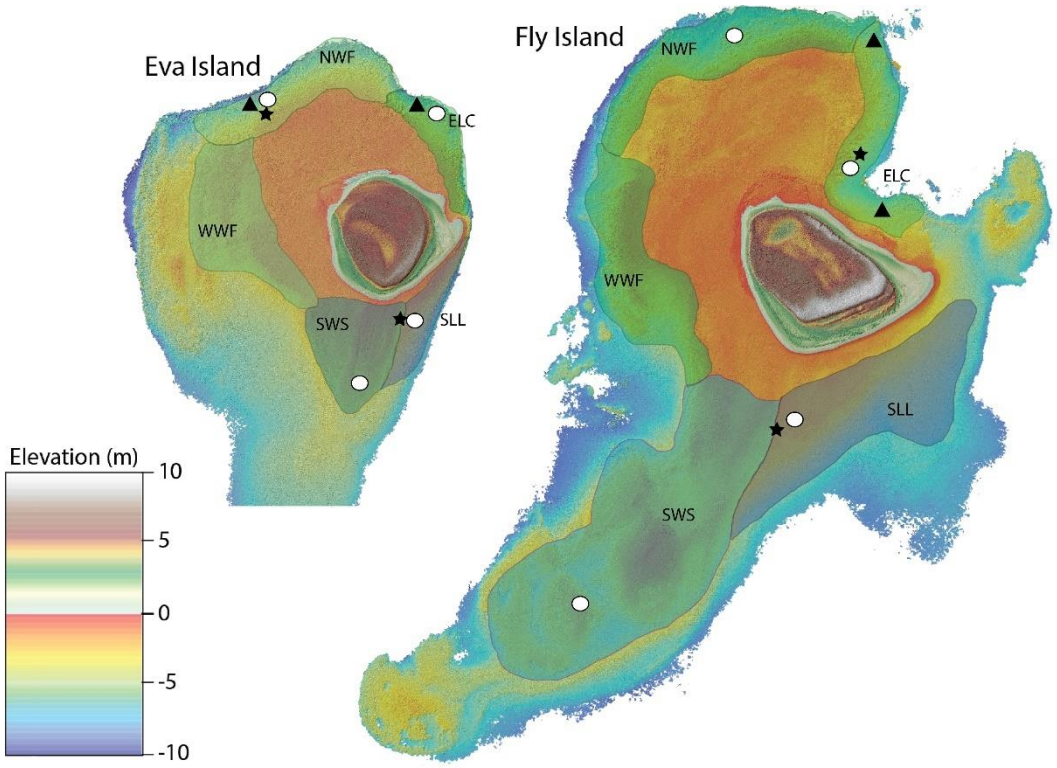

Figure 5.2 Bathymetric imagery of Fly and Eva reefs with transparent overlay displaying the range of each geomorphic reef zone. Reef zones include north windward forereef (NWF), east leeward crest (ELC), southern leeward lagoon (SLL), southern windward sandbar (SWS), and western windward forereef (WWF). White circles represent the location of encruster and bioerosion experiments from chapters 3 and 4, while black stars represent location of where temperature and light loggers were deployed at the benthos, and black triangles show the location of coral growth experiments.

5.3.3 Environmental data

Monthly water quality data (chlorophyll-a, conductivity, salinity, pH, turbidity) was collected offshore of each reef (Figure 5.1) during neap tides between February 2019 and February 2020 (12 months). *In situ* sampling was undertaken using a vertical profiling method with a multi-parameter EXO Sonde 2 (YSI Inc./Xylem Inc.), with detailed methods given in chapter 3. Temperature loggers (°C; Hobo Pendant UA-001-64) and photosynthetic active radiation (PAR) loggers (µmol photons m^{-2} s^{-1}; Odyssey submersible PAR logger) were deployed at each site from March 2019 to April 2020 (collected and replaced in September 2019) with logging intervals of 60 minutes for benthic temperature and 10 minutes for PAR loggers (Chapter 3).

5.3.4 Coral Carbonate Production

Calcification rates for *Acropora spp.* and *Pocillopora damicornis* were measured at four sites across Eva and Fly reefs using the buoyant weight method (Bak 1973; Jokiel et al. 1978; Spencer Davies 1989). These coral species were used as they are abundant across all zones of each reef, are easy to samplewithout damaging large sections of the colony, and are faster growing so are more reflective of environmental conditions at the time of budget assessment (Ross et al. 2017). Calcification rates for all other coral genre were sourced from literature (Table 5.2). Importantly, we included rates of calcification from local studies (e.g., *Acropora, Pocillopora, Goniastrea, Favia, Porites, Turbinaria;* Foster et al. 2014; Dandan et al. 2015; Ross et al. 2015, 2019; Lough et al. 2016) and studies from inshore turbid reefs (e.g., Browne et al. 2013), where possible.

A total of 30 coral nubs (15 *Acropora* and 15 *P.damicornis*) were gathered among eastern and northern sites where coral cover is greatest, and transported to land where they were individually weighed in seawater and then attached to a PVC plate with marine epoxy. Once the epoxy was dry, corals were reweighed to determine the combined weight of the coral, plate and epoxy. Tiles were then attached to metal tripods (n =15) and deployed at the fragment sampling sites (Fig. 5.2). After 13 months of deployment (September 2019 - October 2020) approximately 40% of all coral nubbins had survived. The remaining live samples (total n=16 *Acropora*, and 9 *P.damicornis*) were again buoyantly weighed and coral skeletal mass (g) were calculated using the following equation:

$$M_{air} = \frac{M_{sw} Rho_{CaCO3}}{Rho_{CaCO3} - Rho_{sw}} \qquad \textit{(Eq.5-2)}$$

Where M_{air} is the dry weight of the coral skeleton (g), M_{sw} is the mass of the sample in seawater (g; minus the weight of the tile and epoxy), and Rho_{CaCO3} and Rho_{sw} are the densities of coral and seawater, respectively (Jokiel et al 1978). Rho_{sw} was measured each time samples were being weighed with a hydrometer, and Rho_{CaCO3} is the density of aragonite (2.93 g cm^3). Rates of coral carbonate production were calculated relative to coral surface area (Foster et al. 2014; Ross et al. 2019). The surface area of *Acropora* and *P.damicornis* samples were determined using the surface area to dry weight regressions from Foster et al. (2014), which was based on the same genera and species collected from a reef ~150 km to the south (Coral Bay;

Figure 5.1). Foster et al (2014) found strong linear relationships between and skeletal weight and colony surface area for *Acropora* (R^2=0.98) and *P.damicornis* (R^2=0.97). Relative carbonate production of each coral genus (CCP; kg yr^{-1}) was calculated for each zone from the percent cover and calcification rate of each genus, multiplied by the habitat area (*Az*) of the zone as follows:

$$CCP = coral\,\% \times A_Z \times Calcification\ rate \quad \text{(Eq.5-3)}$$

Gross coral carbonate production (∑CCP; Kg yr^{-1}) of each zone is then the sum of each genus CCP within a zone. In addition, we also quantified carbonate production using calcification rates determined from average linear growth rates and densities for corals (as opposed to the buoyant weight method) measured within the Indo-Pacific (as per *ReefBudget*; Perry et al. 2018a) to compare the difference in total rates of net carbonate production estimates between the two methodologies (Supplementary Table 7Supplementary Table **8**).

5.3.5 Encruster Carbonate Production

To obtain encruster carbonate production rates, encruster growth tiles were deployed at four locations around each of the two reefs (Chapter 3). Eight PVC tiles (10 cm x 10 cm) were deployed at each of the four locations (32 tiles per reef) in April 2019. Four tiles at each site were removed after a six month winter period (April 2019 to September 2019) and replaced with four clean tiles to capture the summer growth period (September 2019 to April 2020). The remaining four tiles stayed *in situ* for a whole year to provide annual encruster growth and calcification rates. Once collected, tiles were treated with a 5% solution of sodium hypochlorite (NaClO) for 24 hours to remove all organic tissue, leaving carbonate deposits intact. After rinsing in distilled water, tiles were dried at 50°C for 24 hrs. Each tile was weighed and then placed in a dilute (10%) solution of hydrochloric acid (HCl) to dissolve all calcium carbonate. Tiles were again rinsed, dried, and reweighed. Rates of encrusting carbonate production were calculated as follows:

$$\text{ECR} = \left(\frac{(ig-eg)}{days} \div SA\right) \times 365 \quad \textit{(Eq.5-4)}$$

Encrusting calcification rate (ECR; kg m^{-2} yr^{-1}) was calculated as the total mass (g) of net carbonate accretion (initial weight (*ig*) minus end weight (*eg*)), divided by the

deployment duration (*days*) and surface area of the tile (*SA*), and multiplied by 365 to provide annual rates (Mallela 2013; Morgan and Kench 2017). Zonal encruster carbonate production (ECP; kg yr^{-1}) was then calculated as the percent cover of CCA multiplied by the encrusting calcification rate, and the habitat area (A_z) of each zone (Eq.5-5).

$$ECP = CCA\ cover\ \% \times encrusting\ calcification\ rate \times A_Z \quad \textit{(Eq.5-5)}$$

CCA benthic cover (%) determined from the *in situ* transects was used to represent calcifying encruster abundance as CCA was the dominant encruster on the tiles (Chapter 3).

As encruster tiles were not deployed in the western zones, theoretical calcification rates were applied matching that of the northern zones, which had a similar environmental profile (i.e., wave exposure, depth, light, temperature, substrate cover). This same approach was taken for bioerosion rates and environmental conditions. We strongly ephasis that the results recorded in this chapter for the WWC zones is hypothetical.

5.3.6 Gross carbonate production

Gross carbonate framework production (GF kg yr^{-1}) for each zone was calculated as the sum of the total mass produced by corals and encrusting organisms (Eq.5-6). The normalized gross framework production rate (GFN kg m^{-2} yr^{-1}) for each zone was calculated by dividing the total mass of carbonate produced by the zone area (Eq.5-7).

$$GF = \sum CCP + \sum ECP \quad \textit{(Eq.5-6)}$$

$$GFN = GF \div A_Z \quad \textit{(Eq.5-7)}$$

5.3.7 Framework Bioerosion

Bioerosion monitoring units (BMU) were used to independently measure endolithic bioerosion across reef zones. Clean cores of *Porites lutea* collected from the South Cay of Willis Island (Great Barrier Reef) were cut into 2 x 5 x 1 cm blocks. As *Porites lutea* is a dominant coral species at Eva and Fly reefs, these blocks were considered suitable representative for Eva and Fly reefs (Chapter 4*)*. 16 BMUs were deployed across each reef for a total of one year. Once BMUs were collected, they

were individually soaked in 5% NaClO for 24 hours to remove organic matter, rinsed with distilled water, and dried at 50°C for 24 hours. Prior to deployment, BMUs were scanned using a Micro computed tomography (micro-CT; Skyscan1176, 90 kV, 273 µA), which was then repeated after collected BMUs were cleaned of organic matter to determine volume lost due to bioerosion. Details of scan settings and methodology are reported in Chapter 4. By comparing BMU carbonate volume before and after deployment, total bioerosion rate (kg m^{-2} yr^{-1}) was calculated as:

$$Bioerosion\ rate\ = (Vol_i\ \times Rho_i) \div (SA_i\ \times\ T) \qquad (Eq.5\text{-}8)$$

where i refers to the individual BMU, Vol_i is the volume lost (m^3) during deployment, SA_i is the surface area of the BMU pre-deployment, Rho_i is the original density of the BMU pre-deployment, and T is the time in years that the unit was deployed for (DeCarlo et al. 2014; Silbiger et al. 2016).

External bioerosion (grazing) rates were quantified using urchin abundance estimates along 20 m transects (15 per reefs) and diver-operated stereo-video (DOV) to collect data on fish abundance and biomass. Given very low urchin abundance across both reefs (<5 individuals per reef), urchins were excluded from the analysis. Bioerosion rates for fish were determined using the "Indo-Pacific" data spreadsheet available from the *Reef Budget* website (https://geography.exeter.ac.uk/reefbudget/indopacific/). Zonal bioerosion rates (Br, kg yr^{-1}) were calculated as follows:

$$Br\ = Bioerosion\ rate \times \%\ available\ substrate\ \times A_Z \qquad (Eq.5\text{-}9)$$

$$BrN\ =\ Br\ \div\ A_Z \qquad (Eq.5\text{-}10)$$

where the bioerosion rate (combination of internal measured from BMU and external measured by DOV) is zone specific, available substrate represents the percent cover of dead carbonate substrate (turfing algae), and *Az* is the zone area. The normalized bioerosion rate (*BrN*, kg m^{-2} yr^{-1}) is then calculated as total zonal bioerosion divided by the habitat area.

5.3.8 Reef accretion and growth

To calculate net carbonate framework production (*G*, kg m^{-2} yr^{-1}) the following equation was applied:

$$G = GFN - GBrN \quad \textit{(Eq.5-11)}$$

Where GFN is the gross normalized framework carbonate production by corals and encrusting organisms, and GBrN is the gross normalized bioerosion rate across the zone. The reef accretion potential (RAP mm yr^{-1}; Eq 12) for each zone is determined by dividing the net framework production (*G*) by the density of aragonite (2.93 g cm^3) and correcting for reef porosity (Rpor), which is taken as 20% as observed within reef cores extracted from turbid zone reefs on the GBR (Palmer et al. 2010).

$$RAP = (G \times 2.93) \div (100 - Rpor) \times 100 \quad \textit{(Eq.5-12)}$$

5.3.9 Direct sediment production

Sediment samples were taken from each transect location (15 samples per reef). Samples were carefully collected by hand with a scoop (250 cm^3) from the upper layer and carefully placed into a zip-lock bag. Sediments were soaked with bleach for 24 hours to remove organic matter and were then rinsed with distilled water and dried at 50°C for 24 hours before being weighed. Carbonate content was determined using approximately 5–7 g of the original sample to which 10% HCl solution was added to dissolve the calcium carbonate. After 24 hours the non-carbonate residue was filtered through a pre-weighed 90 µm pore size filter paper using a suction filter and oven dried at 50°C for 24 hours. Once the filter paper was dry, the paper and the sample were reweighed. Carbonate content (%) was calculated by subtracting the post-dissolved sample minus filter paper weight (S_p) from the pre-dissolved sample minus filter paper weight (S_i), divided by S_i and then multiplied by 100.

$$CaCO_3\ \% = \frac{(S_i - S_p)}{S_i} \times 100 \quad \textit{(Eq.13)}$$

Sediment type was determined using a stereo microscope (Nikon SMZ745T). A subsample (~200 g) was dry sieved into five sieve fractions (<63 µm, 63-150 µm, 150-250 µm, 0.25-0.5 mm, 0.5-1 mm, 1-2 mm, >2 mm) and composition was assessed by identifying 100 sediment grains for each size class. Grains were identified for fractions >150 µmm as one of the following: hard coral, bivalve, gastropod, CCA, foraminifera, serpulid worms, crustacean, sponge spicules, echinoderm spine, unknown, or terrigenous. Sediment composition was expressed as the relative percentage abundance of the total sample and for each of the sieved sub-samples. Direct carbonate sediment production (SPR, kg m^{-2} yr^{-1}) by molluscs, CCA and foraminifera (typically the most abundant organisms with the exception of coral

fragments, table 5) was determined by calculating the sediment biomass (dry weight of field sample ÷ estimated surface area harvested, 0.1m^2) and multiplying the biomass by the organism's abundance (% of sample), the percentage of calcium carbonate (%$CaCO_3$) and the organism's turnover rate as per follows:

$$SPR = (Biomass \times abundance) \times \%CaCO3 \times turnover\ rate \qquad (Eq.5\text{-}13)$$

Turnover rates represent an estimate of calcium carbonate that is deposited into the reef system when an organism dies (Odum 1959). As such, a turnover rate of 1 per year was applied to foraminifera (Hallock et al. 1995), a rate of 2 per year was applied to molluscs, and a rate of 0.5 per year was applied to CCA (Harney and Fletcher 2003). Annual sediment production (*ASP*, kg yr^{-1}) for each zone is then calculated as the total direct sediment production by molluscs, CCA and foraminifera ($\sum SPR$) multiplied by the habitat area (A_Z) and the zonal percentage sediment cover (Eq.5-14). Normalized direct sediment production rates (SPR_N, kg m^{-2} yr^{-1}) can then be calculated by dividing annal sediment production (*ASP*) by the habitat area (A_Z; *Eq 5-15*).

$$ASP = \sum SPR \times A_Z \times \%\ sediment\ cover \qquad (Eq.5\text{-}14)$$

$$SPR_N = ASP \div A_Z \qquad (Eq.5\text{-}15)$$

5.3.10 Sediment budget

The net sediment budget was calculated from calculating gross sediment production and subtracting a rate of sediment dissolution. Gross carbonate sediment production was determined by adding the yearly amount of bioeroded sediment from macroborers and grazers to the yearly amount of carbonate sediments produced by the direct sediment producers. Sediment produced by macroborers is considered to be 80% of total macroboring as approximately 20% of eroded volume is estimated to be lost through chemical dissolution (Nava and Carballo 2008). Rates from microborers were excluded as majority of microboring processes involve chemical dissolutions (i.e., no sediment is formed; Perry et al. 2017). Sediment dissolution (SD) for each zone was estimated from rates recorded in Brown et al (2020) based on zone geomorphic setting. A sediment dissolution rate of 0.296 kg m^{-2}yr^{-1} was applied to forereef zones (NWF, ELC, WWF), while a rate of 1.07 kg m^{-2}yr^{-1} was applied for lagoonal settings (SLL, SWS; Brown et al. 2020)

$$SD = sediment\ dissolution\ rate\ \times \%\ sediment\ cover \quad (Eq.5\text{-}16)$$

The gross sediment production *(GSP,* kg m^{-2} yr^{-1}*)* for each zone is the sum of annual direct carbonate sediment production (*ASP*) and the rate of external erosion by grazers (*BrG*), minus sediment dissolution (SD; Eq 17). This is then normalized by dividing the GSP by the habitat area (*Az; Eq. 18*).

$$GSP = (ASP + BrG) - SD \quad (Eq.5\text{-}17)$$

$$GSPN = SB\ \div A_Z \quad (Eq.5\text{-}18)$$

5.4 Results

5.4.1 Benthic community description

Benthic cover was comparable between reefs with similar coral cover (8% at Fly, 10% at Eva) and fleshy algal cover dominating the benthos (macroalgae = 56% at Eva, and 35% at Fly; turfing algae = 16% at Eva, and 15% at Fly; Chapter 1). Both reefs displayed distinct differences in benthic cover between south and north/east reef zones. Southern zones were characterised by higher macroalgae cover (52-67% for Fly and Eva respectively) and exceptionally low coral cover (0-2%). Whereas northern and eastern zones displayed lower macroalgae cover (0-28%) and higher coral cover (29-37%), and high cover of turfing algae (16-35%) with the latter growing predominantly on dead coral substrate. Eva reef hosts a higher percentage of branching corals compared to Fly (Eva = 26%, Fly =15%), while there is a higher percentage of massives at Fly (Eva = 35%, Fly =45%), and an equal percentage of foliose corals between reefs (Eva = 39%, Fly =40%; Figure 5.3). The highest coral cover recorded at Eva reef was 62% within the northern zone, while a maximum cover of 48% was recorded within the eastern zone of Fry reef.

5.4.2 Environment

Some environmental variables had minimal variation between reefs, such as average benthic water temperature (Fly 24.9 ± 0.02°C; Eva 24.8 ± 0.02°C), salinity (Fly mean = 38.16 ± 0.42; Eva mean = 38.34 ± 0.46), and conductivity (Fly mean = 57149 ± 982 µS cm^{-1}; Eva mean = 57150 ± 965 µS cm^{-1}; Table 5.1). However, Fly reef experienced annual mean turbidity levels nearly 50% higher than Eva reef (Fly mean = 2.27 ± 0.36 FNU; Eva mean = 1.48 ± 0.33 FNU), as well as slightly higher

chlorophyll-a (Fly mean = 0.49 ± 0.05 µg L^{-1}; Eva mean = 0.38 ± 0.05 µg L^{-1}) and pH (Fly mean = 8.19 ± 0.03; Eva mean = 8.17 ± 0.01), whereas Eva recorded higher levels of light at the benthos (Fly mean = 177.52 ± 1.73µmol photons m^{-2} s^{-1}; Eva mean = 228.06 ± 2.38µmol photons m^{-2} s^{-1}).

5.4.3 Gross Carbonate Production

Calcification rates measured in this study were low (*Acropora* = 0.25 g cm^{-2} yr^{-1}, *Pocillopora* = 0.21 g cm^{-2} yr^{-1}), yet comparable to buoyant weight measures of these and other taxa along the Western Australian coast (Foster et al. 2014; Dandan et al. 2015; Ross et al. 2015, 2019, Table 5.2). As such, Eva and Fly reefs both displayed low average coral carbonate production rates (Eva = 0.97 ± 0.26 kg m^{-2} yr^{-1}, Fly = 0.54 ± 0.49 kg m^{-2} yr^{-1}). The largest zones of coral carbonate production were the northern zone (NWF) of Eva (2.54 ± 1.33 kg m^{-2} yr^{-1}) and the eastern zone (ELC) of Fly (2.03 ± 0.98 kg m^{-2} yr^{-1}), while the lowest coral carbonate production at both reefs was among the southern sand-bar zone (SWS; 0.08 ± 0.01 kg m^{-2} yr^{-1} and 0.00 kg $m^{-2}yr^{-1}$ at Eva and Fly, respectively Table 5.3). The two dominant carbonate producing genera across both reefs were *Turbinaria* (26-38%) and *Porites* (27-33%), while *Pavona* had the highest relative contribution to Eva reef's gross carbonate production (~30%; Figure 5.3).

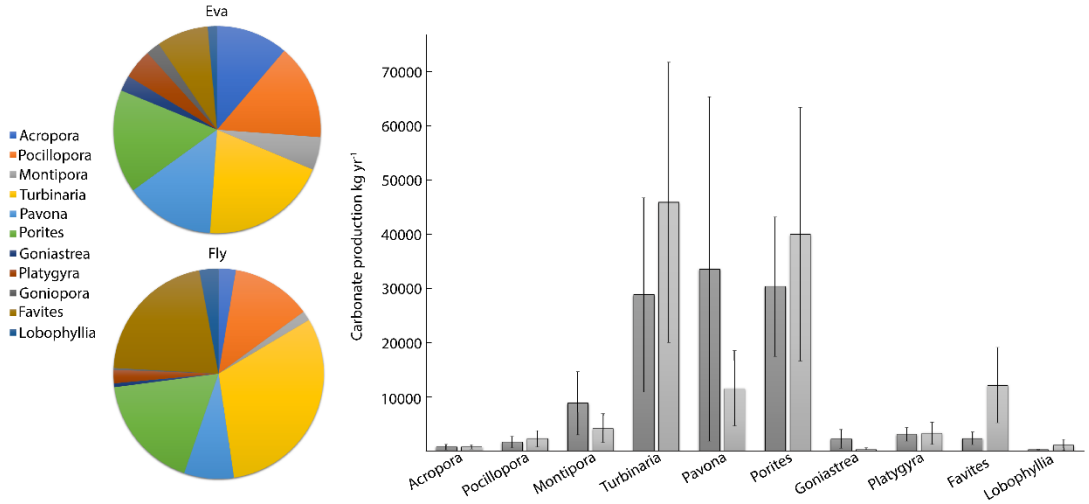

Figure 5.3 The relative cover (a) and contribution of each major coral genera to the overall coral carbonate production (b) at Eva and Fly reefs, error bars represent standard error.

Table 5.1 Benthic habitat and environmental characteristics of each geomorphic zone together with the mean annual estimates of the environmental variables. Geomorphic zones of each reef are northern windward forereef (NWF; characterised by high cover of live coral and turfing algae), eastern leeward reef crest and forereef (ELC; characterised by high live coral cover), southern windward sandbar (SWS; dominated by macroalgae and rubble), southern leeward lagoon (SLL; high sand cover with occasional small coral bombie or sponges), and western windward forereef (WWF; consisting of high sediment cover with spurs and buttresses. Note that light and temperature were measured at the benthos at two sites per reef whereas chlorophyll-a, pH, salinity and turbidity were measured offshore of both Eva and Fly; Figure 5.1).

					Substrate cover (%)				Environment					
Reef	Zone	Habitat size (m^2)	Average Rugosity	Depth (m)	Coral	MA	Old dead coral	Sand	Light (PAR)	Temperature (°C)	Chlorophyll ($\mu g\ L^{-1}$)	pH	Turbidity (FNU)	Salinity
Eva	NWF	156316	1.6	3.5	23	56	11	2	142.04 (±59.90)	27.15 (±0.80)	0.38 (±0.05)	8.18 (±0.01)	1.48 (±0.33)	38.16 (±0.42)
Eva	ELC	85589	1.4	3.1	11	38	38	6	311.17 (±73.15)	27.15 (±0.80)				
Eva	SWS	125198	1.3	3.6	2	65	4	11	142.04 (±59.90)	26.90 (±0.86)				
Eva	SLL	54307	1.4	2.7	6	66	6	15	311.17 (±73.15)	26.90 (±0.86)				
Eva	WWC	182116	1.3	3.4	5	55	6	13	142.04 (±59.90)	27.15 (±0.80)				
Fly	NWF	274563	1.5	4.0	6	21	22	12	106.62 (±36.10)	27.20 (±0.89)	0.49 (±0.06)	8.19 (±0.03)	2.27 (±0.36)	38.34 (±0.46)
Fly	ELC	157566	1.7	4.5	23	16	27	15	106.62 (±36.10)	27.20 (±0.89)				
Fly	SWS	429132	1.1	3.1	0	73	0	19	127.08 (±65.53)	27.32 (±0.89)				
Fly	SLL	253656	1.0	3.0	1	27	2	40	127.08 (±65.53)	27.32 (±0.89)				
Fly	WWC	334414	2.1	2.7	1	48	17	5	106.62 (±36.10)	27.20 (±0.89)				

Table 5.2 Coral calcification rates for each major coral genera recorded at Eva and Fly reefs. Here we compare the calcification rates of branching corals measured *in situ* with offsite rates from local studies. Local calcification rates for some of the massive corals were available but were supplemented with studies outside of WA (shaded in grey). Methodologies used to measure calcification rates were buoyant weight (BW), linear growth bands (LG) or coral core growth bands (CC). All rates of foliose and plating corals were only available from external studies. * indicates calcification rate used in this study

Morphology	Genus	Calcification Rate ($g\ cm^{-2}\ yr^{-1}$)	Region	Method	Source
Branching	*Acropora*	0.25*	Exmouth Gulf	BW	This study
		0.44	Pilbara and Kimberly	BW	Dandan 2015
		0.61	Rottnest Island	BW	Ross 2015
		0.42	Coral Bay	BW	Foster 2016
	Pocillopora	0.21*	Exmouth Gulf	BW	This study
		0.23	Rottnest Island	BW	Ross 2015
		0.34	Coral Bay	BW	Foster 2016
Foliose/plate	*Montipora*	1.52*	Inshore GBR	LG	Browne 2012
	Turbinaria	1.37*	Inshore GBR	LG	Browne 2012
		0.16	Bremer Bay	BW	Ross 2019
	Pavona	1.25*	Central Mexican Pacific	LG	Tortolero-Langarica et al. 2020
Massive	*Porites*	1.62*	Pilbara Islands	CC	Lough 2015
	Goniastrea	0.45*	Coral Bay	BW	Foster 2016
	Favia	0.37*	Pilbara and Kimberly	BW	Dandan 2015
	Lobophyllia	0.23*	Pilbara and Kimberly	BW	Dandan 2015
	Platygyra	1.10*	Persian Gulf	LG	Howells et al. 2018

Average encruster carbonate production rates at Eva and Fly reef were 0.12 ± 0.05 kg $m^{-2}\ yr^{-1}$ and 0.08 ± 0.03 kg $m^{-2}\ yr^{-1}$, respectively (Chapter 3, Table 5.3). The eastern zone (ELC) of Eva reef produced the highest average carbonate production rates (0.31 ± 0.01 kg $m^{-2}\ yr^{-1}$, while the southern zone (SWS) of each reef produced the lowest (0.03 ± 0.01 kg $m^{-2}\ yr^{-1}$ at both reefs).

Total annual gross carbonate production was 117×10^3 kg yr^{-1} at Eva Reef of which 88% was produced by corals, and 125×10^3 kg yr^{-1} at Fly reef, of which 82% was produced by corals.

5.4.4 Bioerosion

A total of 449 fish were recorded on DOV surveys, with only 13 of these being the herbivorous parrotfish *Scarus ghobban.* These counts translated to a relative abundance of 2.6 ± 0.75 individauals per km^2 and biomass of 2.2 ± 1.4 kg km^{-2}, with parrotfish mostly being observed in macroalgae dominated habitats (e.g., SWS). Invertivores (fish that feed on invertebrates) displayed the largest relative biomass of 4.5 kg km^2.

Total average bioerosion rates were low across both reefs (0.17 ± 0.03 kg m^{-2} yr^{-1} at Eva, and 0.16 ± 0.02 kg m^{-2} yr^{-1} at Fly: Table 5.4). The majority of bioerosion at Eva reef was due to grazing by parrotfish (67%), while macroboring was the dominant source of bioerosion at Fly reef (47%) closely followed by grazing (45%). The highest rates of total bioerosion were recorded in the SWS zone of Eva (0.22 ± 0.05 kg m^{-2} yr^{-1}), and the SLL at Fly (0.23 ± 0.05 kg m^{-2} yr^{-1}). The NWF zones of both reefs displayed the lowest rates of bioerosion (0.06 ± 0.01 kg m^{-2} yr^{-1}, and 0.09 ± 0.004 kg m^{-2} yr^{-1} at Eva and Fly respectively).

Table 5.3 Carbonate production (kg yr^{-1}), and normalised carbonate production (kg $m^{-2}yr^{-1}$) from corals and calcifying encrusters, as well as gross normalised carbonate production (kg $m^{-2}yr^{-1}$) per reef zone across Eva and Fly reefs.

	Coral carbonate production		Encruster carbonate production		
	Carbonate production $x10^3$ kg yr^{-1}	Normalised Carbonate production kg $m^{-2}yr^{-1}$	Carbonate production $x10^3$ kg yr^{-1}	Normalised Carbonate production kg $m^{-2}yr^{-1}$	Gross Normalised Carbonate production kg $m^{-2}yr^{-1}$
Eva					
NWF	397.00	2.54 ± 1.33	18.30	0.12 ± 0.01	2.66 ± 1.34
ELC	16.51	0.88 ± 0.21	26.33	0.31 ± 0.01	1.18 ± 0.21
SWS	9.85	0.08 ± 0.05	3.63	0.03 ± 0.01	0.11 ± 0.05
SLL	43.48	1.09 ± 0.42	2.25	0.04 ± 0.00	1.13 ± 0.42
WWC	48.66	0.27 ± 0.25	38.03	0.21 ± 0.01	0.48 ± 0.26
Mean	**221.46**	**0.97 ± 0.45**	**17.71**	**0.12 ± 0.05**	**1.11 ± 0.26**
Fly					
NWF	146.09	0.53 ± 0.47	23.350	0.09 ± 0.04	0.62 ± 0.47
ELC	319.63	2.03 ± 1.73	4.911	0.03 ± 0.01	2.06 ± 1.74
SWS	0.00	0.00 ± 0.00	12.503	0.03 ± 0.01	0.03 ± 0.00
SLL	15.88	0.06 ± 0.04	45.457	0.18 ± 0.04	0.24 ± 0.04
WWC	29.01	0.09 ± 0.21	27.926	0.08 ± 0.02	0.17 ± 0.21
Mean	**102.12**	**0.54 ± 0.38**	**22.83**	**0.08 ± 0.03**	**0.62 ± 0.49**

5.4.5 Net Carbonate Framework production and accretion

Mean net carbonate framework production at Eva reef was 1.01 ± 0.46 kg m^{-2} yr^{-1}, while Fly produced a mean net carbonate framework production rate of 0.47 ± 0.38 kg m^{-2} yr^{-1}. Across Eva reef net carbonate framework production ranged from -0.11kg m^{-2} yr^{-1} in the SWS zone to 2.59 kg m^{-2} yr^{-1} in the NWF zone. Net carbonate framework production at Fly ranged from -0.16 kg m^{-2} yr^{-1} in the SWS zone to 1.91 kg m^{-2} yr^{-1} in the ELC.

The NWF zone of Eva reef showed the greatest RAP at 1.11 mm yr^{-1}, followed by the ELC and SLL zones at 0.46 and 0.45 mm yr^{-1}, respectively. The ELC zone of Fly showed the greatest RAP at 0.65 mm yr^{-1}. The SWS zone of each reef showed negative RAP (Eva = -0.05 mm yr-1; Fly = -0.06 mm yr^{-1}).

Table 5.4 Carbonate production and bioerosion rates (kg $m^{-2}yr^{-1)}$ for each geomorphic zone across Eva and Fly reefs, with resulting net carbonate production rate (G; kg $m^{-2}yr^{-1}$) and estimated reef accretion potential (RAP; mm yr^{-1}) ± standard error

	Carbonate production kg $m^{-2}yr^{-1}$	Bioerosion kg $m^{-2}yr^{-1}$	Net carbonate production kg $m^{-2}yr^{-1}$	Net reef accretion mm yr^{-1}
Eva				
NWF	2.66 ± 0.33	0.06 ± 0.01	2.59 ± 0.34	1.11
ELC	1.18 ± 0.21	0.10 ± 0.01	1.09 ± 0.23	0.46
SWS	0.11 ± 0.05	0.22 ± 0.05	-0.11 ± 0.10	-0.05
SLL	1.13 ± 0.42	0.07 ± 0.01	1.06 ± 0.44	0.45
WWC	0.48 ± 0.26	0.07 ± 0.01	0.40 ± 0.26	0.17
Mean	**1.11 ± 0.44**	**0.17 ± 0.03**	**1.01 ± 0.46**	**0.43 ± 0.19**
Fly				
NWF	0.62 ± 0.47	0.09 ± 0.00	0.53 ± 0.48	0.18
ELC	2.06 ± 1.74	0.15 ± 0.02	1.91 ± 1.75	0.65
SWS	0.03 ± 0.00	0.19 ± 0.06	-0.16 ± 0.06	-0.06
SLL	0.24 ± 0.04	0.23 ± 0.05	0.02 ± 0.09	0.01
WWC	0.17 ± 0.21	0.04 ± 0.03	0.04 ± 0.24	0.01
Mean	**0.62 ± 0.37**	**0.16 ± 0.02**	**0.47 ± 0.38**	**0.16 ± 0.13**

5.4.6 Direct Sediment Production

The average direct sediment production rate at Eva reef was 1.18 ± 0.03 kg m^{-2} yr^{-1}. Approximately 90% of non-coral sediment production was from mollusc (Table 5.5), producing an average 0.10 ± 0.02 kg m^{-2} yr^{-1} non-coral carbonate sediment. The remaining 10% was from foraminifera (9%) and CCA (1%). The average $CaCO_3$

content for sediment samples taken from Eva was 94.6%, with corals contributing to the majority of the sample (36.5%; Table 5.5).

Fly had a larger average direct sediment production rate of 3.14 ± 0.59 kg m^{-2} yr^{-1}. Similar to Eva, molluscs at Fly reef contributed approximately 88% of non-coral sediment production, resulting in an average 2.54 ± 0.58 kg m^{-2} yr^{-1} of non-coral carbonate sediment, while forams contributed 10.5% and CCA 1.5%. The average $CaCO_3$ content of samples at from Fly was 86.2%, with molluscs contributing to the majority of sediment grains (40.1%; Table 5.5).

Table 5.5 Generalised sediment characteristics of Eva and Fly reef

	Dominant grain size	Size classification	$CaCO_3$ %	% of identified grains across all fractions			
				Coral	Mollusc	Foraminifera	CCA
Eva	0.5-1mm (38.6%)	Coarse sand	94.6	36.5	34.2	6.7	6.0
Fly	0.5-1mm (29.9%)	Coarse sand	86.2	34.9	40.1	8.9	6.8

5.4.7 Net Carbonate Sediment Production

Across Eva reef, the average amount of bioeroded sediment produced from macroborers and grazers was 17.59 $x10^3$ ± 3.64 $x10^3$ kg yr^{-1} (Table 5.6). When combined with direct sediment produced by mollusc, foraminifera, and CCA, the average normalised gross sediment production rate of Eva reef was 1.27 ± 0.317 kg m^{-2} yr^{-1}. The average amount of bioeroded sediment produced at Fly reef was higher at 39.31 $x10^3$ ± 11.72 $x10^3$ kg yr^{-1}, which when combined with direct sediment production resulted in a greater average normalised gross sediment production rate of 3.27 ± 0.77 kg m^{-2} yr^{-1} (Table 5.6).

The average sediment dissolution rate at Eva and Fly reef was 0.07 ± 0.00 kg m^{-2} yr^{-1} and 0.16 ± 0.08 kg m^{-2} yr^{-1}, respectively. The highest rates of dissolution were measured within the SLL zones at both reefs (Table 5.6). However, zones with the highest dissolution rates did not correspond with zones with the lowest net carbonate sediment production illustrating that gross rates of sediment production were driving spatial differences in net carbonate sediment production. The average rate of net sediment production at Fly reef (3.11 ± 0.71 kg m^{-2} yr^{-1}) was almost double that estimated at Eva reef (1.20 ± 0.30 kg m^{-2} yr^{-1}) due to very high rates of direct sediment production in Fly's NWF and SWW zones (Table 5.6).

Table 5.6 Sediment budget for Eva and Fly reefs including calculated gross sediment production (kg $cm^{-2}yr^{-1}$) from direct sediment production and sediment derived from bioerosion ($x10^3$ kg yr^{-1}), estimated sediment dissolution rates (kg $cm^{-2}yr^{-1}$), and net carbonate sediment production rates for each geomorphic zone.

	Total direct sediment $x10^3$ kg/yr^{-1}	*Total bioeroded sediment $x10^3$ kg/yr^{-1}*	*Gross sediment production rate kg $m^{-2}yr^{-1}$*	*Sediment dissolution kg $m^{-2}yr^{-1}$*	*Net Carbonate sediment production kg $m^{-2}yr^{-1}$*
Eva					
NWF	30.71	7.98	0.25	0.01	0.24
ELC	75.33	6.83	0.96	0.02	0.94
SWS	147.23	24.50	1.37	0.11	1.26
SLL	87.87	3.53	1.68	0.17	1.51
WWC	368.24	9.93	2.08	0.05	2.03
Mean	**141.9 ± 59.6**	**17.59 ±3.64**	**1.27 ± 0.31**	**0.07 ± 0.03**	**1.20 ± 0.30**
Fly					
NWF	1177.11	16.33	4.35	0.09	4.26
ELC	302.49	18.51	2.04	0.04	2.00
SWS	1215.41	80.42	3.02	0.20	2.82
SLL	1373.63	47.49	5.60	0.46	5.15
WWC	412.39	33.81	1.33	0.02	1.32
Mean	**896.2 ± 223.1**	**39.31 ± 11.72**	**3.27 ± 0.77**	**0.16 ± 0.08**	**3.11 ± 0.71**

5.5 Discussion

5.5.1 Pilbara islands reef carbonate budgets

Eva and Fly reefs currently have a low budgetary state with net carbonate framework production at 1.01 ± 0.46 and 0.47 ± 0.38 kg m^{-2} yr^{-1}, respectively. In contrast, neighbouring Ningaloo Reef, which lies in the clear waters off the western side of the Exmouth peninsula, has a greater net carbonate production rate between 1.4 and 3.9 kg m^{-2} yr^{-1} (see Perry et al. 2018b) suggesting that Ningaloo is in a healthier state and actively accreting. Rates of net carbonate production measured in this study are more comparable to clear water Indo-Pacific reefs considered to be degraded either following acute disturbance events or from reefs exposed to chronic stressors such as poor water quality. For example, Perry and Morgan (2017) recorded a mean net budget of -3.0 kg m^{-2} yr^{-1} on a reef platform of the Maldives, while Januchowski-Hartley et al. (2017) recorded net budgets ranging from -3.9 to 5.8 kg m^{-2} yr^{-1} across

the Seychelles. These reefs were in a negative budget state due to high coral mortality following bleaching events (1998 and 2016) and increased rates of parrotfish bioerosion. Similar carbonate budget states have been recorded among turbid reefs of the Indo-Pacific. A recent study on Singapore's inshore turbid reefs recorded a low mean net carbonate budget of 0.68 kg m^{-2} yr^{-1} (Januchowski-Hartley et al. 2020) while Edinger et al. (2000) recorded variable, yet comparable, net carbonate production rates for turbid and polluted reef sites in Indonesia (-7.38 to 2.51 kg m^{-2} yr^{-1}). Both of the sites studied in Singapore and Indonesia have moderate coral cover (~21-25%) dominated by slower-growing stress-tolerant species, and higher rates of endolithic bioerosion traditionally expected of marginal reef systems. These comparisons support previous assumptions that southern Pilbara reefs are existing in marginal settings and are vulnerable despite a lack of local anthropogenic stressors.

5.5.2 Carbonate production rates

Low coral calcification rates across Eva and Fly reefs could either reflect the reduced capacity of corals to produce carbonate, or the different methodologies used between carbonate budget studies. Across all sites, we recorded average calcification rates of 0.25 g cm^{-2} yr^{-1} for *Acropora.spp* and 0.21 g cm^{-2} yr^{-1} for *Pocillopora damicornis,* which were comparable to studies at healthy clear water reefs of Western Australia using the same buoyant weighing method. These studies included Foster et al (2014) which recorded an *Acropora* calcification rate of 0.42 g cm^{-2} yr^{-1} in Coral Bay and Ross et al. (2015) where *Acropora* calcification rates of 0.61 g cm^{-2} yr^{-1} from Rottnest Island were observed (Figure 5.1). Most previous carbonate budget studies have used linear extension rates, which typically estimate greater rates of coral calcification for branching corals (e.g., 6.2 g cm^{-2} yr^{-1} Browne et al. 2013; 1.75 g cm^{-2} yr^{-1} Morgan and Kench 2012). Given the impact that these calcification rates have on the final net carbonate production rate, it is critically important that we acknowledge these methodological differences when comparing between carbonate budget studies.

To illustrate the influence of calcification rates and the variable methods that are used to quantify them, we calculated carbonate production a second time employing

calcification rates obtained from average linear growth rates for corals among Indo-Pacific reefs from the *ReefBudget* data sheet (Perry et al. 2018a). This resulted in average coral carbonate production rates of 2.10 and 1.33 kg m^{-2} yr^{-1} across Eva and Fly reefs respectively, which is approximately a 216% and 245% increase to that measured using local buoyant weight derived calcification rates. Given that the buoyant weight method is considered to be the most accurate method for measuring calcification rates in the field (Jokiel et al. 1978; Herler and Dirnwöber 2011; Ross et al. 2019), it is likely that our net carbonate production estimates, although lower, are more accurate than studies using linear extension rates. As the majority of carbonate budget studies use calcification rates derived from linear growth measures, it may be argued that this should remain the standardised methodological approach going forward thus allowing for spatial and temporal comparisons. However, interpreting rates of net carbonate production using linear extension rates and associated estimates of reef accretion with future reef trajectories under variable climate scenarios are likely to over-estimate a reef's ability to keep up with SLR.

5.5.3 Bioerosion rates

Much like coral carbonate production rates, bioerosion rates across Eva and Fly reefs were also comparatively low. Average total bioerosion rates were 0.18 kg m^{-2} yr^{-1} at Eva and 0.26 kg m^{-2} yr^{-1} at Fly. Bioerosion rates vary spatially from inshore to offshore (Sammarco and Risk 1990; Cooper et al. 2008), with inshore sites typically experiencing higher macroboring and lower external grazing than offshore reefs (Tribollet et al. 2002; Hutchings et al. 2005). High sedimentation and turbidity on inshore reefs are known to negatively affect the abundance of herbivorous reef fish (Cheal et al. 2013), reducing what can be a dominant driver of bioerosion rates. Additionally, sedimentation may inhibit the settlement and development of microboring taxa such as endolithic algae (Hutchings et al. 2005). In contrast, higher rates of macro-boring on inshore reefs has been linked to higher levels of nutrients in coastal waters (Edinger et al. 2000; Le Grand and Fabricius 2011). As such, previous carbonate budgets studies conducted on reefs close to urban centres (e.g., Singapore, Januchowski-Hartley et al. 2020; Jepara , Edinger et al. 2000; Townsville Browne et al. 2013) have found macro-borers to be the dominant bioeroding group resulting in

high levels of bioerosion. In contrast, although macro-borers were also the dominant bioeroder at Eva and Fly reef, rates of bioerosion were comparatively low, which could potentially be appointed to the lack of local anthropogenic pressure (e.g., urban runoff, pollutants, nutrients). Under this "natural" setting, low bioerosion pressure has facilitated a positive budgetary state despite low net carbonate production.

5.5.4 Spatial variations and environmental pressure

Carbonate production and removal varied spatially within and between both reefs likely reflecting small-scale spatial differences in both environmental and biological drivers. In particular, Eva reef showed the greatest rates of carbonate production, potentially driven by the higher light levels measured at this reef. In contrast, Fly reef was exposed to higher levels of turbidity and chlorophyll-a, which may have hindered carbonate production rates as well as increased endolithic bioerosion (Le Grand and Fabricius 2011). Rates of bioerosion were, however, greater in the SWW zones of each reef. These zones were dominated by macroalgae, which leads to a higher density of herbivorous grazers (Friedlander and Parrish 1998) and associated rates of bioerosion. These small-scale (1 to 10 km) spatial differences highlight the need for caution when up-scaling rates of net carbonate production from a limited number of transects to whole reef systems. A potential approach that could improve the upscaling of carbonate budgets to reef systems is to develop empirical relationships that describe how key ecological processes that drive budgets (e.g., calcification rates, bioerosion) are responding to individual as well as interacting environmental drivers. These quantified relationships could then be combined with remotely sensed habitat maps to estimate net carbonate production at the reef scale and better predict future rates of change.

5.5.5 Sediment Budget

The carbonate sediment budgets of Eva and Fly reefs are comparable to rates estimated for clear-water reefs. Here we measured rates of 1.2 ± 0.3 kg m^{-2} yr^{-1} and 3.1 ± 0.7 kg m^{-2} yr^{-1} for Eva and Fly, respectively. Net sediment production rates of 2.4-2.7 kg m^{-2} yr^{-1} have been reported for Green Island on the northern GBR (Yamano et al. 2000), and a rate of 2.82 kg m^{-2} yr^{-1} has been estimated for Heron

Island reef on the southern GBR (Brown et al. 2021). Additionally, Perry et al., (2017) estimated a net sediment budget of 1.04 kg m^{-2} yr^{-1} among a reef platform in the Maldives, driven by parrotfish bioerosion. Interestingly, direct sediment production quantified here is a magnitude greater than that of turbid inshore reefs of the GBR (~0.2 kg m^{-2} yr^{-1} Browne et al. 2013). This likely reflects the higher rates of terrigenous sediment inputs into the GBR's inshore coastal system as well as the high rates of wave-driven sediment resuspension and chronically turbid environment (Browne et al. 2012, Browne et al 2013). This highlights the negative influence of river runoff and terrigenous inputs on net carbonate sediment budgets. Regardless, the high rates of net sediment production recorded at Eva and Fly reef are encouraging as they suggest that despite low net framework carbonate productivity, these reefs can currently provide carbonate sediments to support island accretion with SLR.

The dominant driver of the high net sediment production at Eva and Fly reef was relative abundance of molluscs. It has been well established that parrotfish are leading producers of carbonate sediments among tropical clear water reefs (Bellwood 1996), but this is not always the case. For example, reef sediments have been found to be dominated by fragments of *Halimeda* spp. (e.g., Timor Sea, North-western Australia; Hayward et al. 1997), foraminifera (e.g. Green Island and Raine Island, North-eastern Australia; Yamano et al. 2000; Dawson et al. 2014) and molluscs (e.g. Lagoonal waters of New Caledonia; Chevillon 1996), highlighting the role of other organisms in carbonate sediment production, and supply. Across Eva and Fly reefs, mollusc (bivalve and gastropod) fragments made up the majority (34 and 40%) of the sediment. The shallow macroalgae dominated substrate (~30% of reef cover) at Eva and Fly provides the ideal habitat for bivalves and gastropods (Roy et al. 2000; Beasley et al. 2005). Ideal habitat coupled with the high abundance of invertivores (fish that feed on invertebrates) recorded in DOV surveys, potentially explains the high abundance of mollusc shell in reef sediments. This demonstrates the importance of identifying the dominant sediment producer among different reef settings as a means of better understanding how net sediment production rates may then be impacted by climate change.

5.5.6 Reef accretion and future island stability

Reef accretion potential (RAP) rates varied between -0.06 to 1.11 mm yr^{-1} with an average rate of 0.43 ± 0.19 mm yr^{-1} for Eva and 0.16 ± 0.13 mm yr^{-1} for Fly reef. If we apply the use of linear extension rates as per the *ReefBudget* methodology, average RAP are increase to 0.91 and 0.43 mm yr^{-1} for Eva and Fly, respectively. These estimates all fall below even the most conservative global mean SLR prediction of 4.4 mm yr^{-1} under ICPP RCP scenarios 2.6, and is well below current globally averaged SLR of approximately 3 mm yr^{-1} (Church and Gregory 2019). Recent research into the morphodynamics of Eva and Fly islands showed that these island features have remained stable over the past two decades, despite displaying dynamic responses to seasonal shifts in wave climate and water levels (Cuttler 2020). However, Bonesso et al. (2020) displayed that the reef platform area of Eva and Fly reef was directly linked to the net volume of their associated islands, as a larger platform area represented a greater sediment factory, suggesting a loss of reef framework would have a negative impact on island stability.

Currently, assuming the reef sediment composition is closely reflective of island sediments, these reefs are likely aiding in the maintenance of island stability through a continual/relatively large supply of sediment. However, estimates of framework accretion with predicted SLR suggests the reef will eventually be inundated and offer less shoreline protection. Under these condition, island volumes may remain stable through nourishment from reef derived sediment production. Recent works on hydrodynamic modelling of sediment transport have demonstrated that under current SLR predictions morphological responses of islands will be diverse, with predicted increases in island height and lagoonal migration maintaining island volume (See East et al. 2020; Masselink et al. 2020; Tuck et al. 2021). However, as the production of carbonate sediments heavily depends upon the reef framework (coral fragments, CCA, habitat for mollusc and other calcifying taxa), the reef's response to SLR and climate change may impact sediment production, which in turn may influence the supply of sediment to islands and impact island stability.

Ultimately, there remains a level of uncertainty regarding how reefs will respond to SLR. An increase in depth will increase light attenuation and may reduce calcification (Perry et al. 2018), or alternatively, the increase in depth (over reef flats currently at sea level) may prompt a response of rapid accretion to catch up with SLR

(Perry and Smithers 2011). Given that reefs exposed to periods of high turbidity are considered to be more resilient to lower light levels (Cacciapaglia and van Woesik 2016), it could be suggested that they may withstand an initial increase in depth and thrive with the increased accommodation space. If this is the case, Eva and Fly may sustain island stability into the future through positive sediment production and breakwater functionality, although this will only be possible under combined environmental variables supportive of a positive carbonate budget state.

5.5.7 Conclusions

We quantified the reef carbonate budgets for two inshore island reefs of the Pilbara, Eva and Fly, to be 1.01± 0.46 and 0.47 ± 0.38 kg m^{-2} yr^{-1}, respectively. These budgetary states are low due to low levels of coral cover and relatively slow coral growth rates, with positive budget states being facilitated by similarly low rates of framework bioerosion. These systems supported high rates of direct sediment production, and therefore healthy net carbonate sediment budgets (1.20 ± 0.30 and 3.11 ± 0.71 kg m^{-2} yr^{-1} at Eva and Fly, respectively). Reef accretion potential varied between -0.06 and 1.11 mm yr^{-1}, which is well below conservative SLR estimates of 4.4 mm yr^{-1} (RCP 2.6), suggesting Eva and Fly islands may be at risk of inundation and erosion if reef accretion remains at current rates into the future.

Carbonate budgets provide a comprehensive assessment of reef health and framework production, if applied correctly. Currently, inconsistencies between methodologies and the use of offsite or historic data, may result in significant over- or underestimation of reef framework production. This then has the potential to significantly shift estimates of carbonate budget assessments and therefore estimated reef accretionary potential. Although not always applied in this study, we strongly encourage the use of current onsite data, as well as the use of accurate and comparable methodologies when conducting carbonate budget studies (see Browne et al. 2021 for a detailed review). Further, we encourage future carbonate budget studies to incorporate reef sediment budgets to support landform management, and environmental data to improve our understanding on how the various components of carbonate budgets quantitatively respond to environmental change.

Postscript: The focus of next chapter is to discuss the key findings and significance of the previous chapters of this thesis, as well as future directions for the field of carbonate budget research.

Chapter 6 General Discussion

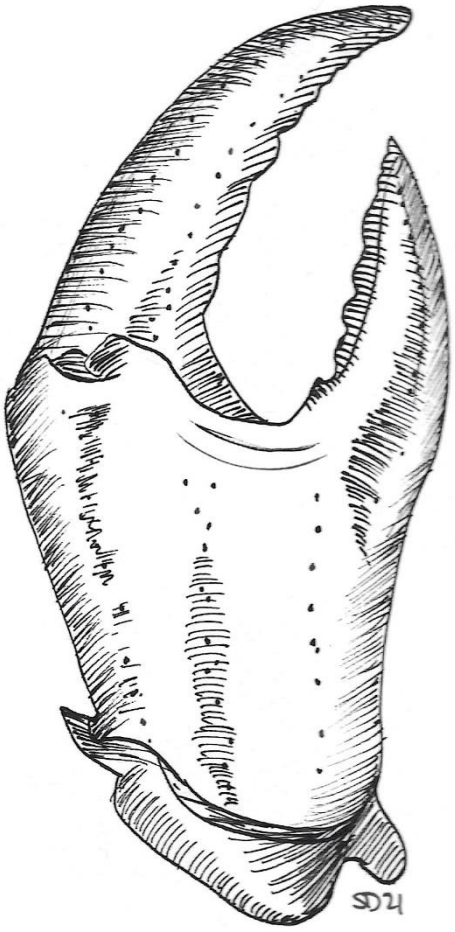

6.1 Summary of findings

This thesis investigated critical components that contribute to the carbonate budget of island reefs of the Pilbara, which are exposed to episodes of high turbidity. The outputs provide a greater understanding of longer-term stability of these remote and "marginal" reef systems, and offer insights into key knowledge gaps pertinent to carbonate budgets (more generally) and their interpretation. This final discussion chapter draws together the main concepts, findings and significance of each data chapter and addresses the limitations of this thesis. Lastly, future research directions for carbonate budgets, in relation to broader reef ecology and carbonate island management, are outlined.

Chapter two investigated the practicality of applying remotely-sensed bathymetric data to quantify reef rugosity and compared this to the traditional chain and tape method. The chain and tape method is limited as it only provides a two dimensional measure of rugosity and is time consuming. Alternatively, remote sensing offers a repeatable measure of reef rugosity over a large three-dimensional area, which is has the potential to be beneficial for rapid and broad-scale reef assessments. These direct comparisons suggested that remote sensing was not able to measure reef rugosity at the resolution required for carbonate budget assessments. Rugosity values from Lidar were often close to 1 suggesting that the reef was flat even where coral cover was >60%. Importantly, remotely sensed rugosity values of close to 1 are not uncommon, with multiple previous studies using remote sensing reporting similar values (Du Preez 2015; Storlazzi et al. 2016; Hamylton and Mallela 2019). When assessing the relationships between coral cover and rugosity for each method, rugosity measured with the chain and tape method were highly correlated to all levels of coral cover, while the LiDAR derived rugosity measures lacked any significant correlations. Further, when applying rugosity measures to calculate carbonate production by corals, LiDAR derived rugosities yielded ~30% less carbonate production. Key conclusions of this chapter were that current resolutions of remote sensing data hinder its application for colony scale measures of reef rugosity. As such, the chain and tape method is more applicable to reef ecological surveys including carbonate budgets.

Chapter three explored and quantified the relative carbonate production of encrusting taxa across Eva and Fly reefs. PVC recruitment tiles were deployed during a six month "winter" season followed by a six month "summer" season, as well as annually to measure any temporal variation in encruster cover and carbonate production. During the summer season, Exmouth Gulf experienced sea surface temperature anomalies up to 3.6°C, which had the potential to cause stress and mortality to sensitive encrusting taxa. Spatially, there was a strong correlation between environmental and habitat data with encruster carbonate production rates (R^2=0.61), with high variation between north and southern zones (p= <0.001). Encruster cover varied seasonally (p= <0.001), with the highest cover of encrusters recorded during the winter season. A decline in cover on the annual tiles compared to tiles deployed over the winter, suggested a potential die-off during the summer season which correlated with significantly less CCA cover during the summer season. However, carbonate production rates were relatively constant across deployment periods suggesting that either encrusters may be preferring vertical or thicker growth during the warmer summer season rather than lateral growth, or that there may have been a shift in species recruitment during this time. Further, encrusters were found to have a high contribution to the overall estimated carbonate production of Eva and Fly reefs, which suggests that encrusters could be critical in maintaining a positive carbonate budget during periods where carbonate production from corals may be impeded (i.e., following bleaching events).

While Eva and Fly reefs experienced high production from encrusting taxa, all measures of bioerosion across reefs were relatively low (Chapter 4). Blocks of *Porites lutea* were used to measure levels of endolithic and external bioerosion using MicroCT technology, where blocks were scanned before and after deployment to quantify direct volume loss. Macroboring worms were found to excavate the greatest volume from coral blocks while microboring and grazing were significantly lower across sites (p= <0.001). Diver operated video (DOV) surveys recorded low abundance of herbivorous grazers (*Scarus ghobban),* which further supports the conclusion that grazing pressure is low across these reefs. When comparing bioerosion rates with environmental data, the only relationships evident were between macroboring rates with temperature and light, which were both negative (temperature r^2= 0.23, p= 0.008, light r^2= 0.16, p= 0.037). These data highlights how

even small changes at the reef spatial scale can have significant influences on bioerosion rates, and how limited measures of bioerosion may not be representative of reef wide bioerosion activity. To further assess the influence of environmental variables on endolithic bioerosion, data from studies across the globe that reported macroboring rates on coral substrate as well as environmental data were compared. Unfortunately, there were only seven studies that met this prerequisite, highlighting the lack of data linking environmental drivers to endolithic bioerosion, and so no clear relationships could be investigated.

Chapter five highlighted the influence of methodological choice for estimating coral calcification rates and, as such, carbonate budgets. Coral calcification rates measured across Eva and Fly reefs using the buoyant weight method were comparable to other reefs in Western Australia, but were much lower than calcification rates calculated using linear growth measures across the Indo Pacific. Linear growth measures may overestimate calcification rates as this method does not account for uneven growth across the surface of many coral morphologies, or variation in skeletal density. Alternatively, the buoyant weight technique directly measures the increase in weight of carbonate over time, and so, is considered to be more accurate. Average coral carbonate production rates derived using on site and local calcification rates from buoyant weight was from 0.97 kg m^{-2} yr^{-1} at Eva reef and 0.54 kg m^{-2} yr^{-1} at Fly reef. When applying off-site linear growth derived calcification rates (from similar reefs) to calculate coral carbonate production across Eva and Fly reefs, rates were approximately 230% greater. The difference in the amount of carbonate produced from corals between methods highlights important issues for both spatial comparisons (between studies using different methods) as well as the interpretation and use of the final coral carbonate production estimates. For example, if over-inflated coral carbonate production rates are then used to estimate net carbonate production and reef accretionary potential, it's likely that the rates of reef accretion will be over-estimated, which then influences future predictions of reef growth and stability with SLR.

This final chapter provides much needed data on key processes of turbid reefs and demonstrates that these inshore island reefs are currently stable. As such, these reefs exist in a delicate equilibrium where low rates of carbonate production are facilitated

by particularly low rates of bioerosion, and where rates of sediment production are driven by high abundance of molluscs. As these reefs are not under local anthropogenic pressures (e.g., pollution, tourism etc.) this delicate balance may be more vulnerable to rapid environmental changes at the local or even global scale.

Predicted reef accretion potential (RAP) from the reef framework budget was estimated to be between -0.06 to 1.11 mm yr^{-1} with an average rate of 0.43 ± 0.19 mm yr^{-1} for Eva and 0.16 ± 0.13 mm yr^{-1} for Fly reef. This is below the most conservative SLR predictions of 4.4 mm yr^{-1} under ICPP RCP scenarios 2.6, as well as under current rates of SLR at 3mm yr^{-1}. Our estimates of framework accretion with predicted SLR suggests the reef framework of Eva and Fly will eventually be inundated and offer less protection from wave energy to the island shorelines, unless a significant increase in reef accretion occurs. This could potentially occur if new suitable substrate for coral settlement and growth become available as predicted SLR has the potential to open up greater accommodation space for coral growth, and thus increasing the reef carbonate budget.

Currently, very few carbonate budgets have incorporated estimates of carbonate sediment production, despite the important influence on adjacent landform growth and stability. Here we found carbonate sediment budget of Eva and Fly reefs showed high levels of sediment supply, the majority of which was from molluscs. Overall sediment budgets produced 0.2 and 2.2 kg m^{-2} yr^{-1} more carbonate compared to the reef framework of Eva and Fly, respectively. Previous sediment budgets producing similar volumes of carbonate from non-coral sources tend to be clearwater shallow environments with high abundance of foraminifera, *Halimeda*, and CCA. Hence, we show that it is important to assess sediment production in additional settings where other non-coral sources could play an important role in sediment production and potential island growth

6.2 Limitations of this thesis

Chapter two focused on reef rugosity and the variation between common *in situ* and remote methods. Further to this, it would have been useful to compare the variation in rugosity measures using chains with different linkage lengths. As the scale of

remote DEM data was 0.1 m^2 having chain lengths closer to 10cm would have been more compareable and offered an opportunity to apply a scaling coefficient between the two methodologies. Logically, smaller chain links would capture more detail in topographic complexity (although only at a 2D scale). Currently, the only remote method offering such finescale resolutions (e.g., 0.15m chain link) is photogramettry. Although this method has the potential to be even more labour intensive than the chain and tape method and requires expensive software and relatively high computer power for analyis.

Within this study, carbonate budget estimates were limited to the forereef and sandy lagoonal zones of Eva and Fly reefs. Given that we have seen high levels of heterogeneity, it would have been beneficial to run additional transects across the reef flat and back reef to gather a greater understanding of the entirety of these reef systems. Additionally, increasing the number of transects across the zones already covered would have increased spatial resolution and likely increased the robustness and accuracy of the dataset. When investigating encruster abundance and carbonate production, I would have liked to deploy more tiles across the reefs across a greater depth range to add another environmental element to the analysis. Similar to encrusting tiles, deployment of more bioerosion monitoring units would have been beneficial to further assessing the variation in bioerosion activities across the reefs. A further limitation of measuring bioerosion in chapter 4 was the size of experimental blocks. Although blocks of this size are the standard used in previous studies, they may not seem appealing to grazing taxa that have a large amount of available substrate on the reef benthos. Further, these blocks being raised limites the succession and predation of taxa such as urchins, mullusc, and sponges, which are typically dominant bioeroding taxa.

A greater temporal resolution of this study would have been beneficial and increased the undertsanding on environmental drivers on these carbonate budgets. Deploying bioerosion blocks and encruster settlement tiles for longer periods could have allowed recruitment of a larger number of taxa, giving a more in depth and accurate understanding of encruster and bioeroding taxa abundance in the reef framework. Looking at encruster growth inter-annually, where tiles are swapped seasonally and annually for several years, would provide longer temporal resolution and greater

understanding on the influence of environmental shifts seasonally and annually. Further, conducting molecular work on the samples deposited onto the tiles would have allowed species identification of CCA, which could have provided knowledge on potential shifts on species abundance seasonally. This would have also allowed for identification of other organisms growing on the tiles that could have been contributing a greater amount of carbonate production than observed visually.

In the current study, a more classical method (although still widely applied) was used to estimate carbonate production from corals across each zone. This method calculate carbonate production of each coral genera per zone by the percentage cover of this coral genera, multiplied by the mean calcification rate, normalised by dividing by the surface are of the zone. As all coral colonies grow in different ways, carbonate production rates are independent of each coral colony and should therefore be measured for each individual colony along survey transects.This adapted, and more detailed method was introduced in mid – late 2018, and was unfortuneatley not learned of before data collection was conducted in September 2018. Due to time limitations and logistical restrictions for field work, this was not possible for this study, as hence the use of the classical method may result in overestimation in coral carbonate production rates in chapter 5.

Finally, collecting data on sediment transport as well as direct sediment and coral carbonate dissolution are steps that should be included in future studies as these functions are relevant when linking carbonate budgets to island stability, and would have been highly beneficial to this study.

6.3 Significance

This thesis quantified the first comprehensive assessment of carbonate framework production and removal for turbid reefs of Western Australia, using a census-based carbonate budget approach. This study not only provides further understanding of the health and function of these under-studied reefs but provides a comprehensive assessment of the environmental conditions (e.g., temperature, light, turbidity, nutrients) that are driving reef functions in these marginal settings. As such, this study is one of a very small number of studies that has provided empirical data for the quantification of relationships between drivers (cause) and biological responses

(effect), which is critical for developing predictive models of reef health and accretion with future climate change. Further, this study took place in a region with very minimal localized anthropogenic impacts, offering a unique “baseline” setting where these reefs are largely responding to changes in the global climate regime as opposed to local influences.

In addition, this is the second study globally that combines reef framework production with carbonate sediment production within a turbid reef environment. The sediment budget gives important insights into the amount of carbonate sediment available for island shoreline nourishment, which is increasingly critical for island stabilization under anthropogenic pressures and predicted SLR.

6.4 Future directions

The comprehensive census-based carbonate budget approach provides a valuable method for evaluating and comparing ecological change with shifting climates. To do this effectively, there needs to be a consistent application of methodologies used in order to ensure that the data are comparable over space and time. Importantly, every effort should be made to use onsite data rather than offsite or historical data. If this is not possible, then there needs to be an acknowledgment of this limitation and results should be interpreted appropriately. For example, this thesis displayed encrusting organisms and macroboring worms were having significant influences on the state of the framework budget, yet, in most carbonate budget studies CCA calcification and endolithic bioerosion rates are often estimated from offsite data. Furthermore, this thesis displayed how using offsite calcification rates (and those gathered from multiple methods) for corals can overestimate carbonate production rates by more than 30%, which can be the difference in determining if is reef is within a positive or negative budget state.

Considering Western Australian reefs, a valuable next step would be to conduct a detailed methodological study comparing the accuracy and fluctuations of calcification rates estimated from linear growth and buoyant weight methods. This study should also include modern methods such as structure from motion to ensure researchers are adopting the more accurate and applicable method when making these measures. Measuring growth rates of foliose corals would also be beneficial as

there is currently no data on this for tropical Western Australia, even though corals of this morphology are highly abundant.

Given that for many studies there are logistical and budgetary constraints on field work that limit the assessment of key carbonate budget parameters (e.g., growth rates, bioerosion rates), it is important that we improve our knowledge on how key ecological processes that influence carbonate budgets vary with environmental change. These data will enable future ecological modelling to make predictions for management and conservation. This can be achieved by collecting on site environmental and water quality data to set a baseline understanding of what conditions ecological reef processes are currently functioning among. Further laboratory research investigating how reef taxa and their functions (e.g., carbonate production, bioeroding activity, dissolution rates) may shift under variable environmental conditions and under the influence of multiple stressors, will strengthen this knowledge and facilitate the establishment of empirical relationships between reef functions and environmental change.

The inclusion of complimentary sediment budgets are highly important for reefs adjacent to carbonate landforms and shorelines. Understanding sediment production and supply is valuable knowledge to future landform management, particularly among low-lying carbonate islands and atolls. Future studies should attempt to measure sediment production and transport rates, as well as sediment dissolution rates to gather a more complete knowledge of the sediment budget. The deployment of various sediment trap designs (e.g., bidirectional, sand export, gravel export; see Morgan and Kench 2014a) gather data on the rate, magnitude, and direction of sediment transport, which is valuable in understanding the ability of reef derived sediments to nourish shorelines. Further, modelling of hydrodynamic processes that impact the reef system will allow predictions to be made in relation to impacts storm events will have on sediment loads.

Literature cited

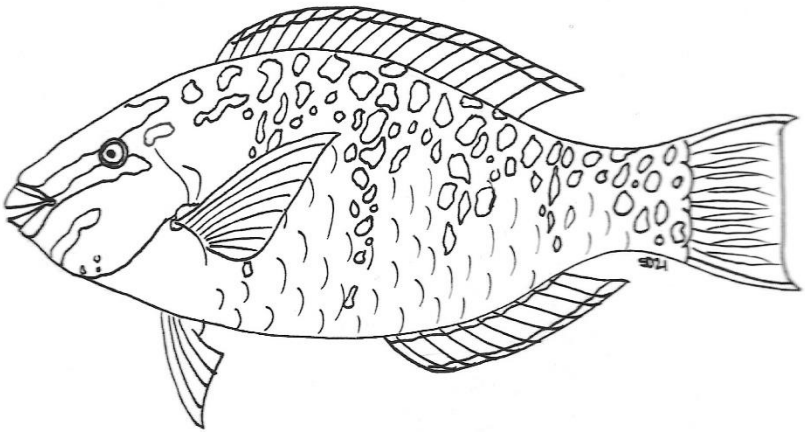

Adey, W H and McKibbin, D L.. "Studies on the Maerl Species Phymatolithon calcareum (Pallas) nov. comb. and Lithothamnium coralloides Crouan in the Ria de Vigo" , vol. 13, no. 2, 1970, pp. 100-106.

W. H. Adey & J. Michael Vassar (1975) Colonization, succession and growth rates of tropical crustose coralline algae (Rhodophyta, Cryptonemiales), Phycologia, 14:2, 55-69, DOI: 10.2216/i0031-8884-14-2-55.1

Achlatis M, Van Der Zande RM, Schönberg CHL, Fang JKH, Hoegh-Guldberg O, Dove S (2017) Sponge bioerosion on changing reefs: Ocean warming poses physiological constraints to the success of a photosymbiotic excavating sponge. Sci Rep 7:1–14. doi: 10.1038/s41598-017-10947-1

Alvarez-Filip L, Carricart-Ganivet JP, Horta-Puga G, Iglesias-Prieto R (2013) Shifts in coral-assemblage composition do not ensure persistence of reef functionality. Sci Rep 3:1–6. doi: 10.1038/srep03486Anthony KRN, Kline DI, Diaz-Pulido G, Dove S, Hoegh-Guldberg O (2008) Ocean acidification causes bleaching and productivity loss in coral reef builders. Proc Natl Acad Sci U S A 105:17442–17446

Andersson AJ (2015) A fundamental paradigm for coral reef carbonate sediment dissolution. Front Mar Sci 2:1–8. doi: 10.3389/fmars.2015.00052

Baird AH, Blakeway DR, Hurley TJ, Stoddart JA (2011) Seasonality of coral reproduction in the Dampier Archipelago, northern Western Australia. Mar Biol 158:275–285

Bak RPM (1973) Coral weight increment in situ. A new method to determine coral growth. Mar Biol 20:45–49. doi: 10.1007/BF00387673

Baker AC, Glynn PW, Riegl B (2008) Climate change and coral reef bleaching: An ecological assessment of long-term impacts, recovery trends and future outlook. Estuar Coast Shelf Sci 80:435–471. doi: 10.1016/j.ecss.2008.09.003

Bakker DM De, Meesters EH, Bak RPM, Nieuwland G (2016) Long-term shifts in coral communities on shallow to deep reef slopes of Curaçao and Bonaire : are there any winners ? Front Mar Sci 3:1–14. doi: 10.3389/fmars.2016.00247

Bakker DM, van Duyl FC, Perry CT, Meesters EH (2019) Extreme spatial heterogeneity in carbonate accretion potential on a Caribbean fringing reef linked to local human disturbance gradients. Glob Chang Biol 25:4092–4104. doi: 10.1111/gcb.14800

Beasley C, Fernandes C, Gomes C, Brito B, Lima dos Santos S, Tagliaro C (2005) Molluscan Diversity and Abundance Among Coastal Habitats of Northern Brazil. Ecotropica 11:9–20.

Belliveau SA, Paul VJ (2002) Effects of herbivory and nutrients on the early colonization of crustose coralline and fleshy algae. Mar Ecol Prog Ser 232:105–114

Bellwood D (1995) Direct estimate of bioerosion by two parrotfish species on the Great Barrier Reef, Australia. Mar Biol 121:419–429.

Bellwood DR (1996) Production and reworking of sediment by parrotfishes (family Scaridae) on the Great Barrier Reef , Australia. Mar Biol 125:795–800.

Beuck L, Vertino A, Stepina E, Karolczak M, Pfannkuche O (2007) Skeletal response of Lophelia pertusa (Scleractinia) to bioeroding sponge infestation visualised with micro-computed tomography. Facies 53:157–176. doi: 10.1007/s10347-006-0094-9

Blake C, Maggs CA (2003) Comparative growth rates and internal banding periodicity of maerl species (Corallinales, Rhodophyta) from northern Europe. Phycologia 42:606–612

BOM (2021) Climatology of Tropical Cyclones in Western Australia. In: Aust. Gov. Bur. Meteorol.

Bonaldo RM, Bellwood DR (2009) Dynamics of parrotfish grazing scars. Mar Biol 156:771–777. doi: 10.1007/s00227-009-1129-x

Bozec YM, Alvarez-Filip L, Mumby PJ (2014) The dynamics of architectural complexity on coral reefs under climate change. Glob Chang Biol 21:223–235

Brock JC, Wright CW, Clayton TD, Nayegandhi A (2004) LIDAR optical rugosity of coral reefs in Biscayne National Park, Florida. Coral Reefs 23:48–59

Brock JC, Wright CW, Kuffner IB, Hernandez R, Thompson P (2006) Airborne lidar sensing of massive stony coral colonies on patch reefs in the northern Florida reef tract. Remote Sens Environ 104:31–42

Brown KT, Bender-Champ D, Achlatis M, van der Zande RM, Kubicek A, Martin SB, Castro-Sanguino C, Dove SG, Hoegh-Guldberg O (2021) Habitat-specific biogenic production and erosion influences net framework and sediment coral reef carbonate budgets. Limnol Oceanogr 66:349–365. doi: 10.1002/lno.11609

Browne NK, Smithers SG, Perry CT (2012a) Coral reefs of the turbid inner-shelf of the Great Barrier Reef, Australia: An environmental and geomorphic perspective on their occurrence, composition and growth. Earth-Science Rev 115:1–20. doi: 10.1016/j.earscirev.2012.06.006

Browne NK (2012) Spatial and temporal variations in coral growth on an inshore turbid reef subjected to multiple disturbances. Mar Environ Res 77:71–83

Browne NK, Smithers SG, Perry CT (2013) Carbonate and terrigenous sediment budgets for two inshore turbid reefs on the central Great Barrier Reef. Mar Geol 346:101–123. doi: 10.1016/j.margeo.2013.08.011

Browne NK, Cuttler MVW, Moon K, Morgan KM, Ross CL, Castro-Sanguino C, Kennedy E V., Harris DL, Barnes P, Bauman AG, Beetham EP, Bonesso J, Bozec Y, Cornwall CE, Dee S, Decarlo TM, D'olivo JP, Doropoulos C, Evans RD, Eyre, Bradley D., Gatenby P, Gonzalez M, Hamylton S, Hansen JE, Lowe RJ, Mallela J, O'Leary MJ, Roff, George, Saunders BJ, Zweifler A (2021) Predicting Responses of Geological Carbonate Reef Systems to Climate Change: a Conseptual Model and Review. In: Oceanography and Marine Biology. pp 229–370

Bruggemann JH, Vanoppen MJH, Breeman AM (1994) Foraging by the stoplight-parrotfish Sparisoma viride. 1.Food selection in different socially determined habitats. Mar Ecol Prog Ser 106:41–56. doi: 10.3354/meps106041

Brunskill GJ, Orpin AR, Zagorskis I, Woolfe KJ, Ellison J (2001) Geochemistry and particle size of surface sediments of Exmouth Gulf , Northwest Shelf , Australia. Cont Shelf Res 21:157–201

Cacciapaglia C, van Woesik R (2016) Climate-change refugia: Shading reef corals by turbidity. Glob Chang Biol 22:1145–1154. doi: 10.1111/gcb.13166

Carreiro-Silva M, McClanahan TR, Kiene WE (2005) The role of inorganic nutrients and herbivory in controlling microbioerosion of carbonate substratum. Coral Reefs 24:214–221. doi: 10.1007/s00338-004-0445-3

Carreiro-Silva M, McClanahan TR (2012) Macrobioerosion of dead branching Porites, 4 and 6 years after coral mass mortality. Mar Ecol Prog Ser 458:103–122. doi: 10.3354/meps09726

Carreiro-Silva M, McClanahan TR, Kiene WE (2009) Effects of inorganic nutrients and organic matter on microbial euendolithic community composition and microbioerosion rates. Mar Ecol Prog Ser 392:1–15. doi: 10.3354/meps08251

Celis-Plá PSM, Hall-Spencer JM, Horta PA, Milazzo M, Korbee N, Cornwall CE, Figueroa

FL (2015) Macroalgal responses to ocean acidification depend on nutrient and light levels. Front Mar Sci 2:doi: 10.3389/fmars.2015.00026

Chave KE, Smith S V., Roy KJ (1972) Carbonate production by coral reefs. Mar Geol 12:123–140. doi: 10.1016/0025-3227(72)90024-2

Chazottes V, Campion-Alsumard T Le, Peyrot-Clausade M (1995) Bioerosion rates on coral reefs: interactions between macroborers, microborers and grazers (Moorea, French Polynesia). "Palaeogeography, Palaeoclimatol Palaeoecol 113:189–198. doi: 10.1016/0031-0182(95)00043-L

Chazottes V, Le Campion-Alsumard T, Peyrot-Clausade M, Cuet P (2002) The effects of eutrophication-related alterations to coral reef communities on agents and rates of bioerosion (Reunion Island, Indian Ocean). Coral Reefs 21:375–390. doi: 10.1007/s00338-002-0259-0

Chazottes V, Hutchings P, Osorno A (2017) Impact of an experimental eutrophication on the processes of bioerosion on the reef: One Tree Island, Great Barrier Reef, Australia. Mar Pollut Bull 118:125–130. doi: 10.1016/j.marpolbul.2017.02.047

Cheal AJ, Emslie M, MacNeil MA, Miller I, Sweatman H (2013) Spatial variation in the functional characteristics of herbivorous fish communities and the resilience of coral reefs. Ecol Appl 23:174–188. doi: 10.1890/11-2253.1

Chevillon C (1996) Skeletal composition of modern lagoon sediments in New Caledonia: Coral, a minor constituent. Coral Reefs 15:199–207. doi: 10.1007/BF01145892

Chisholm JRM (2000) Calcification by crustose coralline algae on the northern Great Barrier Reef, Australia. Limnol Oceanogr 45:1476–1484

Chisholm JRM (2003) Primary Productivity of Reef-Building Crustose Coralline Algae. Limnol Oceanogr 48:1376–1387

Church JA, Gregory JM (2019) Sea level change. Encycl Ocean Sci 493–499. doi: 10.1016/B978-0-12-409548-9.10820-6

Cinner J (2014) Coral reef livelihoods. Curr Opin Environ Sustain 7:65–71. doi: 10.1016/j.cosust.2013.11.025

Comeau S, Cornwall CE, Pupier CA, DeCarlo TM, Alessi C, Trehern R, McCulloch MT (2019) Flow-driven micro-scale pH variability affects the physiology of corals and coralline algae under ocean acidification. Sci Rep 9:1–12

Cooper TF, Ridd P V., Ulstrup KE, Humphrey C, Slivkoff M, Fabricius KE (2008) Temporal dynamics in coral bioindicators for water quality on coastal coral reefs of the Great Barrier Reef. Mar Freshw Res 59:703–716. doi: 10.1071/MF08016

Cornwall CE, Comeau S, Decarlo TM, Moore B, Alexis QD, Mcculloch MT (2018) Resistance of corals and coralline algae to ocean acidification : physiological control of calcification under natural pH variability. R Soc

Cornwall CE, Diaz-Pulido G, Comeau S (2019) Impacts of ocean warming on coralline algae: Knowledge gaps and key recommendations for future research. Front Mar Sci 6:1–10

Cornwall CE, Comeau S, Kornder NA, Perry CT, van Hooidonk R, DeCarlo TM, Pratchett MS, Anderson KD, Browne N, Carpenter R, Diaz-Pulido G, D'Olivo JP, Doo SS, Figueiredo J, Fortunato SAV, Kennedy E, Lantz CA, McCulloch MT, González-Rivero M, Schoepf V, Smithers SG, Lowe RJ (2021) Global declines in coral reef calcium carbonate production under ocean acidification and warming. Proc Natl Acad Sci U S A. doi: 10.1073/pnas.2015265118

Crook ED, Cohen AL, Rebolledo-Vieyra M, Hernandez L, Paytan A (2013) Reduced

calcification and lack of acclimatization by coral colonies growing in areas of persistent natural acidification. Proc Natl Acad Sci U S A 110:11044–11049. doi: 10.1073/pnas.1301589110

Cuttler MVW, Hansen JE, Lowe RJ, Trotter JA, McCulloch MT (2019) Source and supply of sediment to a shoreline salient in a fringing reef environment. Earth Surf Process Landforms 44:552–564. doi: 10.1002/esp.4516

Cuttler MVW, Vos K, Branson P, Hansen JE, O'leary M, Browne NK, Lowe RJ (2020) Interannual response of reef islands to climate-driven variations in water level and wave climate. Remote Sens 12:1–18

Cyronak T, Santos IR, Eyre BD (2013) Permeable coral reef sediment dissolution driven by elevated pCO 2 and pore water advection. Geophys Res Lett 40:4876–4881. doi: 10.1002/grl.50948

Dahl AL (1973) Surface Area in Ecological Analysis : Quantification of Benthic Coral-Reef Algae. Mar Biol 249:239–24

Darling ES, Graham NAJ, Januchowski-Hartley FA, Nash KL, Pratchett MS, Wilson SK (2017) Relationships between structural complexity, coral traits, and reef fish assemblages. Coral Reefs 36:561–575

Dandan SS, Falter JL, Lowe RJ, McCulloch MT (2015) Resilience of coral calcification to extreme temperature variations in the Kimberley region, northwest Australia. Coral Reefs 34:1151–1163. doi: 10.1007/s00338-015-1335-6

Davidson TM, Altieri AH, Ruiz GM, Torchin ME (2018) REVIEW AND Bioerosion in a changing world : a conceptual framework. Ecol Lett 21:422–438. doi: 10.1111/ele.12899

Davies S P (1989) Short-term growth measurements of corals using an accurate buoyant weighing technique. Mar Biol 101:389–395. doi: 10.1007/BF00428135

Dawson JL, Smithers SG, Hua Q (2014) The importance of large benthic foraminifera to reef island sediment budget and dynamics at Raine Island, northern Great Barrier Reef. Geomorphology 222:68–81. doi: 10.1016/j.geomorph.2014.03.023

Davies PJ, Hutchings PA (1983) Initial colonization, erosion and accretion of coral substrate - Experimental results, Lizard Island, Great Barrier Reef. Coral Reefs 2:27–35. doi: 10.1007/BF00304729

Dean AJ, Steneck RS, Tager D, Pandolfi JM (2015) Distribution, abundance and diversity of crustose coralline algae on the Great Barrier Reef. Coral Reefs 34:581–594

DeCarlo TM, Cohen AL, Barkley HC, Cobban Q, Young C, Shamberger KE, Brainard RE, Golbuu Y (2014) Coral macrobioerosion is accelerated by ocean acidification and nutrients. Geology 43:7–10. doi: 10.1130/G36147.1

Dee S, Cuttler M, O'Leary M, Hacker J, Browne N (2020) The complexity of calculating an accurate carbonate budget. Coral Reefs 39:1525–1534

Dee S, Cuttler M, Cartwright P, McIlwain J, Browne N (2021) Encrusters maintain stable carbonate production despite temperature anomalies among two inshore island reefs of the Pilbara, Western Australia. Mar Environ Res. doi: 10.1016/j.marenvres.2021.105386

Denis V, Ribas-Deulofeu L, Sturaro N, Kuo CY, Chen CA (2017) A functional approach to the structural complexity of coral assemblages based on colony morphological features. Sci Rep 7:1–11

Depczynski M, Gilmour JP, Ridgway T, Barnes H, Heyward AJ, Holmes TH, Moore JAY, Radford BT, Thomson DP, Tinkler P, Wilson SK (2013) Bleaching, coral mortality and

subsequent survivorship on a West Australian fringing reef. Coral Reefs 32:233–238. doi: 10.1007/s00338-012-0974-0

Dethier MN (1994) The ecology of intertidal algal crusts: variation within a functional group. J Exp Mar Bio Ecol 177:37–71

Diaz MC, Rützler K (2001) Sponges: An essential component of Caribbean coral reefs. Bull Mar Sci 69:535–546.

Diaz-Pulido G, Anthony KRN, Kline DI, Dove S, Hoegh-Guldberg O (2012) Interactions between ocean acidification and warming on the mortality and dissolution of coralline algae. J Phycol 48:32–39

Dinno A (2017) Package 'dunn.test.' CRAN Repos 1–7

Doropoulos C, Ward S, Diaz-Pulido G, Hoegh-Guldberg O, Mumby PJ (2012) Ocean acidification reduces coral recruitment by disrupting intimate larval-algal settlement interactions. Ecol Lett 15:338–346

Dufois F, Lowe R, Branson P, Fearns P (2017) Tropical Cyclone-Driven Sediment Dynamics Over the Australian North West Shelf. J Geophys Res Ocean 122:225–244

Dustan P, Doherty O, Pardede S (2013) Digital Reef Rugosity Estimates Coral Reef Habitat Complexity. PLoS One 8:1–10

Du Preez C (2015) A new arc-chord ration (ACR) rugosity index for quantifying three-dimensional landscape structural complexity. Landscape Ecology 30:181-192. doi: 10.1007/s10980-014-0118-8

Eakin CM (1996) A model comparison of calcium carbonate budgets before and after the 1982-1983 El Nino at Uva Island in the eastern Pacific. Coral Reefs 15:109–119.

East HK, Perry CT, Beetham EP, Kench PS, Liang Y (2020) Modelling reef hydrodynamics and sediment mobility under sea level rise in atoll reef island systems. Glob Planet Change 192:103196. doi: 10.1016/j.gloplacha.2020.103196

Edinger EN, Limmon G V, Jompa J, Widjatmoko W (2000) Normal Coral Growth Rates on Dying Reefs : Are Coral Growth Rates Good Indicators of Reef Health ? 40:404–425

Enochs IC, Manzello DP, Kolodziej G, Noonan SHC, Valentino L, Fabricius KE (2016) Enhanced macroboring and depressed calcification drive net dissolution at high-CO2 coral reefs. Proc R Soc B Biol Sci. doi: 10.1098/rspb.2016.1742

EPA (2021) Potential cumulative impacts of proposed activities and developments on the environmental , social and cultural values of Exmouth Gulf in accordance with section 16 (e) of the Environmental Protection Act 1986.

Evans RD, Wilson SK, Fisher R, Ryan NM, Babcock R, Blakeway D, Bond T, Dorji P, Dufois F, Fearns P, Lowe RJ, Stoddart J, Thomson DP (2020) Early recovery dynamics of turbid coral reefs after recurring bleaching events. J Environ Manage 268:110666

Eyre BD, Andersson AJ, Cyronak T (2014) Benthic coral reef calcium carbonate dissolution in an acidifying ocean. Nat Clim Chang 4:969–976. doi: 10.1038/nclimate2380

Fabricius KE, De'ath G (2001) Environmental factors associated with the spatial distribution of crustose coralline algae on the Great Barrier Reef. Coral Reefs 19:303–309

Feng M, McPhaden MJ, Xie SP, Hafner J (2013) La Niña forces unprecedented Leeuwin Current warming in 2011. Sci Rep 3:1–9

Ferrari R, Malcolm HA, Byrne M, Friedman A, Williams SB, Schultz A, Jordan AR, Figueira WF (2018) Habitat structural complexity metrics improve predictions of fish abundance and distribution. Ecography (Cop) 41:1077–1091

Foster T, Short JA, Falter JL, Ross C, Mcculloch MT (2014) Reduced calcification in Western Australian corals during anomalously high summer water temperatures. J Exp

Mar Bio Ecol 461:133–143. doi: 10.1016/j.jembe.2014.07.014

Friedlander AM, Parrish JD (1998) Habitat characteristics affecting fish assemblages on a Hawaiian coral reef. J Exp Mar Bio Ecol 224:1–30. doi: 10.1016/S0022-0981(97)00164-0

Friedman A, Pizarro O, Williams SB, Johnson-Roberson M (2012) Multi-Scale Measures of Rugosity, Slope and Aspect from Benthic Stereo Image Reconstructions. PLoS One 7:e50440

Gischler E (2006) Sedimentation on Rasdhoo and Ari Atolls, Maldives, Indian ocean. Facies 52:341–360

Gilmour JP, Smith LD, Heyward AJ, Baird AH, Pratchett MS (2013) Recovery of an isolated coral reef system following severe disturbance. Science (80-) 340:69–71. doi: 10.1126/science.1232310

Goetze JS, Bond T, McLean DL, Saunders BJ, Langlois TJ, Lindfield S, Fullwood LAF, Driessen D, Shedrawi G, Harvey ES (2019) A field and video analysis guide for diver operated stereo-video. Methods Ecol Evol 10:1083–1090. doi: 10.1111/2041-210X.13189

Gómez-Lemos LA, Doropoulos C, Bayraktarov E, Diaz-Pulido G (2018) Coralline algal metabolites induce settlement and mediate the inductive effect of epiphytic microbes on coral larvae. Sci Rep 8:1–11

Graham NAJ, Nash KL (2013) The importance of structural complexity in coral reef ecosystems. Coral Reefs 32:315–326

Guest JR, Low J, Tun K, Wilson B, Ng C, Raingeard D, Ulstrup KE, Tanzil JTI, Todd PA, Toh TC, McDougald D, Chou LM, Steinberg PD (2016) Coral community response to bleaching on a highly disturbed reef. Sci Rep 6:1–11. doi: 10.1038/srep20717

Hallock P, Talge HK, Cockey EM, Muller RG (1995) A new disease in reef-dwelling forminifera: implications for coastal sedimentation. J Foraminifer Res 25:280–286. doi: 10.2113/gsjfr.25.3.280

Hamylton S, Silverman J, Shaw E (2013) The use of remote sensing to scale up measures of carbonate production on reef systems : a comparison of hydrochemical and census-based estimation methods. 34:6451–6465.

Hamylton SM, Carvalho RC, Duce S, Roelfsema CM, Vila-Concejo A (2016) Linking pattern to process in reef sediment dynamics at Lady Musgrave Island, southern Great Barrier Reef. Sedimentology 63:1634–1650. doi: 10.1111/sed.12278

Hamylton SM, Mallela J (2019) Reef development on a remote coral atoll before and after coral bleaching: A geospatial assessment. Mar Geol 418:106041

Harney JN, Fletcher CH (2003) A budget of carbonate framework and sediment production, Kailua Bay, Oahu, Hawaii. J Sediment Res 73:856–868. doi: 10.1306/051503730856

Harrell Jr FE, Harrell Jr MFE (2015) Package ‘ Hmisc .’ CRAN2018 235–236

Harris DL, Pomeroy A, Power H, Casella E, Rovere A, Webster JM, Parravicini V, Canavesio R, Collin A (2018) Coral reef structural complexity provides important coastal protection from waves under rising sea levels. Sci Adv 4:7. doi: 10.1126/sciadv.aao4350

Heery EC, Hoeksema BW, Browne NK, Reimer JD, Ang PO, Huang D, Friess DA, Chou LM, Loke LHL, Saksena-Taylor P, Alsagoff N, Yeemin T, Sutthacheep M, Vo ST, Bos AR, Gumanao GS, Syed Hussein MA, Waheed Z, Lane DJW, Johan O, Kunzmann A, Jompa J, Suharsono, Taira D, Bauman AG, Todd PA (2018) Urban coral reefs:

Degradation and resilience of hard coral assemblages in coastal cities of East and Southeast Asia. Mar Pollut Bull 135:654–681. doi: 10.1016/j.marpolbul.2018.07.041

Herler J, Dirnwöber M (2011) A simple technique for measuring buoyant weight increment of entire, transplanted coral colonies in the field. J Exp Mar Bio Ecol 407:250–255. doi: 10.1016/j.jembe.2011.06.022

Hernández-Ballesteros LM, Elizalde-Rendón EM, Carballo JL, Carricart-Ganivet JP (2013) Sponge bioerosion on reef-building corals: Dependent on the environment or on skeletal density? J Exp Mar Bio Ecol 441:23–27. doi: 10.1016/j.jembe.2013.01.016

Herrán N, Narayan GR, Reymond CE, Westphal H (2017) Calcium carbonate production, coral cover and diversity along a distance gradient from Stone Town: A case study from Zanzibar, Tanzania. Front Mar Sci 4:1–14

Hetzinger S, Halfar J, Zack T, Mecking J V., Kunz BE, Jacob DE, Adey WH (2013) Coralline algal Barium as indicator for 20th century northwestern North Atlantic surface ocean freshwater variability. Sci Rep 3:1–9

Heyward AJ, Pinceratto E, Smith L, Science AI of M, Petroleum B (1997) Big bank shoals of the Timor Sea : an environmental resource atlas. Townsville, QLD

Heyward AJ, Negri AP (1999) Natural inducers for coral larval metamorphosis. Coral Reefs 18:273–279

Highsmith RC (1979) Coral growth rates and environmental control of density banding. Exp Mar Biol Ecol 37:105–125

Hoegh-Guldberg O (2004) Coral reefs in a century of rapid environmental change. In: Symbiosis.

Hoegh-Guldberg O, Harvell CD, Sale PF, Edwards AJ, Caldeira K, Knowlton N, Eakin CM, Muthiga N, Bradbury RH, Dubi A, Hatziolos ME, Mumby PJ, Hooten A, Steneck RS, Greenfield P, Gomez E (2007) Coral Reefs Under Rapid Climate Change and Ocean Acidification. Science (80-) 318:1737–1742

Hofmann LC, Heiden J, Bischof K, Teichberg M (2014) Nutrient availability affects the response of the calcifying chlorophyte Halimeda opuntia (L.) J.V. Lamouroux to low pH. Planta 239:231–242

Holmes KE, Edinger EN, Hariyadi, Limmon G V., Risk MJ (2000) Bioerosion of live massive corals and branching coral rubble on Indonesian coral reefs. Mar Pollut Bull 40:606–617. doi: 10.1016/S0025-326X(00)00067-9

van Hooidonk R, Maynard J, Tamelander J, Gove J, Ahmadia G, Raymundo L, Williams G, Heron SF, Planes S (2016) Local-scale projections of coral reef futures and implications of the Paris Agreement. Sci Rep 6:1–8. doi: 10.1038/srep39666

Howells EJ, Dunshea G, McParland D, Vaughan GO, Heron SF, Pratchett MS, Burt JA, Bauman AG (2018) Species-specific coral calcification responses to the extreme environment of the southern Persian Gulf. Front Mar Sci 4:1–13. doi: 10.3389/fmars.2018.00056

Hubbard DK, Miller AI, David A, Islands USV (1990) To the Nature of Reef Systems in the Fossil Record t. 60:335–360.

Hutchings P (2008) Role of polychaetes in bioerosion of coral substrates. Curr Dev Bioerosion 249–264. doi: 10.1007/978-3-540-77598-0_13

Hutchings P (2011) Bioerosion. In: Hopley D (ed) Encyclopedia of Modern Coral Reefs: Structure, Form and Process. Springer Netherlands, Dordrecht, pp 139–156

Hutchings P, Peyrot-Clausade M, Osnorno A (2005) Influence of land runoff on rates and agents of bioerosion of coral substrates. Mar Pollut Bull 51:438–447. doi: 10.1016/j.marpolbul.2004.10.044

Hutchings PA (1986) Biological destruction of coral reefs - A review. Coral Reefs 4:239–252. doi: 10.1007/BF00298083

Hutchings PA, Peyrot-Clausade M (2002) The distribution and abundance of boring species of polychaetes and sipunculans in coral substrates in French Polynesia. J Exp Mar Bio Ecol 269:101–121. doi: 10.1016/S0022-0981(02)00004-7

Isenburg, M "LAStools - efficient LiDAR processing software" (version 141017, unlicensed), obtained from http://rapidlasso.com/LAStools

Januchowski-Hartley FA, Graham NAJ, Wilson SK, Jennings S, Perry CT (2017) Drivers and predictions of coral reef carbonate budget trajectories. Proc R Soc B Biol Sci. doi: 10.1098/rspb.2016.2533

Januchowski-Hartley FA, Bauman AG, Morgan KM, Seah JCL, Huang D, Todd PA (2020) Accreting coral reefs in a highly urbanized environment. Coral Reefs 39:717–731. doi: 10.1007/s00338-020-01953-3

Johansson CL, Bellwood DR, Depczynski M (2010) Sea urchins, macroalgae and coral reef decline: A functional evaluation of an intact reef system, Ningaloo, Western Australia. Mar Ecol Prog Ser 414:65–74. doi: 10.3354/meps08730

Jokiel PL, Maragos J, Franzisket L (1978) Coral growth: buoyant weight technique. Coral reefs Res methods 529–541.

Jenness JS (2004) Calculating landscape surface area from digital elevation models. Wildl Soc Bul 32:829–839

Kamenos NA, Law A (2010) Temperature controls on coralline algal skeletal growth. J Phycol 46:331–335

Kane HH, Fletcher CH (2020) Rethinking Reef Island Stability in Relation to Anthropogenic Sea Level Rise. Earth's Futur. doi: 10.1029/2020EF001525

Karakulak FS, Erk H, Bilgin B (2006) Length-weight relationships for 47 coastal fish species from the northern Aegean Sea, Turkey. J Appl Ichthyol 22:274–278. doi: 10.1111/j.1439-0426.2006.00736.x

Kench PS (1998) Physical controls on development of lagoon sand deposits and lagoon infilling in an Indian Ocean atoll. J Coast Res 14:1014–1024.

Kench PS, Cowell PJ (2006) Variations in sediment production and implications for atoll island stability under rising sea level.

Kennedy E V., Perry CT, Halloran PR, Iglesias-Prieto R, Schönberg CHL, Wisshak M, Form AU, Carricart-Ganivet JP, Fine M, Eakin CM, Mumby PJ (2013) Avoiding coral reef functional collapse requires local and global action. Curr Biol 23:912–918. doi: 10.1016/j.cub.2013.04.020

Kennedy E V., Ordoñez A, Lewis BE, Diaz-Pulido G (2017) Comparison of recruitment tile materials for monitoring coralline algae responses to a changing climate. Mar Ecol Prog Ser 569:129–144

Kiene WE, Hutchings PA (1994) Bioerosion experiments at Lizard Island, Great Barrier Reef. Coral Reefs 13:91–98. doi: 10.1007/BF00300767

King RJ, Schramm W (1982) Calcification in the maerl coralline alga Phymatolithon calcareum: Effects of salinity and temperature. Mar Biol 70:197–204

Kittinger JN, Bambico TM, Minton D, Miller A, Mejia M, Kalei N, Wong B, Glazier EW (2016) Restoring ecosystems, restoring community: socioeconomic and cultural

dimensions of a community-based coral reef restoration project. Reg Environ Chang 16:301–313. doi: 10.1007/s10113-013-0572-x

Kleypas JA (1996) Coral reef development under naturally turbid conditions: Fringing reefs near Broad Sound, Australia. Coral Reefs 15:153–167. doi: 10.1007/BF01145886

Kleypas JA, McManus JW, Mene LAB (1999) Environmental limits to coral reef development: Where do we draw the line? Am Zool 39:146–159. doi: 10.1093/icb/39.1.146

Knudby A, LeDrew E (2007) Measuring Structural Complexity on Coral Reefs. Proc Am Acadamy Underw Sci 26th Symp 181–188

Kohler KE, Gill SM (2006) Coral Point Count with Excel extensions (CPCe): A Visual Basic program for the determination of coral and substrate coverage using random point count methodology. Comput Geosci 32:1259–1269

Kuffner IB, Andersson AJ, Jokiel PL, Rodgers KUUS, Mackenzie FT (2008) Decreased abundance of crustose coralline algae due to ocean acidification. Nat Geosci doi:10.1038/ngeo100

Kuffner IB, Hickey TD, Morrison JM (2013) Calcification rates of the massive coral Siderastrea siderea and crustose coralline algae along the Florida Keys (USA) outer-reef tract. Coral Reefs 32:987–997

Lafratta A, Fromont J, Speare P, Schönberg CHL (2017) Coral bleaching in turbid waters of north-Western Australia. Mar Freshw Res 68:65–75

Langdon MW, Van Keulen M, Paling EI (2013) Distribution, abundance and bioerosion of the grazing sea urchin *Echinometra mathaei* at Ningaloo Marine Park, Western Australia. J R Soc West Aust 96:19.

Lange ID, Perry CT, Alvarez-Filip L (2020) Carbonate budgets as indicators of functional reef "health": A critical review of data underpinning census-based methods and current knowledge gaps. Ecol Indic 110:105857. doi: 10.1016/j.ecolind.2019.105857

Le Grand HM, Fabricius KE (2011) Relationship of internal macrobioeroder densities in living massive Porites to turbidity and chlorophyll on the Australian Great Barrier Reef. Coral Reefs 30:97–107. doi: 10.1007/s00338-010-0670-x

Le Nohaïc M, Ross CL, Cornwall CE, Comeau S, Lowe R, McCulloch MT, Schoepf V (2017) Marine heatwave causes unprecedented regional mass bleaching of thermally resistant corals in northwestern Australia. Sci Rep 7:1–11. doi: 10.1038/s41598-017-14794-y

Lei X, Huang H, Lian J, Zhou G, Jiang L (2018) Community structure of coralline algae and its relationship with environment in Sanya reefs, China. Aquat Ecosyst Heal Manag 21:19–29

Liu G, Heron SF, Mark Eakin C, Muller-Karger FE, Vega-Rodriguez M, Guild LS, de la Cour JL, Geiger EF, Skirving WJ, Burgess TFR, Strong AE, Harris A, Maturi E, Ignatov A, Sapper J, Li J, Lynds S (2014) Reef-scale thermal stress monitoring of coral ecosystems: New 5-km global products from NOAA coral reef watch. Remote Sens 6:11579–11606

Loiola M, Cruz ICS, Lisboa DS, Mariano-Neto E, Leão ZMAN, Oliveira MDM, Kikuchi RKP (2019) Structure of marginal coral reef assemblages under different turbidity regime. Mar Environ Res 147:138–148. doi: 10.1016/j.marenvres.2019.03.013

Lough JM, Barnes DJ (2000) Environmental controls on growth of the massive coral Porites. J Exp Mar Bio Ecol 245:225–243

Lough JM, Cantin NE, Benthuysen JA, Cooper TF (2016) Environmental drivers of growth in massive Porites corals over 16 degrees of latitude along Australia's northwest shelf. Limnol Oceanogr 61:684–700. doi: 10.1002/lno.10244

Magel JMT, Burns JHR, Gates RD, Baum JK (2019) Effects of bleaching-associated mass coral mortality on reef structural complexity across a gradient of local disturbance. Sci Rep 1–12

Mallela J, Perry CT (2007) Calcium carbonate budgets for two coral reefs affected by different terrestrial runoff regimes, Rio Bueno, Jamaica. Coral Reefs 26:129–145. doi: 10.1007/s00338-006-0169-7

Mallela J (2013) Calcification by Reef-Building Sclerobionts. PLoS One 8:1–13

Marcia MA, Kain JM, Norton TA (1996) Biotic interactions in the colonization of crustose coralline algae by epiphytes. J Exp Mar Bio Ecol 199:303–318

Mariath R, Rodriguez RR, Figueiredo MAO (2013) Succession of crustose coralline red algae (Rhodophyta) on coralgal reefs exposed to physical disturbance in the southwest Atlantic. Helgol Mar Res 67:687–696

Martin S, Castets MD, Clavier J (2006) Primary production, respiration and calcification of the temperate free-living coralline alga Lithothamnion corallioides. Aquat Bot 85:121–128

Martin S, Clavier J, Chauvaud L, Thouzeau G (2007) Community metabolism in temperate maerl beds. II. Nutrient fluxes. Mar Ecol Prog Ser 335:31–41

Martin S, Gattuso J-P (2009) Response of Mediterranean coralline algae to ocean acidification and elevated temperature. Glob Chang Biol 15:2089–2100

Mason B, Beard M, Miller MW (2011) Coral larvae settle at a higher frequency on red surfaces. Coral Reefs 30:667–676

Masselink G, Beetham E, Kench P (2020) Coral reef islands can accrete vertically in response to sea level rise. Sci Adv. doi: 10.1126/sciadv.aay3656

Matsuda S (1989) Succession and growth rates of encrusting crustose coralline algae (Rhodophyta, Cryptonemiales) in the upper fore-reef environment off Ishigaki Island, Ryukyu Islands. Coral Reefs 7:185–195

McClanahan TR, Shafir S. (1990) Causes and consequences of sea urchin abundance and diversity in Kenyan coral reef lagoons. Oecologia 83:362–370

McCoy SJ, Kamenos NA (2015) Coralline algae (Rhodophyta) in a changing world: Integrating ecological, physiological, and geochemical responses to global change. J Phycol 51:6–24

McIlwain JL (2002) Link between reproductive output and larval supply of a common damselfish species , with evidence of replenishment from outside the local population. Mar Ecol Prog Ser 236:219–232.

Mollica NR, Guo W, Cohen AL, Huang KF, Foster GL, Donald HK, Solow AR (2018) Ocean acidification affects coral growth by reducing skeletal density. Proc Natl Acad Sci U S A 115:1754–1759. doi: 10.1073/pnas.1712806115

Moore JAY, Bellchambers LM, Depczynski MR, Evans RD, Evans SN, Field SN, Friedman KJ, Gilmour JP, Holmes TH, Middlebrook R, Radford BT, Ridgway T, Shedrawi G, Taylor H, Thomson DP, Wilson SK (2012) Unprecedented Mass Bleaching and Loss of Coral across 12° of Latitude in Western Australia in 2010-11. PLoS One 7:e51807. doi: 10.1371/journal.pone.0051807

Morgan KM, Kench PS (2012) Skeletal extension and calcification of reef-building corals in the central Indian Ocean. Mar Environ Res 81:78–82. doi:

10.1016/j.marenvres.2012.08.001

Morgan KM, Kench PS (2014a) A detrital sediment budget of a Maldivian reef platform. Geomorphology 222:122–131. doi: 10.1016/j.geomorph.2014.02.013

Morgan K, Kench P (2014b) Carbonate production rates of encruster communities on a lagoonal patch reef: Vabbinfaru reef platform, maldives. Mar Freshw Res 65:720–726

Morgan KM, Kench PS (2016) Reef to island sediment connections on a Maldivian carbonate platform: using benthic ecology and biosedimentary depositional facies to examine island-building potential. Earth Surf Process Landforms 41:1815–1825. doi: 10.1002/esp.3946

Morgan KM, Kench PS (2017) New rates of Indian Ocean carbonate production by encrusting coral reef calci fi ers : Periodic expansions following disturbance in fl uence reef-building and recovery. Mar Geol 390:72–79

Morgan KM, Perry CT, Arthur R, Williams HTP, Smithers SG (2020) Projections of coral cover and habitat change on turbid reefs under future sea-level rise. Proc R Soc B Biol Sci 287:20200541. doi: 10.1098/rspb.2020.0541Moustaka M, Langlois TJ, McLean D, Bond T, Fisher R, Fearns P, Dorji P, Evans RD (2018) The effects of suspended sediment on coral reef fish assemblages and feeding guilds of north-west Australia. Coral Reefs 37:659–673. doi: 10.1007/s00338-018-1690-1

Morgan KM, Perry CT, Johnson JA, Smithers SG, Morgan KM, Perry CT (2017) Nearshore Turbid-Zone Corals Exhibit High Bleaching Tolerance on the Great Barrier Reef Following the 2016 Ocean Warming Event. Front Mar Sci 4:1–13. doi: 10.3389/fmars.2017.00224

Morgan KM, Perry CT, Smithers SG, Johnson JA, Daniell JJ (2016) Evidence of extensive reef development and high coral cover in nearshore environments : implications for understanding coral adaptation in turbid settings. Nat Publ Gr 1–10. doi: 10.1038/srep29616

Murphy GN, Perry CT, Chin P, McCoy C (2016) New approaches to quantifying bioerosion by endolithic sponge populations: applications to the coral reefs of Grand Cayman. Coral Reefs 35:1109–1121. doi: 10.1007/s00338-016-1442-z

Nava H, Carballo JL (2008) Chemical and mechanical bioerosion of boring sponges from Mexican Pacific coral reefs. J Exp Biol 211:2827–2831. doi: 10.1242/jeb.019216

Nott J, Hubbert G (2005) Comparisons between topographically surveyed debris lines and modelled inundation levels from severe tropical cyclones Vance and Chris , and their geomorphic impact on the sand coast. 54:187–196

dre P, Mcglinn D, Minchin PR, O'hara RB, Simpson GL, Solymos P, Henry M, Stevens H, Szoecs E, Maintainer HW (2019) Package "vegan" Title Community Ecology Package. Community Ecol Packag 2:1–297

Odum E (1959) Fundameittals of Ecology. Sci Educ 19015.

Ogston AS, Field ME (2010) Predictions of Turbidity Due to Enhanced Sediment Resuspension Resulting from Sea-Level Rise on a Fringing Coral Reef: Evidence from Molokai, Hawaii. J Coast Res 26:1027–1037. doi: 10.2112/JCOASTRES-D-09-00064.1

Ordoñez A, Kennedy E V., Diaz-Pulido G (2017) Reduced spore germination explains sensitivity of reef-building algae to climate change stressors. PLoS One 12:1–19

Osorno A, Peyrot-Clausade M, Hutchings PA (2005) Patterns and rates of erosion in dead

Porites across the Great Barrier Reef (Australia) after 2 years and 4 years of exposure. Coral Reefs 24:292–303. doi: 10.1007/s00338-005-0478-2

Padilla D (1984) The importance of form: difference in competitive ability, resistanc to consumers and environmental stress in an assemblage of coralline algae. J Exp Mar Bio Ecol 79:105–127

Pagès-Escolà M, Hereu B, Garrabou J, Montero-Serra I, Gori A, Gómez-Gras D, Figuerola B, Linares C (2018) Divergent responses to warming of two common co-occurring Mediterranean bryozoans. Sci Rep 8:1–9

Palmer SE, Perry CT, Smithers SG, Gulliver P (2010) Internal structure and accretionary history of a nearshore, turbid-zone coral reef: Paluma Shoals, central Great Barrier Reef, Australia. Mar Geol 276:14–29. doi: 10.1016/j.margeo.2010.07.002

Pari N, Peyrot-Clausade M, Le Campion-Alsumard T, Hutchings P, Chazottes V, Golubic S, Le Campion J, Fontaine MF (1998) Bioerosion of experimental substrates on high islands and on atoll lagoons (French Polynesia) after two years of exposure. Mar Ecol Prog Ser 166:119–130

Pari N, Peyrot-clausade M, Hutchings PA (2002) Bioerosion of experimental substrates on high islands and atoll lagoons (French Polynesia) during 5 years of exposure. 276:109–127.

Perry CT (1999) Reef framework preservation in four contrasting modern reef environments, Discovery Bay, Jamaica. J Coast Res 15:796–812.

Perry CT (2005) Structure and development of detrital reef deposits in turbid nearshore environments, Inhaca Island, Mozambique. Mar Geol 214:143–161

Perry CT, Alvarez-Filip L (2019) Changing geo-ecological functions of coral reefs in the Anthropocene. Funct Ecol 33:976–988. doi: 10.1111/1365-2435.13247

Perry CT, Edinger EN, Kench PS, Murphy GN, Smithers SG, Steneck RS, Mumby PJ (2012) Estimating rates of biologically driven coral reef framework production and erosion: A new census-based carbonate budget methodology and applications to the reefs of Bonaire. Coral Reefs 31:853–868. doi: 10.1007/s00338-012-0901-4

Perry CT, Kench PS, Smithers SG, Riegl B, Yamano H, O'Leary MJ (2011) Implications of reef ecosystem change for the stability and maintenance of coral reef islands. Glob Chang Biol 17:3679–3696. doi: 10.1111/j.1365-2486.2011.02523.x

Perry CT, Morgan KM (2017) Bleaching drives collapse in reef carbonate budgets and reef growth potential on southern Maldives reefs. Sci Rep 7:1–9. doi: 10.1038/srep40581

Perry CT, Murphy GN, Kench PS, Smithers SG, Edinger EN, Steneck RS, Mumby PJ (2013) Caribbean-wide decline in carbonate production threatens coral reef growth. Nat Commun 4:1402–1407

Perry CT, Murphy GN, Kench PS, Edinger EN, Smithers SG, Steneck RS, Mumby PJ (2014) Changing dynamics of Caribbean reef carbonate budgets: Emergence of reef bioeroders as critical controls on present and future reef growth potential. Proc R Soc B Biol Sci 281:20142018. doi: 10.1098/rspb.2014.2018

Perry CT, Morgan KM, Yarlett RT (2017) Reef Habitat Type and Spatial Extent as Interacting Controls on Platform-Scale Carbonate Budgets. Front Mar Sci 4:1–13. doi: 10.3389/fmars.2017.00185

Perry CT, Smithers SG (2011) Cycles of coral reef 'turn-on', rapid growth and 'turn-off' over the past 8500 years: a context for understanding modern ecological states and trajectories. Glob Chang Biol 17:3679–3696. doi: 10.1111/j.1365-2486.2011.02523.x

Perry CT, Spencer T, Kench PS (2008) Carbonate budgets and reef production states: A

geomorphic perspective on the ecological phase-shift concept. Coral Reefs 27:853–866
Perry CT, Lange I, Januchowski-Hartley FA (2018a) ReefBudget Indo Pacific: online resource and methodology. Retrieved from http://geography.exeter.ac.uk/reefbudget/

Perry CT, Alvarez-Filip L, Graham NAJ, Mumby PJ, Wilson SK, Kench PS, Manzello DP, Morgan KM, Slangen ABA, Thomson DP, Januchowski-Hartley F, Smithers SG, Steneck RS, Carlton R, Edinger EN, Enochs IC, Estrada-Saldívar N, Haywood MDE, Kolodziej G, Murphy GN, Pérez-Cervantes E, Suchley A, Valentino L, Boenish R, Wilson M, MacDonald C (2018b) Loss of coral reef growth capacity to track future increases in sea level. Nature 558:396–400. doi: 10.1038/s41586-018-0194-z

Pielke R, Ritchie J (2021) Distorting the view of our climate future: The misuse and abuse of climate pathways and scenarios. Energy Res Soc Sci 72:101890. doi: 10.1016/j.erss.2020.101890

Potin P, Floc'h JY, Augris C, Cabioch J (1990) Annual growth rate of the calcareous red alga Lithothamnion corallioides (Corallinales, Rhodophyta) in the Bay of Brest, France. Hydrobiologia 204–205:263–267
Du Preez C (2015) A new arc–chord ratio (ACR) rugosity index for quantifying three-dimensional landscape structural complexity. Landsc Ecol 30:181–192
Prouty NG, Cohen A, Yates KK, Storlazzi CD, Swarzenski PW, White D (2017) Vulnerability of Coral Reefs to Bioerosion From Land-Based Sources of Pollution. J Geophys Res Ocean 122:9319–9331. doi: 10.1002/2017JC013264
Putnam HM, Barott KL, Ainsworth TD, Gates RD (2017) The Vulnerability and Resilience of Reef-Building Corals. Curr Biol 27:R528–R540. doi: https://doi.org/10.1016/j.cub.2017.04.047
Pygas DR, Ferrari R, Figueira W, Pygas DR, Ferrari R, Figueira W (2019) complexity in marine ecology Review and Meta-analysis of the Importance of Remotely Sensed Habitat Structural Complexity in Marine Ecology. Estuar Coast Shelf Sci 106468
Rasser MW, Riegl B (2002) Holocene coral reef rubble and its binding agents. Coral Reefs 21:57–72
Rice MM, Maher RL, Correa AMS, Moeller H V., Lemoine NP, Shantz AA, Burkepile DE, Silbiger NJ (2020) Macroborer presence on corals increases with nutrient input and promotes parrotfish bioerosion. Coral Reefs 39:409–418. doi: 10.1007/s00338-020-01904-y
Richards ZT, Garcia RA, Wallace CC, Rosser NL, Muir PR (2015) A diverse assemblage of reef corals thriving in a dynamic intertidal reef setting (Bonaparte archipelago, Kimberley, Australia). PLoS One 10:1–17. doi: 10.1371/journal.pone.0117791
Ridgway T, Inostroza K, Synnot L, Trapon M, Twomey L, Westera M (2016) Temporal patterns of coral cover in the offshore Pilbara, Western Australia. Mar Biol 163:1–9
Risk MJ (1972) Fish Diversity on a Coral Reef in the Virgin Islands. Atoll Res Bull 153:
Roik A, Roder C, Rothig T, Voolstra CR (2016) Spatial and seasonal reef calcification in corals and calcareous crusts in the central Red Sea. 681–693
Roik A, Röthig T, Pogoreutz C, Voolstra CR (2018) Coral reef carbonate budgets and ecological drivers in the naturally high temperature and high alkalinity environment of the Red Sea. Coral reef carbonate budgets Ecol drivers Nat high Temp high Total alkalinity Environ Red Sea 203885. doi: 10.1101/203885

Ross CL, Falter JL, Schoepf V, McCulloch MT (2015) Perennial growth of hermatypic corals at Rottnest Island, Western Australia (32°S). PeerJ 2015:1–26. doi:

10.7717/peerj.781
Ross CL, Falter JL, McCulloch MT (2017) Active modulation of the calcifying fluid carbonate chemistry (δ11B, B/Ca) and seasonally invariant coral calcification at sub-Tropical limits. Sci Rep 7:1–11. doi: 10.1038/s41598-017-14066-9
Ross CL, DeCarlo TM, McCulloch MT (2019) Environmental and physiochemical controls on coral calcification along a latitudinal temperature gradient in Western Australia. Glob Chang Biol 25:431–447. doi: 10.1111/gcb.14488
Rosser NL (2012) Abundance , distribution and new records of scleractinian corals at Barrow Island and Southern Montebello Islands. J R Soc West Aust 95:155–165
Roy K, Jablonski D, Valentine JW (2000) Dissecting latitudinal diversity gradients: Functional groups and clades of marine bivalves. Proc R Soc B Biol Sci 267:293–299. doi: 10.1098/rspb.2000.0999
Rutzler K (1975) The Role of Burrowing Sponges in Bioerosion *. Oecologia 216:203–216.
Ryan EJ, Hanmer K, Kench PS (2019) Massive corals maintain a positive carbonate budget of a Maldivian upper reef platform despite major bleaching event. Sci Rep 9:1–11. doi: 10.1038/s41598-019-42985-2
Ryan EJ, Smithers SG, Zhao SELTRCJX (2016) The influence of sea level and cyclones on Holocene reef flat development : Middle Island , central Great Barrier Reef. Coral Reefs 35:805–818. doi: 10.1007/s00338-016-1453-9
Sadd J. (1984) Sediment transport and CaCO3 budget on a fringing reef, Cane Bay, St. Croix, US Virgin Islands. Bull Mar Sci 35:221–238.
Sammarco P, Risk M (1990) Large-scale patterns in internal bioerosion of Porites: cross continental shelf trends on the Great Barrier Reef. Mar Ecol Prog Ser 59:145–156. doi: 10.3354/meps059145
Scoffin TP (1993) The geological effects of hurricanes on coral reefs and the interpretation of storm deposits. Coral Reefs 12:203–221
Schiel DR, Steinbeck JR, Foster MS (2014) Ten Years of Induced Ocean Warming Causes Comprehensive changes in marine benthic communies. Ecology 85:1833–1839.
Schönberg ACHL (2015) Monitoring Bioeroding Sponges : Using Rubble , Quadrat , or Intercept Surveys ? 228:137–155.
Schönberg CHL, Fang JKH, Carreiro-Silva M, Tribollet A, Wisshak M (2017) Bioerosion: The other ocean acidification problem. ICES J Mar Sci 74:895–925. doi: 10.1093/icesjms/fsw254
Short J, Foster T, Falter J, Kendrick GA, Mcculloch MT (2015) Crustose coralline algal growth , calcification and mortality following a marine heatwave in Western Australia. Cont Shelf Res 106:38–44
Schramm KD, Marnane MJ, Elsdon TS, Jones CM, Saunders BJ, Newman SJ, Harvey ES (2021) Fish associations with shallow water subsea pipelines compared to surrounding reef and soft sediment habitats. Sci Rep 11:1–15. doi: 10.1038/s41598-021-85396-y
Silbiger NJ, Guadayol Ò, Thomas FIM, Donahue MJ (2014) Reefs shift from net accretion to net erosion along a natural environmental gradient. Mar Ecol Prog Ser 515:33–44. doi: 10.3354/meps10999
Silbiger NJ, Guadayol O, Thomas FIM, Donahue MJ (2015) Impacts of multiple environmental stressors on coral reef erosion and secondary accretion. PeerJ Prepr 3:e1451. doi: 10.7287/peerj.preprints.1190v1
Silbiger NJ, Guadayol O, Thomas FOM, Donahue MJ (2016) A novel μct analysis reveals different responses of bioerosion and secondary accretion to environmental variability.

PLoS One 11:11–16. doi: 10.1371/journal.pone.0153058
Silbiger NJ, Donahue MJ, Brainard RE (2017) Environmental drivers of coral reef carbonate production and bioerosion: A multi-scale analysis. Ecology 98:2547–2560. doi: 10.1002/ecy.1946
Speed CW, Babcock RC, Bancroft KP, Beckley LE, Bellchambers LM, Depczynski M, Field SN, Friedman KJ, Gilmour JP, Hobbs JPA, Kobryn HT, Moore JAY, Nutt CD, Shedrawi G, Thomson DP, Wilson SK (2013) Dynamic Stability of Coral Reefs on the West Australian Coast. PLoS One. doi: 10.1371/journal.pone.0069863
Stearn W, Scoffin TP (1977) Calcium Carbonate Budget of a Fringing Reef on the West Coast of Barbados. Bull Mar Sci 27:479–510
Steneck RS (1986) The Ecology of Coralline Algal Crusts : Convergent Patterns and Adaptative Strategies. Annu Rev Ecol Syst 17:273–303
Steneck RS (2011) Mechanisms of Competitive Dominance Between Crustose Coralline Algae : An Herbivore- Mediated Competitive Reversal. Ecology 72:938–950
Storlazzi CD, Dartnell P, Hatcher GA, Gibbs AE (2016) End of the chain? Rugosity and fine-scale bathymetry from existing underwater digital imagery using structure-from-motion (SfM) technology. Coral Reefs 35:889–894
Tortolero-Langarica JJA, Rodríguez-Troncoso AP, Carricart-Ganivet JP, Cupul-Magaña AL (2016) Skeletal extension, density and calcification rates of massive free-living coral Porites lobata Dana, 1846. J Exp Mar Bio Ecol 478:68–76
Tortolero-Langarica JJA, Rodríguez-Troncoso AP, Cupul-Magaña AL, Rinkevich B (2020) Micro-fragmentation as an effective and applied tool to restore remote reefs in the eastern tropical pacific. Int J Environ Res Public Health 17:1–18. doi: 10.3390/ijerph17186574
Tribollet A (2008) The boring microflora in modern coral reef ecosystems: a review of its roles. In: Wisshak M, Tapanila L (eds) Current Developments in Bioerosion. Springer Berlin Heidelberg, Berlin, Heidelberg, pp 67–94
Tribollet A, Golubic S (2005) Cross-shelf differences in the pattern and pace of bioerosion of experimental carbonate substrates exposed for 3 years on the northern Great Barrier Reef, Australia. Coral Reefs 24:422–434. doi: 10.1007/s00338-005-0003-7
Tribollet A, Decherf G, Hutchings PA, Peyrot-Clausade M (2002) Large-scale spatial variability in bioerosion of experimental coral substrates on the Great Barrier Reef (Australia): importance of microborers. Coral Reefs 424–432. doi: 10.1007/s00338-002-0267-0
Tuck ME, Ford MR, Kench PS, Masselink G (2021) Sediment supply dampens the erosive effects of sea-level rise on reef islands. Sci Rep 11:1–10. doi: 10.1038/s41598-021-85076-x
Vásquez-Elizondo RM, Enríquez S (2016) Coralline algal physiology is more adversely affected by elevated temperature than reduced pH. Sci Rep 6:1–14
Venti A, Andersson A, Langdon C (2014) Multiple driving factors explain spatial and temporal variability in coral calcification rates on the Bermuda platform. Coral Reefs 33:979–997. doi: 10.1007/s00338-014-1191-9
Vermeij MJA, Dailer ML, Smith CM (2011) Crustose coralline algae can suppress macroalgal growth and recruitment on hawaiian coral reefs. Mar Ecol Prog Ser 422:1–7
Vogel K, Gektidis M, Golubic S, Kiene WE, Radtke G (2000) Experimental studies on microbial bioerosion at Lee Stocking Island, Bahamas and One Tree Island, Great Barrier Reef, Australia: Implications for paleoecological reconstructions. Lethaia

33:190–204. doi: 10.1080/00241160025100053
Vogel N, Cantin NE, Strahl J, Kaniewska P, Bay L, Wild C, Uthicke S (2016) Interactive effects of ocean acidification and warming on coral reef associated epilithic algal communities under past, present-day and future ocean conditions. Coral Reefs 35:715–728
Walbridge S, Slocum N, Pobuda M, Wright DJ (2018) Unified Geomorphological Analysis Workflows with Benthic Terrain Modeler. Geosciences 8:doi:10.3390
Webb AE, van Heuven SMAC, de Bakker DM, van Duyl FC, Reichart GJ, de Nooijer LJ (2017) Combined effects of experimental acidification and eutrophication on reef sponge bioerosion rates. Front Mar Sci 4:1–15. doi: 10.3389/fmars.2017.00311
Weber JN, White EW (1974) Activation energy for skeletal aragonite deposited by the hermatypic coral Platygyra spp. Mar Biol 26:353–359
Webster NS, Soo R, Cobb R, Negri AP (2011) Elevated seawater temperature causes a microbial shift on crustose coralline algae with implications for the recruitment of coral larvae. ISME J 5:759–770
Wedding LM, Friedlander A (2008) Determining the influence of seascape structure on coral reef fishes in Hawaii using a geospatial approach. Mar Geod 31:246–266
Welle PD, Small MJ, Doney SC, Azevedo L (2017) Estimating the effect of multiple environmental stressors on coral bleaching and mortality. PLoS One 12:1–15
Wellington GM, Glynn PW (1983) Environmental influences on skeletal banding in eastern Pacific (Panama) corals. Coral Reefs 1:215–222
Wickham H (2011) Review Reviewed Work (s): ggplot2 : Elegant Graphics for Data Analysis by H . WICKHAM Review by : Leland Wilkinson Published by : International Biometric Society Stable URL : https://www.jstor.org/stable/41242513. Int Biometric Soc 67:678–679
Wild C, Hoegh-Guldberg O, Naumann MS, Colombo-Pallotta MF, Ateweberhan M, Fitt WK, Iglesias-Prieto R, Palmer C, Bythell JC, Ortiz JC, Loya Y, Van Woesik R (2011) Climate change impedes scleractinian corals as primary reef ecosystem engineers. Mar Freshw Res 62:205–215
Wisshak M, Schönberg CHL, Form AU, Freiwald A (2012) Ocean Acidification Accelerates Reef Bioerosion. PLoS One. doi: 10.1371/Citation
Wizemann A, Nandini SD, Stuhldreier I, Sánchez-Noguera C, Wisshak M, Westphal H, Rixen T, Wild C, Reymond CE (2018) Rapid bioerosion in a tropical upwelling coral reef. PLoS One 13:1–23. doi: 10.1371/journal.pone.0202887
van Woesik R, Cacciapaglia C (2018) Refining reef-coral refugia. Glob Chang Biol 24:e400–e401
Yamano H, Miyajima T, Koike I (2000) Importance of foraminifera for the formation and maintenance of a coral sand cay : Green Island , Australia. Coral Reefs An Ecosyst Transit 19:51–58.
Yamano H, Kayanne H, Chikamori M (2005) An Overview of The Nature and Dynamics of Reef Islands. Glob Environ Res 9:9–20
Yarlett RT, Perry CT, Wilson RW, Philpot KE (2018) Constraining species-size class variability in rates of parrotfish bioerosion on Maldivian coral reefs: Implications for regional-scale bioerosion estimates. Mar Ecol Prog Ser 590:155–169. doi: 10.3354/meps12480
Yarlett RT, Perry CT, Wilson RW, Harborne AR (2020) Inter-habitat variability in parrotfish bioerosion rates and grazing pressure on an indian ocean reef platform. Diversity

12:1–17. doi: 10.3390/d12100381
Zoffoli ML, Frouin R, Kampel M (2014) Water Column Correction for Coral Reef Studies by Remote Sensing. Sensors 14:16881–16931
Zubia M, Peyrot-Clausade M (2001) Internal bioerosion of Acropora formosa in Réunion (Indian Ocean): Microborer and macroborer activities. Oceanol Acta 24:251–262. doi: 10.1016/S0399-1784(01)01144-6
Zweifler A, O'leary M, Morgan K, Browne NK (2021) Turbid coral reefs: Past, present and future—a review. Diversity 13:1–23. doi: 10.3390/d13060251

Appendices

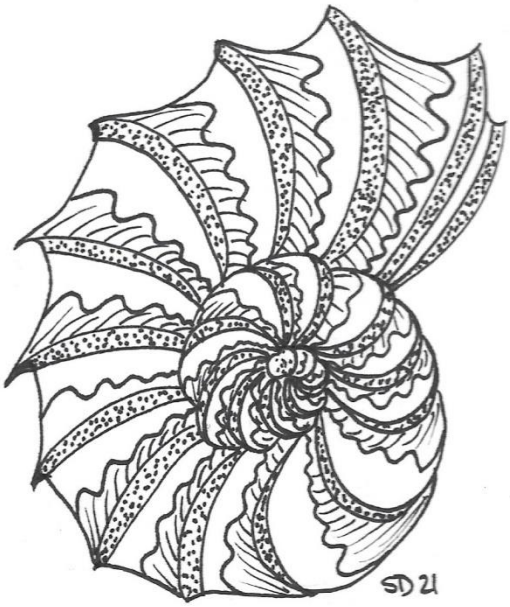

1.1 Copyright statements

2.1 Supplementary material

Supplementary Table 1 Summary of census based carbonate budget studies since the 1970's with regards to the method used to assess reef rugosity

Year	*Location/s*	*Rugosity method*	*References*
1977 & 1980	Bellairs Reef, Barbados	CT method (version of)	Stearn et al., 1977 and Scoffin et al., 1980.
1990	St Croix, US Virgin Islands	CT method	Hubbard 1990
1996	Uva Island, Eastern Pacific	CT method	Eakin 1996
2001	Uva Island, Eastern Pacific	CT method	Eakin 2001
2003	Kailua Bay, Oahu, Hawaii	CT method	Harney and Fletcher 2003
2007	Rio Bueno, Jamaica	CT method	Mallela and Perry 2007
2007	Warraber Island, Torres Strait, Australia	CT method	Hart and Kench 2007
2012	Bonaire	CT method	Perry et al., 2012
2013	19 reefs in the Caribbean	CT method	Perry et al., 2013
2013	Middle Reef and Paluma Shoals, Great Barrier Reef, Australia	CT method	Browne et al., 2013
2013	Warrabar Reef and Bet Reef, Torres strait	CT method	Leon and Woodroffe 2013
2013	One Tree Island, Australia	Remote sensing	Hamylton et al., 2013
2014	Vabbinfaru Reef, North Malé Atoll, Maldives	CT method	Morgan and Kench 2014b
2015	75 sites across the Caribbean	CT method	Perry et al., 2015a
2015	Great Chagos Bank, Peros Banhos, Salomon	CT method	Perry et al., 2015b
2017	Seychelles Islands	CT method	Januchowski-Hartley et al., (2017)
2017	Zanzibar Island chain, close to Stone Town, Zanzibar	CT method	Herrán et al., 2017
2017	Gaafu Dhalu Atoll, Southern Maldives	CT method	Perry and Morgan 2017
2017	Lhaviyani Atoll, Central Maldives	CT method	Perry et al., 2017
2018	Cheeca Rocks, Florida Keys	CT method	Manzello et al., 2018
2018	86 sites across the Caribbean and 68 sites in the Indo-Pacific region	CT method	Perry et al., 2018
2018	Red Sea, Saudi Arabia	CT method	Roik et al., 2017

2018	Palau & Yap, Western Pacific Ocean	CT method	van Woesik and Cacciapaglia 2018
2019	Cocos Keeling	Remote sensing	Hamylton and Mallela 2019
2019	Great Chagos Bank, Peros Banhos, Salomon in the Chagos Archipelago	CT method	Lange and Perry 2018
2019	Mahutigala reef, Gaafu Dhalu Atoll, Maldives	CT method	Ryan et al., 2019
2019	Bonaire fringing reef, Caribbean	CT method	de Bakker et al., 2019
2020	Offshore coral reefs, Singapore	CT method	Januchowski-Hartley et al., 2020

Supplementary Table 2 Average habitat cover (%), average encruster carbonate production (CP) rate (g $cm^{-2}yr^{-1}$), and tile CCA cover (%), of northern and southern sites across Eva and Fly reefs

		Habitat (% cover)				CP rate (g $cm^{-2}yr^{-1}$)			CCA cover (%)		
Reefs	zone	coral	MA	TA	sand	Winter	Summer	Annual	Winter	Summer	Annual
Eva	*North*	37	28	16	9	0.0537	0.0562	0.0624	93	78	88
	South	2	67	4	14	0.0374	0.0251	0.0241	81	54	65
Fly	*North*	29	0	35	20	0.0413	0.0340	0.0466	89	74	70
	South	1	52	3	28	0.0254	0.0375	0.0331	65	56	59

Supplementary Table 3 Average monthly environmental measures over 12 months of tile deployments. Temperature data provided by NOAA (https://coralreefwatch.noaa.gov/product/5km/, Liu et al. 2014) shows average as well as maximum Sea Surface temperature (SST) and Sea Surface temperature anomaly (SSTA) for each month. Chlorophyll, conductivity, salinity, pH, and turbidity were all measured *in situ* with Sonde probe. *In situ* measurements were not taken at Eva reef during October 2019 due to poor weather, and measurements were not able to be taken at either reef during March 2020 due to COVID 19 travel restrictions.

						Chlorophyll ug/L		Conductivity µS/cm		Salinity psu		pH		Turbidity FNU	
Year	Month	av. SST	Max SST	av. SSTA	Max SSTA	Eva	Fly	Eva	Fly	Eva	Fly	Eva	Fly	Eva	Fly
2019	April	27.6	29.5	0.1	1.6	0.7	0.8	$5.9x10^4$	$5.9x10^4$	36.1	36.0	8.1	8.1	1.6	0.8
2019	May	25.1	25.9	-0.7	0.2	0.3	0.8	$5.3x10^4$	$5.3x10^4$	35.5	36.0	8.2	8.2	0.2	1.6
2019	June	22.6	24.7	-1.8	-0.3	0.6	0.6	$5.5x10^4$	$5.4x10^4$	39.0	39.3	8.2	8.2	1.1	5.0
2019	July	21.6	22.5	-1.5	-0.8	0.4	0.5	$5.4x10^4$	$5.4x10^4$	39.4	38.9	8.15	8.1	1.6	2.5
2019	Aug	21.0	22.4	-1.0	0.4	0.5	0.5	$5.5x10^4$	$5.4x10^4$	38.7	38.7	8.2	8.2	3.6	2.3
2019	Sep	22.8	23.8	0.7	1.7	0.1	0.3	$5.5x10^4$	$5.4x10^4$	39.1	38.8	8.25	8.3	0.7	1.7
2019	Oct	23.7	24.6	1.0	1.5		0.6		$5.7x10^4$		39.5		8.5		1.9
2019	Nov	25.1	26.1	1.3	2.0	0.5	0.5	$5.7x10^4$	$5.7x10^4$	39.5	39.6	8.2	8.2	3.5	3.9
2019	Dec	27.6	29.0	2.6	3.2	0.2	0.2	$5.9x10^4$	$6.1x10^4$	38.2	39.5	8.2	8.2	1.0	1.1
2020	Jan	28.4	29.4	1.8	3.0	0.2	0.2	$6.3x10^4$	$6.4x10^4$	39.4	39.5	8.2	8.2	0.3	0.8
2020	Feb	27.6	28.7	-0.2	0.6	0.5	0.4	$6.2x10^4$	$6.0x10^4$	39.6	38.8	8.1	8.1	0.4	2.8
2020	Mar	29.0	29.5	0.8	1.5										

Supplementary Table 4 Distance based linear modelling marginal test results for individual drivers of spatial variation in CCA cover, as well as carbonate production rates.

Variable	*SS(trace)*	*Pseudo-F*	*P*	*Prop.*
CCA cover				
Benthic Temperature	208.5	4.901	0.036	0.182
Light	81.6	1.688	0.209	0.071
Chlorophyll	40.2	0.801	0.378	0.035
Conductivity	84.6	1.756	0.204	0.074
Salinity	146.5	3.229	0.084	0.128
pH	7.4	0.143	0.726	0.006
Turbidity	21.6	0.423	0.528	0.019
Coral	217.1	5.150	0.033	0.190
Macroalgae	107.7	2.286	0.141	0.094
Turfing algae	63.0	1.282	0.271	0.055
Sand	86.2	1.792	0.195	0.075
Carbonate production				
Temperature	389.7	1.560	0.216	0.066
Light	2.5	0.009	0.990	0.000
Chlorophyll	35.5	0.134	0.792	0.006
Conductivity	18.8	0.070	0.875	0.003
Salinity	139.0	0.532	0.488	0.024
pH	122.6	0.468	0.508	0.021
Turbidity	70.2	0.265	0.649	0.012
Coral	832.7	3.627	0.060	0.142
Macroalgae	1035.6	4.699	0.039	0.176
Turfing algae	703.7	2.988	0.090	0.120
Sand	29.9	0.113	0.811	0.005

Supplementary Table 5 Distance based linear modelling marginal test results for individual drivers of temporal variation in CCA cover temporally, as well as carbonate production rates.

Variable	*SS(trace)*	*Pseudo-F*	*P*	*Prop.*
CCA cover				
Benthic Temperature	360.1	13.18	0.001	0.223
Light	165.3	5.24	0.028	0.102
Chlorophyll-a	164.5	5.21	0.025	0.102
Conductivity	314.2	11.09	0.001	0.194
Salinity	356.4	13.00	0.001	0.220
pH	16.4	0.47	0.499	0.010
Turbidity	19.0	0.55	0.468	0.012
Carbonate production				
Temperature	19.2	0.13	0.820	0.003
Light	68.7	0.46	0.526	0.010
Chlorophyll-a	39.7	0.27	0.659	0.006
Conductivity	6.7	0.04	0.945	0.001
Salinity	18.9	0.13	0.821	0.003
pH	35.6	0.24	0.681	0.005
Turbidity	157.9	1.08	0.307	0.023

Supplementary Table 6 Summary of studies globally that have recorded rates of endolithic bioerosion at the microboring or macroboring scale. Boring shown in red indicates bioerosion purely by sponges and studies shown in blue indicate that the study used non-coral experimental substrate. * indicates the study was used in linear regression analysis

Study	*Region*	*Method*	*Experimental substrate used*	*Reef type*	*Environmental data*	*Notes*	*Units of bioerosion used*	*Grazing*	*Macro*	*Micro*	*Total*
Stearn and Scoffin (1977)	Barbados	Analysis of coral colony X-ray to quantify volume loss	Average	Fringing reef	No		kg m^{-2} yr^{-1}		0.237		
			Orbicella annularis						0.377		
			Porites astreoides						0.148		
			Siderastrea siderea						0.08		
			Agaricia agaricites						0.382		
			Porites porites						0.200		
Scoffin et al. (1980)	Barbados	Buoyant weight of reef substrate	average	Fringing reef	No		kg m^{-2} yr^{-1}		0.301		
			crustose coralline algae						0.511		
			Agaricia agaricites						0.315		
			Orbicella annularis						0.478		
			Porites asteroides						0.207		
			Porites porites						0.196		
			Siderastrea siderea						0.098		
Davies and Hutchings (1983)	Great Barrier Reef	experimental blocks - bioerosion calculated from volume of polychaetes	*Porites letua*	Reef front	No		kg m^{-2} yr^{-1}		0.694		
				Reef flat					0.843		
				Patch reef					1.788		
Sammarco and Risk	Great Barrier Reef	Analysis of coral colony X-ray to quantify volume loss	*Porites lobata*	Fringing reef	No		%				11.13

(1990)				Platform								5.88
				Platform								4.58
				Platform								6.39
				Platform								1.21
Kiene and Hutchings (1994)	Great Barrier Reef	2D Image analysis of borer hole volume from sliced experimental substrate	*Porites letua*	Leeward slope (10m)	No			kg m^{-2} yr^{-1}		1.3		
				Windward reef slope						1.6		
				Lagoon patch reef						1.3		
				Reef flat						1.6		
				Lagoon channel						1.3		
				Leeward slope (20 m)						2.0		
Chazottes et al. (1995)	Moorea, French Polynesia	2D Image analysis of borer hole volume from sliced experimental substrate	*Porites lobata*	Clear water barrier reef	No		2 months	kg m^{-2} yr^{-1}	0.37	0.002	0.57	0.94
							6 months		0.96	0.003	0.2	1.16
							12 months		1.74	0.022	0.14	1.9
							24 months		2.33	0.09	0.2	2.62
Eakin (1996)	Central Pacific	*In situ* "bucket" measurements		Back reef	No			kg m^{-2} yr^{-1}	0.10	6.29		
				Reef flat					1.16	3.67		
				Fore reef					2.32	5.95		
				Reef base					5.63	8.01		
Vogel et al. (2000)	Great Barrier Reef	Microscope, SEM	*Tridacna* shells	Micro atoll	Yes	Nitrates and phosphates		kg m^{-2} yr^{-1}			0.025	
Zubia and Peyrot-Clausade (2001)	Reunion (Indian ocean)	Live samples of Acropora with scanning electron microscopy (SEM) to analyse volume of caco3 extracted by microflora	*Acropora formosa*	Undisturbed reef flat	No		grazed	g cm^{-3}			0.24	
				Undisturbed reef flat			ungrazed				0.22	
				Disturbed reef flat			grazed				0.38	
				Disturbed reef flat			ungrazed				0.34	

Tribollet et al. (2002)	Great Barrier Reef	2D Image analysis of borer hole volume from sliced experimental substrate	*Porites. Sp.*	Inshore reef	No		Snapper	kg m^{-2} yr^{-1}	0.28	0.037	0.12	0.46
				Inshore reef			Low Isles		0.32	0.01	0.15	0.53
				Clear water reef			Lizard		2.77	0.09	0.75	3.6
							Harrier		2.8	0.037	0.38	3.04
							Ribbon		1.24	0.037	1.01	2.2
							Osprey		1.37	0.037	1.34	2.6
Pari et al. (2002)	French Polynesia	2D Image analysis of borer hole volume from sliced experimental substrate	*Porites lutea*	Fringing reef	No			kg m^{-2} yr^{-1}	1.27	0.12		
									1.58	0.33		
									1.42	1.04		
									2.49	0.52		
									1.68	0.12		
									1.48	0.02		
Chazottes et al. (2002)	Reunion (Indian ocean)	2D Image analysis of borer hole volume from sliced experimental substrate	*Porites lobata*	fringing reef	Yes	Salinity, Nutrients		kg m^{-2} yr^{-1}	0.002	0.007	0.058	
									0.003	0.021	0.067	
									0.004	0.032	0.044	
Harney and Fletcher (2003)	Hawaii	% Eroded from coral rubble		Nearshore	No			kg m^{-2} yr^{-1}				0.133
				Reef platform								0.13
				Channel margins								0.15
				Reef platform								0.197
				Reef front								0.39
Tribollet and Golubic (2005)	Great Barrier Reef	2D Image analysis of borer hole volume from sliced experimental substrate	*Porites. Spp.*	Inshore reef	No		Snapper	kg m^{-2} yr^{-1}	0.004	0.13	0.15	0.27
				Inshore reef			Low Isles		0.01	0.01	0.16	0.18
				clear water reef			Lizard		0.11	0.11	0.71	1.09
							Harrier		0.02	0.02	0.76	1.22

							Ribbon		0.04	0.04	0.38	1.23
							Osprey		0.03	0.03	1.4	2.19
Osorno et al. (2005)	Great Barrier Reef	2D Image analysis of borer hole volume from sliced experimental substrate	*Porites spp.*	Inshore island reef	No		Snapper	kg m^{-2} yr^{-1} after 2 years exposure	0.02	0.08		
				Inshore island reef			Low Isles		0.05	0.14		
				Mid-shelf reef			Lizard		0.17	0.01		
				Outer shelf reef			Harrier		0.32	0.09		
				Outer shelf reef			Ribbon		0.64	0.02		
				Outer shelf reef			Osprey		0.85	0.04		
				Inshore island reef			Snapper	kg m^{-2} yr^{-1} after 4 years exposure	0.15	0.27		
				Inshore island reef			Low Isles		0.12	0.16		
				Mid-shelf reef			Lizard		0.29	0.10		
				Outer shelf reef			Harrier		0.69	0.22		
				Outer shelf reef			Ribbon		1.85	0.13		
				Outer shelf reef			Osprey		1.22	0.04		
Carreiro-Silva et al. (2005)	Belize	*In situ* shells exposed to levels of herbivory and nutrients - image analysis or borer volume	*Strombus gigas* shell fragments	atoll patch reef	Yes	Nutrients	Ungrazed/ control	kg m^{-2} yr^{-1}	0.062			
							Ungrazed/ enriched		0.452			
							Grazed/ control		0.049			
							Grazed/ enriched		0.200			
Mallela and Perry (2007)	Caribbean	% eroded from coral rubble	*Acropora spp.*	Central embayment	Yes	Temperature, Nutrients		kg m^{-2} yr^{-1}	0.1	0.8	1.7	
				Outer embayment	Yes	Temperature, Nutrients		kg m^{-2} yr^{-1}	0.22	0.7	0.4	

Carreiro-Silva et al. (2009)	Belize	*In situ* shells exposed to levels of herbivory and nutrients - image analysis or borer volume	*Strombus gigas* shell fragments	atoll patch reef		Nitrogen and Phosphate		kg m^{-2} yr^{-1}		0.396
						Nitrogen, Phosphate, and organic matter				0.37
						Organic matter				0.044
						Control				0.048
Carreiro-Silva and McClanahan (2012)*	Kenya	2D Image analysis of borer hole volume from sliced experimental substrate	*Porites* branching	fringing reef MPA	Yes	Nutrients, chlorophyll-a, Total particulate matter, Particulate organic matter, Temperature, Current speed	Malindi	kg m^{-2} yr^{-1} after 4 years of exposure		0.230
				fringing reef-MPA			Watamu			0.195
				fringing reef-MPA			Mombasa			0.220
				patch reef -MPA			Kisite			0.180
				fringing reef-Reserve			Ras Iwatine			0.270
				fringing reef Reserve			Mpunguti			0.175
				Fringing- heavily fished			Kanamai			0.220
				patch reef – heavily fished			Diani			0.190
				fringing reef MPA			Malindi	kg m^{-2} yr^{-1} after 6 years of exposure		0.290
				fringing reef-MPA			Watamu			0.370
				fringing reef-MPA			Mombasa			0.230
				patch reef -MPA			Kisite			0.185
				fringing reef-Reserve			Ras Iwatine			0.265
				fringing reef-Reserve			Mpunguti			0.165

				Fringing – heavily fished			Kanamai		0.250
				patch reef – heavily fished			Diani		0.185
Hernández-Ballesteros et al. (2013)	Mexico	Image analysis of x ray images of coral slices	*Montastraea annularis*	turbid	No		bioerosion with skeletal density	%	1.7
			Montastraea annularis	fringing reef					3.81
			Porites astreoides	turbid					3.72
			Porites astreoides	fringing reef					7.45
Browne et al. (2013)	Great Barrier Reef	% Eroded from coral rubble	*Acropora*	Shallow turbid	No			kg m^{-2} yr^{-1}	0.3
				Deep					4.9
				Shallow windward					0.6
				Leeward					4.3
Wisshak et al. (2014)	Helgoland Island	Tank experiments measuring carbonate dissolution by sponges through changes in total alkalinity	*Oyster shells*	tank	Yes	Temperature, Salinity, pH, pCO2, DIC, HCO3, Aragonite Saturation, Nutrients	present day pco2		0.04
							moderately elevated pco2		0.07
							strongly elevated pco2		0.16
DeCarlo et al. (2014)*	Pacific basin	CT scanning coral cores	*Porites spp.*	Fringing reef/ bay	Yes	Aragonite saturation state, Nitrate	Palau	kg m^{-2} yr^{-1}	0.17
				Fringing reef/ bay			Palau		0.11
				Fringing			Palau		0.012
				Barrier			Palau		0.012
				Lagoon/ fringing			Rose Atoll		0
				fringing			Wake Atoll		0
				fringing			Palmyra Atoll		0
				Langoon/fringing			Kingman reef		0.04

				fringing			Jarvis island			0.27		
				fringing			Panama			0.65		
				fringing			Panama			0.68		
Murphy et al. (2016)	Grand Cayman	Erosion in cores/coral heads	*Orbicella annularis*	Fore reef	No		sponge only	kg m^{-2} yr^{-1}		0.10		
Enochs et al. (2016)*	PNG	µCT analysis to measure volume loss of experimental substrate by bioeroders	*Porites spp.*	Volcanic island reefs	Yes	DIC, Total Alkalinity, pH		kg m^{-2} yr^{-1}				0.13
												0.098
												0.065
												0.052
												0.039
												0.026
Silbiger et al. (2017)*	Hawaii	µCT analysis to measure volume loss of experimental substrate by bioeroders	*Porites lobata*	Island/ atolls	Yes	pH, Temperature, Nutrients, Chlorophyll-a, Total Alkalinity		kg m^{-2} yr^{-1}				0.15
												0.15
												0.12
												0.074
												0.094
												0.072
Prouty et al. (2017)*	Hawaii	CT scanning coral cores to measure volume removed by bioeroders	*Porites lobata*	shallow reefs	Yes	Aragonite Saturation, pH, Salinity, Nitrate		kg m^{-2} yr^{-1}				0.072
												0.056
												0.089
												0.039
												0.023
												0.099
Chazottes et al. (2017)*	Great Barrier Reef	2D Image analysis of borer hole volume from sliced experimental substrate	*Porites spp.*	micro atoll	Yes	Sites enriched with Nitrogen and Phosphorus	enriched	kg m^{-2}	1.67	0.016	1.18	
							control		1	0.022	0.99	

Webb et al. (2017)	Caribbean	Dead coral cores	*Diploria spp.*	Tank	Yes	Temperature, Salinity, pCO2, 02%, DIC, pH, HCO3, CO2, Aragonite Saturation, DOC, Nox, NO2, NH4, PO4	present day	mg cm^{-2} h^{-1}	0.0055	
							Bleow-ambient		0.005	
							Reduced-emissions		0.005	
							Business-as-usual		0.007333	
Wizemann et al. (2018)*	Costa Rica	Weight loss and µCT analysis to measure volume loss of experimental substrate by bioeroders	*stylophora pistillata*	protected bay exposed to seasonal upwelling	Yes	DIC, SST, Salinity, pH, co2, Aragonite Saturation, Nutrients	one month	mg		15.225
							two months			147.2333
							three months			161.7
							four months			567.4

Supplementary Table 7 General calcification rates for corals equated from linear extension and density measurements provided from the *Reefbudget* data sheet

Morphology	Genus	Calcification Rate ($g\ cm^{-2}\ yr^{-1}$)
Branching	*Acropora (table)*	10.7
	Pocillopora	3.7
Foliose/plate	*Montipora*	2.7
	Turbinaria	2.6
	Pavona	3.3
Massive	*Porites*	1.5
	Goniastrea	0.9
	Favia	0.9
	Lobophyllia	2.1
	Platygyra	1.1

Supplementary Table 8 Adjusted coral carbonate production, gross carbonate production (kg $m^{-2}yr^{-1}$), net carbonate production (kg $m^{-2}yr^{-1}$), and reef accretion potential (mm yr^{-1}) once *Reef Budget* linear growth calcification rates had been applied

	Coral carbonate production		Adjusted measures		
	Carbonate production $x10^3$ kg yr^{-1}	Normalised Carbonate production kg $m^{-2}yr^{-1}$	Gross normalised carbonate production kg $m^{-2}yr^{-1}$	Net carbonate production kg $m^{-2}yr^{-1}$	Reef accretion potential mm yr^{-1}
Eva					
NWF	894.2 ± 855.1	5.7 ± 2.4	5.8 ± 2.3	5.8 ± 2.3	2.46
ELC	145.7 ± 108.1	2.4 ± 1.1	2.7 ± 1.2	2.6 ± 1.1	1.11
SWS	40.8 ± 18.7	0.3 ± 0.1	0.4 ± 0.1	0.1 ± 0.1	0.06
SLL	111.9 ± 42.6	1.6 ± 0.7	1.6 ± 0.8	1.6 ± 0.4	0.67
WWC	81.3 ± 45.5	0.4 ± 0.2	0.7 ± 0.3	0.6 ± 0.3	0.25
Mean	254.8 ± 113.9	2.1 ± 1.2	2.2 ± 1.3	2.1 ± 1.0	0.91
Fly					
NWF	356.9 ± 219.3	1.3 ± 0.8	1.4 ± 0.9	1.3 ± 0.8	0.44
ELC	724.1 ± 338.2	4.9 ± 2.1	4.9 ± 2.1	4.8 ± 1.8	1.63
SWS	0.0 ± 0.0	0.0 ± 0.0	0.03 ± 0.0	-0.2 ± *0.1*	-0.06
SLL	37.8 ± 20.3	0.2 ± 0.1	0.4 ± 0.1	0.2 ± 0.1	0.05
WWC	58.6 ± 38.2	0.2 ± 0.1	0.3 ± 0.2	0.1 ± 0.1	0.05
Mean	235.5 ± 129.3	1.2 ± 0.9	1.4 ± 1.1	1.2 ± 0.9	0.43

Supplementary Table 9 Equations used throughout carbonate and sediment budgets

Eq. no	Factor	Symbol	Units	Equation
1	Habitat area	A_Z	m^2	$A_Z = A \times Rug_Z$
2	Coral skeletal mass	M_{air}	g	$M_{air} = \frac{M_{sw} Rho_{CaCO3}}{Rho_{CaCO3} - Rho_{sw}}$
3	Coral carbonate production	CCP	Kg yr^{-1}	$CCP = coral\,\% \times A_Z \times Calcification\,rate$
4	Encruster calcification rate	ECR	Kg yr^{-1}	$\mathrm{ECR} = (\frac{(ig - eg)}{days} \div SA) \times 36$
5	Encruster carbonate production	ECP	Kg yr^{-1}	$ECP = CCA\,cover\,\% \times ECR \times A_Z$
6	Gross framework production	GF	Kg yr^{-1}	$GF = \sum CCP + \sum ECP$
7	Normalised framework production	GF_N	Kg m^{-2} yr^{-1}	$GFN = GF \div A_Z$
8	Bioerosion rate		Kg m^{-2} yr^{-1}	$Bioerosion\,rate = (Vol_i \times Rho_i) \div (SA_i \times T)$
9	Zonal bioerosion rate	Br	Kg yr^{-1}	$Br = Bioerosion\,rate \times \%\,available\,substrate \times A_Z$
10	Normalised bioerosion rate	Br_N	Kg m^{-2} yr^{-1}	$BrN = Br \div A_Z$
11	Net framework production	NF	Kg m^{-2} yr^{-1}	$NF = GFN - GBrN$
12	Reef accretion potential	RAP	mm yr^{-1}	$RAP = (NF \times 2.93) \div (100 - Rpor) \times 100$
13	Carbonate content	$CaCO^3$ %	%	$CaCO_3\,\% = \frac{(S_i - S_p)}{S_i} \times 100$
14	Direct sediment production rate	SPR	Kg m^{-2} yr^{-1}	$SPR = (Biomass \times abundance) \times \%CaCO3 \times turnover\,rate$
15	Annual sediment production	ASP	Kg yr^{-1}	$ASP = \sum SPR \times A_Z \times \%\,sediment\,cover$
16	Normalised annual sediment production	ASP_N	Kg m^{-2} yr^{-1}	$ASPN = ASP \div A_Z$
17	Sediment dissolution	SD	Kg m^{-2} yr^{-1}	$SD = sediment\,dissolution\,rate \times \%\,sediment\,cover$
18	Gross sediment production	GSP	Kg m^{-2} yr^{-1}	$NSP = (ASP + BrG) - SD$
19	Normalised net sediment production	NSP_N	Kg m^{-2} yr^{-1}	$GSPN = SB \div A_Z$